Calhoun: The NPS Institutional Archive
DSpace Repository

Theses and Dissertations 1. Thesis and Dissertation Collection, all items

1982

Evaluation of the performance and flow in an axial compressor.

Waddell, John Leighton.

Monterey, California. Naval Postgraduate School

http://hdl.handle.net/10945/20155

Downloaded from NPS Archive: Calhoun

Calhoun is the Naval Postgraduate School's public access digital repository for research materials and institutional publications created by the NPS community. Calhoun is named for Professor of Mathematics Guy K. Calhoun, NPS's first appointed -- and published -- scholarly author.

Dudley Knox Library / Naval Postgraduate School
411 Dyer Road / 1 University Circle
Monterey, California USA 93943

http://www.nps.edu/library

DUDLEY KNOX LIBRARY
NAVAL POSTGRADUATE SCHOOL
MONTEREY, CALIF. 93940

NAVAL POSTGRADUATE SCHOOL
Monterey, California

THESIS

EVALUATION OF THE PERFORMANCE AND FLOW IN AN AXIAL COMPRESSOR

by

John Leighton Waddell

October 1982

Thesis Advisor: R. P. Shreeve

Approved for public release; distribution unlimited

T208072

REPORT DOCUMENTATION PAGE

READ INSTRUCTIONS
BEFORE COMPLETING FORM

1. REPORT NUMBER	2. GOVT ACCESSION NO.	3. RECIPIENT'S CATALOG NUMBER
4. TITLE (and Subtitle) Evaluation of the Performance and Flow in an Axial Compressor		5. TYPE OF REPORT & PERIOD COVERED Master's Thesis October 1982
		6. PERFORMING ORG. REPORT NUMBER
7. AUTHOR(s) John Leighton Waddell		8. CONTRACT OR GRANT NUMBER(s)
9. PERFORMING ORGANIZATION NAME AND ADDRESS Naval Postgraduate School Monterey, California 93940		10. PROGRAM ELEMENT, PROJECT, TASK AREA & WORK UNIT NUMBERS
11. CONTROLLING OFFICE NAME AND ADDRESS Naval Postgraduate School Monterey, California 93940		12. REPORT DATE October 1982
		13. NUMBER OF PAGES 160
14. MONITORING AGENCY NAME & ADDRESS(if different from Controlling Office)		15. SECURITY CLASS. (of this report) Unclassified
		15a. DECLASSIFICATION/DOWNGRADING SCHEDULE

16. DISTRIBUTION STATEMENT (of this Report)

Approved for public release; distribution unlimited

17. DISTRIBUTION STATEMENT (of the abstract entered in Block 20, if different from Report)

18. SUPPLEMENTARY NOTES

19. KEY WORDS (Continue on reverse side if necessary and identify by block number)

Axial Compressor
Secondary Flows
Guide Vanes
Compressor Testing

20. ABSTRACT (Continue on reverse side if necessary and identify by block number)

An experimental evaluation of the axial compressor test rig with one stage of symmetric blading was conducted to determine its suitability for studies of tip clearance effects. Measurements were made of performance parameters and internal flow fields. The configuration tested was found to be unsuitable due to poor flow from the inlet guide vanes, particularly near the tip region. Secondary flows and flaws in

DD FORM 1473 1 JAN 73 EDITION OF 1 NOV 65 IS OBSOLETE
S/N 0102-014-6601

construction of the guide vanes were suggested as probable causes. Recommendations were made for a program to resolve the problem.

Approved for public release; distribution unlimited

Evaluation of the Performance and Flow in an Axial Compressor

by

John Leighton Waddell
Lieutenant, United States Navy
B.S.A.E., Texas A&M University, 1974

Submitted in partial fulfillment of the
requirements for the degree of

MASTER OF SCIENCE IN AERONAUTICAL ENGINEERING

from the

NAVAL POSTGRADUATE SCHOOL
October 1982

2013
2 1

DUDLEY KNOX LIBRARY
NAVAL POSTGRADUATE SCHOOL
MONTEREY, CALIF. 93940

ABSTRACT

An experimental evaluation of the axial compressor test rig with one stage of symmetric blading was conducted to determine its suitability for studies of tip clearance effects. Measurements were made of performance parameters and internal flow fields. The configuration tested was found to be unsuitable due to poor flow from the inlet guide vanes, particularly near the tip region. Secondary flows and flaws in construction of the guide vanes were suggested as probable causes. Recommendations were made for a program to resolve the problem.

TABLE OF CONTENTS

I. INTRODUCTION 15

II. APPARATUS 17

A. COMPRESSOR TEST RIG 17

B. DATA ACQUISITION SYSTEM 19

C. INSTRUMENTATION 19

III. TEST PROGRAM AND RESULTS 24

A. SUMMARY 24

B. PHASE 1 24

C. PHASE 2 26

D. PHASE 3 29

E. SUPPLEMENTAL TESTS 30

IV. DISCUSSION 33

A. FLOW FROM THE INLET GUIDE VANES 33

B. PERFORMANCE DIFFERENCES 37

C. MEASUREMENT UNSTEADINESS 39

V. CONCLUSIONS AND RECOMMENDATIONS 41

TABLES 43

FIGURES 79

APPENDIX A. SURVEY PROBE CALIBRATION 132

APPENDIX B. COMPRESSOR DESIGN DATA 141

APPENDIX C. EXPERIMENTAL DATA FROM BUILD 1 143

APPENDIX D. INTEGRATION OF EXIT RAKES 145

APPENDIX E. DATA REDUCTION EQUATIONS 149

APPENDIX F. DATA REDUCTION SOFTWARE 150

APPENDIX G. SUMMARY OF TEST PROGRAM 155

LIST OF REFERENCES 158

INITIAL DISTRIBUTION LIST 160

LIST OF TABLES

1. Measured Quantities, Typical Set-up 43

2. Measurement Uncertainty 44

3. Performance Parameters (IGVs 0°) 45

4. Mid-span Velocity Vectors (IGVs 0°) 47

5. Mid-span Pressure Variations with Throttling (IGVs 0°) 49

6. Velocity Vectors at 17 Inches Radius (IGVs 0°) . . 51

7. Pressure Variations at 17 Inches Radius (IGVs 0°) 52

8. Performance Parameters (IGVs 4°) 53

9. Mid-span Velocity Vectors (IGVs 4°) 54

10. Mid-span Pressure Variations with Throttling (IGVs 4°) 55

11. Survey Results, Velocity Vectors (IGVs 0°, S2+4) . 56

12. Performance Parameters (IGVs 3°) 57

13. Mid-span Velocity Vectors (IGVs 3°) 58

14. Mid-span Pressure Variations with Throttling (IGVs 3°) 59

15. Survey Results, Velocity Vectors (IGVs 3°, S2+4) . 60

16. Survey Results, Velocity Vectors (IGVs 3°, S1+4) . 61

17. Survey Results, Velocity Vectors (IGVs 3°, S1+2+4) 62

18. Performance Parameters (IGVs 2°) 63

19. Mid-span Velocity Vectors (IGVs 2°) 64

20. Mid-span Pressure Variations with Throttling (IGVs 2°) 65

21. Survey Results, Velocity Vectors (IGVs 2°, S2+4) . 66

22. Survey Results, Velocity Vectors (IGVs 2°, S1+4) . 67

23. Performance Parameters (IGVs 0°) 68

24. Mid-span Velocity Vectors (IGVs 0°) 69

25. Survey Results, Velocity Vectors (IGVs 0°, S1+4) . 70

26. Survey Results, Velocity Vectors (IGVs 0°, S4) . . 72

27. Survey Results, Velocity Vectors (IGVs 0°, S2+3) . 74

28. Off Design Survey Velocity Vectors (IGVs 0°, S1) . 76

29. Off Design Survey Velocity Vectors (IGVs 0°, S2+3+4) 77

30. Velocity Vectors at Station One at Three Survey Locations 78

A1a. "SMITH" Probe Coefficients 135

A1b. "SMITH" Probe Calibration Errors 136

A2a. 539 Probe Coefficients 137

A2b. 539 Probe Calibration Errors 138

A3a. 538 Probe Coefficients 139

A3b. 538 Probe Calibration Errors 140

B1. Summary of Mid-span Design Flow Values 141

B2. Summary of Off Design Calculations 142

C1. Build 1 Velocities at Mid-Span 143

D1. Sub-Area Pressure Determination from Probe Pressures 146

G1. Performance Map, Throttle Configurations 157

LIST OF FIGURES

1. Compressor Schematic 79

2. Measurement Planes for Installed Stage 80

3. Locations of Survey Ports 81

4. Performance Parameters vs Flow Rate (IGVs 0°) . . . 83

5. Comparison of Measured Performance with Design Values and Build One Measurements 84

6. Mid-span Flow Angles vs Flow Rate (IGVs 0°) 85

7. Flow Angles at 17 Inches Radius vs Flow Rate (IGVs 0°) 86

8. Inlet and Exit Pressure Distributions vs Radius at Three Throttle Settings (IGVs 0°) 87

9. Performance Parameters vs Flow Rate (IGVs 4°) . . . 88

10. Mid-span Flow Angles vs Flow Rate (IGVs 4°) 89

11. Inlet and Exit Pressure Distributions vs Radius at Three Throttle Settings (IGVs 4°) 90

12. Measured Flow Angle Radial Distribution at Moderate Throttling (IGVs 4°, S2+S4; — - - — Design) 91

13. Relative Flow Angle Radial Distribution at Moderate Throttling (IGVs 4°, S2+S4; — - - — Design) 92

14. Axial Velocity Radial Distribution at Moderate Throttling (IGVs 4°, S2+S4) 93

15. Intrastage Pressure Radial Distributions at Moderate Throttling (IGVs 4°, S2+S4) 94

16. Performance Parameters vs Flow Rate (IGVs 3°) . . . 95

17. Mid-span Flow Angles vs Flow Rate (IGVs 3°) 96

18. Inlet and Exit Pressure Distributions vs Radius at Three Throttle Settings (IGVs 3°) 97

19. Measured Flow Angle Radial Distribution at Moderate Throttling (IGVs 3°, S2+4) 98

20. Relative Flow Angle Radial Distribution at Moderate Throttling (IGVs 3°, S2+4) 99

21. Axial Velocity Radial Distribution at Moderate Throttling (IGVs 3°, S2+4) 100

22. Intrastage Pressure Radial Distributions at Moderate Throttling (IGVs 3°, S2+4) 101

23. Performance Parameters vs Flow Rate (IGVs 2°) . . . 102

24. Mid-span Flow Angles vs Flow Rate (IGVs 2°) 103

25. Inlet and Exit Pressure Radial Distributions at Three Throttle Settings (IGVs 2°) 104

26. Measured Flow Angle Radius Distributions at Moderate Throttling (IGVs 2°, S2+4) 105

27. Relative Flow Angle Radius Distributions at Moderate Throttling (IGVs 2°, S2+4) 106

28. Axial Velocity Radial Distributions at Moderate Throttling (IGVs 2°, S2+4) 107

29. Intrastage Pressure Radial Distributions at Moderate Throttling (IGVs 2°, S2+4) 108

30. Measured Flow Angle Radial Distributions at Moderate Throttling (IGVs 2°, S1+4) 109

31. Relative Flow Angle Radial Distributions at Moderate Throttling (IGVs 2°, S1+4) 110

32. Axial Velocity Radial Distribution at Moderate Throttling (IGVs 2°, S1+4) 111

33. Measured Flow Angle Radial Distributions with Closely Spaced Data Points (IGV 2°, S1+4) 112

34. Measured Flow Angle Radial Distributions Measured by Yaw Probe 113

35. Performance Parameters vs Flow Rate (IGVs 0°) . . . 114

36. Mid-span Flow Angles vs Flow Rate (IGVs 0°) 115

37. Measured Flow Angle Radial Distribution at Moderate Throttling (IGVs 0°, S1+4) 116

38. Axial Velocity Radial Distribution at Moderate Throttling (IGVs 0°, S1+4) 117

39. Intrastage Pressure Radial Distribution at Moderate Throttling (IGVs 0°, S1+4) 118

40. Off-design Measured Flow Angle Radial Distribution (IGVs 0°, S1; ———— Design) 119

41. Off-design Relative Flow Angle Radial Distribution (IGVs 0°, S1; ———— Design) 120

42. Off-design Axial Velocity Radial Distribution (IGVs 0°, S1; ———— Design) 121

43. Off-design Intrastage Pressure Radial Distribution (IGVs 0°, S1) 122

44. Off-design Measured Flow Angle Radial Distribution (IGVs 0°, S2+3+4; ———— Design) 123

45. Off-design Relative Flow Angle Radial Distributions (IGV 0°, S2+3+4; ———— Design) 124

46. Off-design Axial Velocity Radial Distribution (IGVs 0°, S2+3+4; ———— Design) 125

47. Off-design Intrastage Pressure Radial Distributions (IGV 0°, S2+3+4) 126

48. Comparison of Measured Flow Angle at Three Locations Relative to the Inlet Guide Vane Trailing Edge (IGVs 3°, S2+4; ———— Design) 127

49. Stator Vane Exit Circumferential Survey at Three Radii 128

50. Inlet Total Pressure Radial Survey Results 129

51. Torque and Inlet Nozzle Pressure Fluctuations with Time 130

52. Schematic of Guide Vane Exit Geometry 131

D1. Total Pressure Rake Geometry 147

D2. Pressure Mass Averaging Area Divisions 148

TABLE OF SYMBOLS

ρ_0	Ambient density (Rho0)
P_{amb}	Ambient pressure (Pamb)
P_{t_I}	Inlet (nozzle) total pressure (Ptnoz)
P_I	Inlet (nozzle) static pressure (Pnoz)
C_D	Nozzle discharge coefficient
β_n	Nozzle area ratio
T_{T_I}	Inlet total temperature (T)
R	Gas constant
g_c	Gravitational constant
$\dot{m}$	Mass flow rate (Mflow)
γ	Ratio of specific heats
$\bar{\Phi}$	Flow coefficient based on average velocity (Cflow)
A_C	Compressor test section area
A_I	Duct area
π_{t_2}, π_{t_3}	Total pressure coefficient (Cpt2), (Cpt3)
π_1, π_2, π_3	Static pressure coefficient (Cp1), (Cp2), (Cp3)
HP	Shaft horsepower (Powr)

Rpm	Rotational velocity (Rpm)
Tq	Shaft torque (Torq)
X	Work coefficient (Cwork)
$\bar{\eta}_t$	Average total-to-total efficiency (Etaav)
ϕ_1, ϕ_2, ϕ_3	Respective probe flow pitch angles (Phi)
α_1, α_2, α_3	Respective probe yaw angles (Alfa)
V_1, V_2, V_3	Absolute velocities
W_1, W_2	Velocities relative to rotor
β_1, β_2	Flow angles relative to rotor (Beta)
V_{u_1}, V_{u_2}	Circumferential velocity components
V_{a_1}, V_{a_2}, V_{a_3}	Axial velocity components
U_m	Mean radius wheel speed
R_m	Mean radius
S1, S2, S3, S4, S5	Throttle screen elements

Note: Names in parentheses are those used in the HP 9845A software.

Units are defined in the text as needed and in tables of results.

ACKNOWLEDGMENT

I wish to express my sincere appreciation to the entire Turbopropulsion Laboratory staff for their assistance, encouragement and patience. Without the benefit of their experience and ingenuity many of the steps in this program could not have been completed. My thanks go to Dr. R. P. Shreeve for his direction and his help in putting it all together. I especially thank Mr. Jim Hammer for his constant encouragement and support, for the questions he answered, and for the questions he asked.

I. INTRODUCTION

Secondary flow effects and associated losses that result from finite tip clearances in compressors are not fully understood. The low speed axial flow compressor at the Turbopropulsion Laboratory of the Naval Postgraduate School is currently being used to improve understanding of the tip clearance problem and to generate better prediction methods for the effects. To this end, the axial compressor was reconfigured as described in Ref. 1 to facilitate new experimental studies. The redesign was intended to:

1) provide an axisymmetric flow as uniform as possible ahead of the compressor;
2) provide a means to determine accurately the mass flow rate;
3) allow an easy adjustment of the mass flow rate;
4) minimize the pressure losses at open throttle to provide the maximum range of mass flow rate.

In this configuration, Welch performed preliminary tests with solid body blading, as reported in Ref. 2. Symmetric blading was selected for the tip clearance investigation and new blading was designed and reported in Ref. 3. Initial tests with one stage of the new symmetric blading were made by Moyle but were terminated by an accidental failure which resulted in a total loss of the blading and some instrumentation. Results from these tests, referred to as

Build 1, were reported in Ref. 4. A new set of inlet guide vanes was cast, as detailed in Ref. 5, and the compressor was rebuilt with one stage. This configuration is designated Build 2.

The purpose of the present investigation was to evaluate the current Build 2 and to determine its suitability for studies of tip clearance effects. In the course of the work the performance of individual blade rows as well as the overall compressor performance were examined, measurements were refined where problems were encountered, and the flow fields were examined throughout the stage.

II. APPARATUS

A. COMPRESSOR TEST RIG

The low speed axial flow compressor was designed to provide a large enough scale to allow the insertion of multiple intrastage sensors without altering the flow fields. The three foot diameter compressor, shown in Fig. 1, is capable of one to three stages of operation. When less than three stages are used, the stages may be built up in a normal closely spaced configuration or in an expanded configuration with wide separation between stages or between blade rows of a given stage. There are thirty rotor blades and thirty-two stator vanes per stage and each stage is identical. One row of thirty-two inlet guide vanes and one or two rows of thirty-two exit guide vanes may be installed. For the present measurements, one stage of symmetrical blading was installed in a closely spaced configuration with one row of inlet guide vanes and one row of exit guide vanes. The access ports in the case-wall are arranged in eight axial locations and allow insertion of intrastage probes at various peripheral locations relative to the fixed blading. The survey planes are shown in Figs. 2 and 3. Provisions are made for mounting a traverse rig which allows for circumferential as well as radial surveys in any of six locations. The traverse unit, shown in Fig. 3d, was mounted in the

first access location. Additional sensors may be installed by drilling the test section casing or duct walls.

Flow enters the compressor from outside the laboratory through a twenty-one foot long duct which contains a throttling device. A choice of two inlet bellmouths, used to meter the flow rate, attaches to the front of the ducting and is surrounded by a protective screen enclosure. The large inlet bellmouth with a three foot throat diameter is used for conditions where minimum pressure drop is desired. The smaller 2.1 foot throat diameter bellmouth is used when a greater pressure drop can be accepted. The duct has a section which can be removed, when the large bellmouth is used, to reduce the boundary layer growth. Only the large bellmouth was used here, but the duct section was not removed. Throttling is accomplished, as described in Ref. 6, by the insertion of screens or perforated plates into the inlet flow causing a drop in total pressure. Throttling is therefore fixed for each run and may be changed only by stopping the compressor. Flow exits the compressor and is vented into the building via a conical diffuser.

The compressor is driven by a constant speed electric motor, rated at 150 horsepower, and is coupled to the compressor by ten drive belts. The drive ratio can be changed by changing the drive sheaves, allowing operation at nominally 1588, 1818 and 2290 revolutions per minute. With the low speed drive sheave installed the compressor was operating

at roughly 1616 RPM for all tests reported in the present work.

B. DATA ACQUISITION SYSTEM

Data was acquired using the Hewlett Packard HP 3052 Data Acquisition controlled by an HP 9845A computer. The system included a HP 34495A Scanner, HP 3495 Digital Volt Meter (DVM), HG 78K Scanivalve Controller and signal preprocessor circuits. The HG 78K Scanivalve Controller (manufactured in-house) controlled the two solenoid driven 48 port Scanivalves. Each Scanivalve, referred to ambient pressure, provided the ability to read 48 pressures with a single transducer. All data were recorded by the computer via the scanner, the digital volt meter and interface bus.

Data acquisition was accomplished using the "GENUSE", general acquisition program, described in Ref. 7. Briefly, the program controls the reading of data from up to five Scanivalves and 35 other channels, stores the data on tape and gives a tabulated printed copy. Two modifications were made to the program. An on-line reduction routine was added and a change was made in the non-Scanivalve data reading subroutine to allow a torque reading to be made which was averaged over an extended time.

C. INSTRUMENTATION

The instrumentation consisted of numerous pressure sensors and several other non-pressure devices. The pressure

sensors included three United Sensor five hole probes, two total pressure rakes, four Kiel probes, a simple total pressure probe, twelve static pressure taps, and an ambient pressure sensor. For some tests a cobra probe and a yaw probe were added. The non-pressure devices included three thermocouples, a torquemeter, a tachometer, and six linear potentiometers to record radial and angular positions of the movable probes. Table 1 lists the quantities measured. Where possible, the pressure sensors were connected to one of the Scanivalves because of the ability to do an on-line scale verification. This was done by connecting Scanivalve port one to the transducer reference pressure (atmos) to give the zero reading (or tare) for the transducer while the second port was connected to a manometer column pressurized to a controlled pressure in inches of water. This allowed the scale factor and zero drift to be checked at each data point. Two dedicated transducers were used to measure the bellmouth pressure drop and ambient pressure. The electrical signals from all transducers were conditioned before digitizing by the digital volt meter. Each Scanivalve and non-Scanivalve channel incorporated a signal conditioning circuit to allow the zero point and scale factors to be set.

Ambient pressure within the building was measured using an absolute pressure transducer. Verification readings were made periodically using a Fortin type barometer. Excessive

drift in the absolute transducer generally led to the use of the barometer readings in all calculations. Ambient temperature was sensed using two "J" type thermocouples in the inlet duct with an electrical equivalent ice point reference. The recovery factor of the thermocouples was taken to be unity. Total temperature rise was measured differentially by averaging the outputs of two "J" type thermocouples located at mid-radius at the stator exit and connecting them in series with the thermocouples in the inlet. The rotational speed of the compressor was measured using a magnetic pickup connected to a digital counter. The signal was read manually using a multimeter (although provisions exist for automatic reading through the scanner). Torque was measured using a Lebow Model 1215-6K torquemeter which was statically calibrated periodically between tests. The stability of the torque calibration was verified using an electrical shunt prior to each run. Inlet bellmouth (nozzle) pressure drop was measured using a differential transducer between the pressure (stagnation) within the inlet enclosure and the pressure (static) in the nozzle throat. The two pressures were also measured individually using two adjacent ports on the first Scanivalve. The Scanivalve measurements were used for all calculations since the drift of the dedicated transducer could not be checked over long run periods. One port of the first Scanivalve was connected to a total pressure tube inside the duct at a distance of two duct diameters

downstream of the throttle. This reading was used purely for verification of other readings and was not used for calculations. The test section inlet total pressure was measured using a twelve hole rake at survey plane one. Total pressure was determined using a mass averaging technique described in Appendix D. The exit total pressure was measured using a similar rake, applying the same mass averaging technique. Eight case wall static pressure taps, corresponding to the eight survey planes and two hub static pressure taps were used. Four Kiel probes at mid-radius at the stator exit completed the instrumentation on the first Scanivalve.

The second Scanivalve was used for the three United Sensor five hole probes, and the total pressure on the cobra probe, when it was used. The survey probes, described in Appendix A, provided measurements of yaw, pitch and velocity magnitude at survey plane two (station 1), survey plane three (station 2) and survey plane four (station 3). The radial positions and yaw angles for the probes were recorded from linear potentiometers attached to the probe mounts. For the station 3 probe in the traverse unit, readings were recorded from potentiometers set manually from the digital counters in the traverse unit. A similar technique was used for the cobra probe. The five hole probes were yaw-balanced using a forty-five degree inclined manometer board. Accurate measurements required that the balancing be done very

carefully. In shear layers or turbulent flows, the difficulty involved in yaw-balancing added to the uncertainty in the probe measurements.

III. TEST PROGRAM AND RESULTS

A. SUMMARY

The test program was carried out in three phases. First, a performance map was taken and limited flow field surveys were made. The results from these tests appear in Tables 3 to 8 and Figs. 4 to 8. Second, the inlet guide vanes were adjusted to three different settings to alter the flow angles into the rotor. The results from these tests appear in Tables 9 to 31 and Figs. 9 to 34 and include both performance maps and surveys made near the observed peak efficiency. Third, the inlet guide vanes were returned to the original configuration and surveys were taken at and near the peak efficiency and at two well-off-design throttling conditions. The results from these tests appear in Tables 32 to 40 and Figs. 35 to 47. Other supplemental tests taken concurrently with the other testing include examining fluctuations in torque and flow rate, nozzle flow rate verification, and a comparison of probe results obtained in peripherally displaced survey holes to examine axisymmetry.

B. PHASE 1

The first phase performance map involved twenty-two throttle conditions from fully open throttle through all possible combinations of the screen-type throttle elements.

The three survey probes remained at mid-radius where the flow vectors were determined (Table 4). This is the configuration in which build one data was available for comparison. The performance parameters are listed in Table 3 and plotted in Fig. 4. Comparisons with build one data and the design predictions appear in Fig. 5. Note that the build one data reflects only the mid-span pressure rise and not a spanwise integrated value. The pressure rise was virtually linear with flow rate, never showing a peak but indicating a change in slope at very high throttling. The power and the efficiency both showed a definite rise and fall but the peak values, occurring at a flow rate of roughly ϕ = .76, were obscured due to 2% fluctuations in the torque measurement. The pressure ratio through the stage varied from 1.014 to 1.02.

The flow angle at the inlet guide vane exit (station 1) remained essentially constant through the measured range of flow rates at 17.5 degrees as is plotted in Fig. 6. The mid-span rotor exit angle (station 2) varied nearly linearly with flow rate. The flow angle at station 1 was 3.8 degrees less than the design prediction. A less detailed performance map was taken with the probes at seventeen inches radius. The guide vane exit angle exhibited even more severe underturning than at the mid-radius with the measured angle varying one degree from 23 to 22 degrees (Fig. 7). Limited surveys taken while examining the axisymmetry of the flow

indicated that these angles were quite typical of the condition in the blade-to-blade direction.

Radial flows were noted at all stations. At station 1, there was a consistently inward flow which was most severe at low throttling. At station 2, the radial component shifted from radially outward at low throttling to inward at high throttling. The opposite occurred at station 3. As can be seen in Fig. 7, the station 3 probe showed a relatively constant yaw angle as the flow was throttled initially, but the yaw angle increased rapidly below a flow rate of $\phi = 0.75$.

C. PHASE 2

To "force" the rotor inflow angle to match the design angle at mid-span, the inlet guide vanes were turned four degrees counterclockwise. This resulted in a large reduction in flow rate, pressure rise, and power required, varying from 5.4 to 3.1 percent (Table 8). This came from "unloading" the rotor as the requirement for turning was reduced. The efficiency was significantly reduced at high flow rates but changed little at the moderate and low flow rates (Fig. 9). The flow angles out of the inlet guide vanes at mid-span were closer to design as shown in Fig. 10. However Fig. 12 shows that the guide vane exit flow was still underturning at the outer radii, and now overturning at the inner radii. The angles at station 1 had shifted uniformly across the radius in the direction the guide vanes had been turned.

Also, although the inlet flow angles were somewhat improved, the stator exit angles were not correct for any succeeding stages. The radial flows were altered noticeably. The flow at station 1 showed a minimum inward component near the "maximum" efficiency (Table 9). The flow at station 2 was consistently inward, being somewhat less so away from the peak efficiency condition. The stator exit flow was outward near peak efficiency and inward at lower or higher throttle conditions.

Total and static pressure distributions, taken from the survey probes, showed that the static pressure rise was about equally divided between the rotor and the stator (Fig. 15). The rise was greater at the tip but relatively flat overall. The total pressure rise across the rotor was skewed slightly toward the tip. The overall stage total pressure rise can not be inferred from the data in Fig. 14 since the probe was at a single peripheral position well clear of the stator wakes.

The inlet guide vanes were adjusted back one degree clockwise to be three degrees from the original configuration. The performance, shown in Fig. 16, was found to be similar to that obtained at the four degree setting. However, there were indications of a possible upturn in the efficiency with increased throttling at the lowest flow rate after an apparent peak efficiency at a flow rate of about $\phi = .73$ compared to results at the 4° guide vane setting.

The pressure rise at peak efficiency increased by 4 percent, at low throttling by 2 percent and at highest throttling by 1 percent (Table 12). Shown in Fig. 17, the flow angles at stations 2 and 3 showed similar trends to those measured at the four degree setting. The stator exit radial flow showed a distinct trend from inward at low throttling to outward at high throttling (Table 13).

Several surveys were taken near the peak efficiency. These surveys, concentrated in the hub and tip regions, showed a reversal in flow angle at both the hub and tip. This was true at all three stations. The surveys also showed that the rotor total pressure rise was still slanted toward the outer radii, even slightly below the observed peak performance. The through-flow velocities were also higher at the outer regions, corresponding to regions of greater pressure rise (Fig. 21). Surveys were taken at locations displaced circumferentially relative to the inlet guide vanes. The results shown in Fig. 48 show that the flow angles were much better behaved toward the pressure side of the blade and roughly the same near mid-passage or toward the suction side. The pressure side showed slightly lower velocities and had a much lower radial flow (Table 30).

The inlet guide vane angle was reduced by one additional degree to give a stagger angle two degrees greater than in the original configuration. The performance map was repeated and several surveys were taken. At this point, the

acquisition program was changed to read the torque over a longer period which yielded a more stable reading. The results in Fig. 23 show that the performance again yielded an indistinct peak in the efficiency. In fact, the efficiency appeared to rise again at the highest throttling to the previous peak value. The pressure rise and power required showed no different trends, being similar to the original configuration. The radial flow components also showed similar trends (Table 19).

During the surveys, a lack of stability was noted in the flow angles at station 1 at radii between sixteen and seventeen and a half inches. The flow angle would remain steady for several seconds, then drift to a new value (Fig. 33). The flow appeared to vascillate about an intermediate value that followed a smooth variation as a function of radius. Repeating the survey, using a two tube yaw head probe, the vascillations were not apparent and the flow angles did follow a smooth curve (Fig. 34). With the smaller yaw probe, angles were measured very close to the outer wall. The results showed a strong reversal in the flow angle at the tip at all three stations.

D. PHASE 3

The inlet guide vanes were returned to the original configuration and three surveys were taken with moderate throttling and one was taken at very low (Figs. 40-43) and one at

very high throttling (Figs. 44-47). These surveys showed the changes in the flow fields over the range of flow rates. As throttling was increased, the flow rate decreased and the pressure rise shifted from being greatest at the hub to being greater at the tip. The ill-defined peak efficiency occurred when the distribution in pressure rise was approximately uniform across the blade height. The off-design inlet conditions caused the peak to occur at a flow rate slightly lower than for uniform pressure rise when the bulk of the work and flow rate were concentrated at the outer radii. At the low flow rates the pressure field was the most distorted and the radial components of the velocity were the greatest.

E. SUPPLEMENTAL TESTS

Supplemental tests were conducted during the program to examine three areas. These tests looked at flow rate and torque fluctuations, nozzle flow rate verification, and comparison of results from different peripheral survey locations to examine axisymmetry. The results of these tests appear in Figs. 48 to 51.

Output from the torquemeter and nozzle pressure drop transducer were connected to oscillographs and continuous readings were taken. As seen in Fig. 51, the torque fluctuations were typically plus or minus 15 inch-pounds with a frequency of consistently 5.5 per second. With a compressor speed of 1616 RPM, this was one oscillation per 4.9

revolutions of the drive motor running at 1180 RPM. The nozzle pressure fluctuations had a frequency of three per second. Thus the torque fluctuation varied at a rate of 1.8 oscillations per flow rate oscillation. The amplitude of the nozzle pressure drop variations was unsteady in time and no wave form analysis was done to look for frequency content.

An attempt was made to verify the flow rate measurements, in an approximate way, since an integration of radial probe surveys downstream of the rotor had suggested that the flow rate should be somewhat higher than was measured. The flow at the inlet to the compressor (survey plane 1) was traversed using a cobra probe and the total pressure distribution was recorded (Fig. 50). Assuming axisymmetry and constant static pressure at the value measured at the wall, the mass flux distribution was calculated and integrated to obtain the total flow rate. The result was found to correspond to the use of a discharge coefficient for the large bellmouth of 1.026, rather than 0.98 which had been used to date. This higher value was used in all calculations.

The degree of axisymmetry was examined by moving the survey probes and rakes to various survey ports about the circumference. At survey plane one, rakes were placed in four of the nine ports and good agreement was obtained in the results. Similarly, ports five, seven and nine showed good agreement at survey plane two. The stator exit was surveyed circumferentially at three radii (Fig. 49). The

wake was consistently centered at 9° on the traverse unit at all three radii at moderate throttling. Thus the flow measured at station 3 was clear of the wake for all other runs for which the probe was typically located at the 5° position. The exit rake was moved to 5 ports at 3 survey planes between the stator and exit guide vanes. The locations furthest aft of the stage allowed the best mixing of stator wakes but also reflected the build-up of hub and case wall boundary layers.

IV. DISCUSSION

A. FLOW FROM THE INLET GUIDE VANES

The most significant result from the measurement program was the behavior of the flow angle from the inlet guide vanes. The significant underturning at the outer radii related directly to the alteration of the performance of the compressor. This underturning, roughly ten degrees at 17.5 inches radius and four degrees at mid-radius, required the rotor to do increased work as compared to the design and led to a violation of the radial equilibrium condition. The result was to change the pressure distributions and flow rates through the machine. Comparison with build one showed that the flow angle at mid span was 2° greater in build one, suggesting that there should be a difference in performance in the two builds, and this was observed. Vascillations in flow angle at the outer radii indicated the possibility of the presence of a flow separation. Since these problems affected the performance of the rest of the compressor, any discussion must begin with the inlet guide vanes.

As discussed in Ref. 8 and Ref. 9, secondary flows result when boundary layers pass through a set of stationary turning vanes. In particular, the fluid particles within the case and hub wall boundary layers tend to move toward the convex side of the flow passage and roll up into two trailing

vortices moving downstream. Modeling of this effect using small perturbation theory predicts that there will be overturning within the boundary layer and underturning outside of it. Reference 9 indicates that this is well supported by experimental experience in rectilinear (2D) cascades and that the underturning may be seen in the flow at a distance of three or four boundary layer thicknesses. The compressor is not two dimensional and is imposing on the flow a radial gradient in axial velocity and static pressure. While these are not the conditions as described in Ref. 9, the effect should be similar. With the case wall boundary layer being roughly one inch at moderate throttling, this effect could be expected to be seen inwards towards or even past the mid-radius. The hub boundary layer, with a thickness of about two tenths of an inch, has a much smaller and only local effect. It does however exhibit the same underturning/overturning pattern.

The differences in radial flow component shown in Table 30 tend to support this explanation of the mechanism causing the distorted flow at the guide vane exit. Along the pressure side of the vane, in the outer regions the calculated pitch angle is the most strongly positive. It decreases across the passage as measured in survey ports 7 and 8. Because the pressure taps on the probe are separated radially, the indicated pitch angle in a pressure gradient can be in error as a result of the gradient. Thus an

alternative explanation for the differences in pitch angle is that the radial pressure gradient is steeper along the pressure side of the blade. The hub region exhibits a similar behavior to that described for the outer regions but of smaller magnitude. The shape of the curves in Fig. 48 at the three survey locations support the idea of secondary flows as the cause of underturning since the angles measured away from the vane wakes qualitatively match closely the pattern predicted in Ref. 9. Note that the flow angles at mid-span were closer to the design values in build one than in build two (until the IGV's were adjusted). Thus there is an additional mechanism for underturning in build two in addition to the secondary flow effects discussed here.

Vavra indicates in Ref. 10 that the flow at the exit of a set of guide vanes is very sensitive to the distance a between neighboring blades as defined in Fig. 52. The relationship between passage exit area, blade spacing and efflux angle (at the mean line conditions) is approximated in Ref. 10 by the relationship $\alpha_e = \cos^{-1}(a/s)\left(1+\frac{4te}{s}\right)\left(1-\frac{\cos^{-1}(a/s)}{90}\right)$. The angle will decrease for either an increase in trailing edge thickness or an increase in the distance a for constant spacing. The trailing edge thicknesses are reported in Ref. 11 to be thicker for build two than for build one. For the additional underturning to be solely due to the larger trailing edge thickness it would require even larger thicknesses

than were reported. For a to be larger for the build two blades, the blade thickness would need to be smaller, which was not the case, or the blades would have to have been made with a shorter chord, which is known to be true for some blades. Therefore a combination of thicker trailing edges and shorter chord blades is probably the cause for the additional underturning seen in build two as compared to build one. One possibility for narrower blades would be excessive trimming during the removal of the flashing from the casting process. Another would be shrinkage of the epoxy after moulding but this is considered less likely, since most epoxy materials are known to swell slightly due to the diffusion of water molecules into the material.

Reynolds number effects must also be considered as a possible cause for the general level of underturning. Below a Reynolds number of 2.2×10^5, a decrease in deflection angle could be expected. At moderate throttling the Reynolds number based on mid-span chord was approximately 2.5×10^5 at the most closed throttle condition. Since the guide vane exit angle was essentially constant over the operating flow range, Reynolds number effect appeared to be minimal. The stator exit angle changed appreciably at the lower flow rates but this was probably the result of increased incidence angles from the rotor rather than an effect of Reynolds number.

The presence of a peripheral gradient across the passage could cause an error in yaw angle measurement in view of the separation of the yaw ports in the probe. This was discounted after measurements were made with a yaw probe which had its ports mounted along the same radial line, and similar results were obtained.

The erratic yaw angles experienced on some tests suggested the presence of a flow separation along the suction side of the guide vanes. Should the flow be separated, the flow angles would be expected to be reduced. Consistent with this observation, the flow closest to the pressure side of the blade demonstrated less underturning than at the two locations toward the center of the passage. The frequency of the change in the flow angle that occurred after the probe was balanced did not correlate with any of the measured flow rate oscillations or the typical one half per rotor revolution frequency of a rotating stall. It was clearly an intermittent rather than a periodic condition. It is possible therefore that the flow detaches and reattaches intermittently and further measurements are required to define the process clearly.

B. PERFORMANCE DIFFERENCES

The measured performance departed from the design expectation, shown in Fig. 5. Several factors could have contributed to the differences. For example, the design was

carried out for a single stage operating speed of 2290 RPM whereas the present tests were limited to 1616 RPM. Thus there was a possibility of a small Reynolds number effect on the performance as described in Ref. 8. Secondly, the test rig was intended to be run with the first six-foot section of duct removed in tests with the large inlet bellmouth. The extra length would have contributed a small amount to the boundary layer growth. Clearly, however, these differences are minor in comparison with the likely effect of the underturning of the guide vanes.

Comparisons with build one showed a rise in power, and flow rate in build two. The two degree shift in the rotor inflow angle caused greater loading on the rotor yielding a higher pressure rise and work requirement. The power increased roughly two percent over build one with an increase in flow rate of about 1.5 percent. The pressure rise within the stage was altered appreciably. At mid-span, the static pressure rise shifted more to the rotor; but at the case wall the static pressure rise, as measured by the wall static ports, shifted more toward the stator. No surveys were available from build one to allow a comparison at other radial locations, but the limited data did suggest a significant alteration in the internal flow fields. Further differences were in the radial flows at station two and three which showed much smaller magnitudes in build one.

It was extremely difficult to determine the peak efficiency for several reasons. First, the performance characteristic, which resulted from the incorrect flow fields, was very flat. The fluctuations occurring in the pressure rise and torque compounded the problem. With high flow volumes undergoing only slight pressure rises the work input could be greatly affected by perturbations in the torque or in the nozzle flow rate. Also, the radial exit total pressure rake, situated well aft of the stage, was influenced by the case wall and hub boundary layers and did not fully average the flow from the stators. This generated an uncertainty as to the true variation in the mass-averaged total pressure rise with flow rate.

C. MEASUREMENT UNSTEADINESS

The flow rate and torque fluctuations were apparently not related to any structural or flow feature of the machine. The frequency of the fluctuations did not correlate with each other nor with the (approximately) one per two revolutions of a rotating stall. Nor did they correspond to harmonics of the drive motor which operated at 1180 revolutions per minute. They were not similar to the natural frequencies of the blades given in Ref. 5. The flow vascillations observed at the outer radius occurred with a period estimated to be ten seconds or longer; torque and flow fluctuations were much more rapid. One possible explanation for

the torque fluctuations is that they were a result of play in the drive belts, but no means were available to examine the connection. Thus, there was no evidence that the torque fluctuations produced corresponding fluctuations in the flow fields, and they were accepted as an undesirable contributor to uncertainty in the measurement of efficiency.

V. CONCLUSIONS AND RECOMMENDATIONS

The evaluation of the performance of build two of the compressor indicated that it was not suitable for the intended tip effect research as presently configured. Results indicated that the compressor was operating at neither the design conditions nor the equivalent conditions to build one. The principal reason for the differences was an improper flow from the inlet guide vanes which was probably the result of secondary flows, somewhat aggravated by defects in the cast of the vanes.

The following are therefore recommended:

1. The inlet guide vanes should be recast, taking care to insure an accurate reproduction of the design geometry.
2. The compressor should be reevaluated at a higher speed and in an expanded mode to permit better definition of the flow fields and a better evaluation of the blading design.
3. The inlet boundary layer should be changed to gauge its importance. Methods of changing the boundary layer at the inlet guide vanes include:
    - (i) Install the large bellmouth inside the laboratory without throttle and with minimum ducting. This would minimize the boundary layer and the effect on the inlet guide vane exit angle could be measured (only) at open throttle.
    - (ii) Use of the smaller bellmouth.
    - (iii) Removal of parts of the inlet duct.
    - (iv) Use of controlled boundary layer suction (or blowing) just ahead of the compressor. This

would probably be desirable in the course of the tip clearance investigation to follow.

The logical procedure is to first carry out 3(i) without compressor geometry changes to answer definitively whether secondary flows developing from case wall boundary layer are the primary cause of the observed underturning. Depending on the results of this first test, either new inlet guide vanes should be cast or a new design should be developed which accounts properly for deviation angle in the presence of radial gradients in through flow.

Table 1. Measured Quantities, Typical Set-up

S.V. #4

$P_A - P_A$
$P_{cal} - P_A$
$P_{1_{noz}} - P_A$
$P_{2_{noz}} - P_A$
$P_{t_{pipe}} - P_A$
$P_{s_{pipe}} - P_A$
Inlet Rake $P_t 11.00-P_A$
Inlet Rake $P_t 11.50-P_A$
Inlet Rake $P_t 12.00-P_A$
Inlet Rake $P_t 12.75-P_A$
Inlet Rake $P_t 13.50-P_A$
Inlet Rake $P_t 14.40-P_A$
Inlet Rake $P_t 15.30-P_A$
Inlet Rake $P_t 16.00-P_A$
Inlet Rake $P_t 16.50-P_A$

S.V. #4 (Cont'd)

Inlet Rake P 17.00-P_A
Inlet Rake P 17.50-P_A
Inlet Rake P 17.75-P_A
SP-1 $P_{Hub} - P_A$
SP-1 $P_{Tip} - P_A$
SP-2 $P_{Tip} - P_A$
SP-3 $P_{Tip} - P_A$
SP-4 $P_{Tip} - P_A$
SP-5 $P_{Tip} - P_A$
SP-6 $P_{Tip} - P_A$
SP-7 $P_{Tip} - P_A$
SP-8 $P_{Tip} - P_A$
SP-8 $P_{Hub} - P_A$
Exit $P_t 3-1 - P_A$
Exit $P_t 3-2 - P_A$

S.V. #4 (Cont'd)

Exit $P_t 3-3 - P_A$
Exit $P_t 3-4 - P_A$
Exit Rake $P_t 11.00-P_t$
Exit Rake $P_t 11.50-P_t$
Exit Rake $P_t 12.00-P_t$
Exit Rake $P_t 12.75-P_t$
Exit Rake $P_t 13.50-P_t$
Exit Rake $P_t 14.40-P_t$
Exit Rake $P_t 15.30-P_t$
Exit Rake $P_t 16.00-P_t$
Exit Rake $P_t 16.50-P_t$
Exit Rake $P_t 17.00-P_t$
Exit Rake $P_t 17.50-P_t$
Exit Rake $P_t 17.75-P_t$

S.V. #5

$P_A - P_A$
$P_{cal} - P_A$
Probe "X" $P_1 - P_A$
Probe "X" $P_{23} - P_A$
Probe "X" $P_4 - P_A$
Probe "X" $P_5 - P_A$
Probe "Y" $P_1 - P_A$
Probe "Y" $P_{23} - P_A$
Probe "Y" $P_4 - P_A$
Probe "Y" $P_5 - P_A$
Probe "Z" $P_1 - P_A$
Probe "Z" $P_{23} - P_A$
Probe "Z" $P_4 - P_A$
Probe "Z" $P_5 - P_A$

Scanner #1

T_{t_0} - "J" - IPR
ΔT out 1
ΔT out 2
ΔT Brg. Front
ΔT Brg. Rear
RPM - F/V
P_{Baro} "Hg Abs
ΔP
Torque--in-lbs
Probe "X"--Pos
Probe "X"--Yaw
Probe "Y"--Pos
Probe "Y"--Yaw
Probe "Z"--Pos
Probe "Z"--Yaw

Table 2. Measurement Uncertainty

Scanivalve pressures		±.02 inches H_2O
Ambient pressure		±.01 inches Hg
Ambient temperature		±2°F
Temperature rise		±2°F
Rotor speed		±1 RPM
Torque		±2 inch lb
Probe radial position	better than	±.01 inches
Probe yaw angles		±.25°[1]

---

[1] If carefully balanced

Table 3. Performance Parameters (IGVs 0°)

I	Cflow	POWER	Cwork	Cpt3	Etaav	Etats	T	T3-T	Prise
1	.9888	50.697	.6376	.5566	.8730	.1042	65.81	-.13	1.013
2	.9899	50.745	.6386	.5312	.8318	.0670	66.73	-.78	1.012
3	.9866	51.085	.6417	.5527	.8612	.1026	64.07	-.07	1.013
4	.9510	52.679	.6880	.5965	.8671	.2214	65.15	1.26	1.014
5	.9567	53.343	.6926	.5844	.8438	.1914	65.24	2.15	1.013
6	.9560	53.016	.6899	.5954	.8630	.2160	65.97	.96	1.014
7	.9221	53.460	.7218	.6310	.8742	.2881	66.42	1.52	1.014
8	.9283	54.056	.7239	.6330	.8743	.2909	65.66	1.56	1.015
9	.9249	54.367	.7317	.6332	.8654	.3034	66.34	.95	1.015
10	.8907	54.800	.7664	.6700	.8742	.3861	66.72	1.83	1.015
11	.8915	56.019	.7815	.6793	.8692	.3793	65.90	1.86	1.016
12	.9922	55.750	.7765	.6786	.8739	.3829	65.50	2.25	1.016
13	.8554	55.206	.8063	.7241	.8980	.4607	68.26	.74	1.017
14	.8536	56.066	.8171	.7219	.8835	.4519	66.06	2.05	1.017
15	.8537	55.196	.8055	.7178	.8911	.4574	66.83	.91	1.017
16	.8362	55.739	.8311	.7458	.8974	.4918	67.17	2.12	1.017
17	.8338	55.270	.8271	.7427	.8980	.4946	67.57	.96	1.017
18	.8357	54.900	.8166	.7420	.9087	.4989	66.52	2.14	1.017
19	.8880	54.800	.7685	.6838	.8899	.3987	66.52	2.14	1.016
20	.8830	55.032	.7745	.6767	.8737	.3850	65.50	2:71	1.016
21	.8881	54.879	.7696	.6781	.8810	.3886	66.63	1.49	1.016
22	.8011	56.541	.8775	.7666	.8736	.5156	65.68	1.78	1.018
23	.8016	56.055	.8681	.7630	.8789	.5176	64.93	2.22	1.018
24	.8036	56.146	.8692	.7715	.8876	.5236	66.08	2.00	1.018
25	.8037	55.802	.8677	.7692	.8865	.5320	68.40	1.02	1.018
26	.8033	56.731	.8767	.7669	.8748	.5175	64.92	1.71	1.018
27	.8040	56.494	.8738	.7682	.8791	.5226	65.87	1.18	1.018
28	.7985	55.834	.8725	.7893	.9047	.5586	67.60	1.02	1.018
29	.7963	56.868	.8913	.7894	.8857	.5482	67.74	.79	1.018
30	.7975	56.673	.8832	.7793	.8824	.5320	65.50	1.99	1.018
31	.7787	55.650	.8901	.7858	.8828	.5538	66.65	1.44	1.018
32	.7740	56.557	.9074	.7863	.8665	.5400	65.07	1.74	1.018
33	.7788	56.525	.9029	.7898	.8748	.5456	66.05	2.27	1.018
34	.7715	56.055	.9061	.7987	.8815	.5658	67.28	2.80	1.018
35	.7709	56.520	.9156	.8121	.8870	.5670	68.04	2.08	1.019
36	.7730	56.736	.9147	.8021	.8770	.5609	66.94	1.80	1.019
37	.7555	56.130	.9284	.8019	.8637	.5558	68.35	1.08	1.018
38	.7592	56.304	.9269	.8074	.8710	.5606	68.52	1.45	1.019
39	.7571	56.330	.9262	.8071	.8715	.5584	66.35	2.55	1.019
40	.7546	56.172	.9250	.8147	.8807	.5779	65.38	2.21	1.019

Table 3 (Continued)

41	.7530	55.744	.9219	.8187	.8880	.5835	66.55	1.41	1.019
42	.7526	55.876	.9266	.8137	.8782	.5752	67.73	2.78	1.019
43	.7342	56.140	.9498	.8273	.8711	.5837	65.23	1.76	1.019
44	.7345	56.071	.9473	.8243	.8701	.5815	64.68	3.37	1.019
45	.7361	55.850	.9441	.8261	.8751	.5855	66.13	2.62	1.019
46	.7290	56.151	.9593	.8297	.8649	.5817	66.61	2.15	1.019
47	.7341	56.108	.9539	.8303	.8705	.5848	67.68	1.46	1.019
48	.7326	55.201	.9381	.8294	.8841	.5977	66.42	2.75	1.019
49	.7314	55.586	.9416	.8319	.8835	.5986	63.85	2.63	1.019
50	.7333	56.383	.9526	.8336	.8751	.5909	63.89	3.23	1.019
51	.7348	55.882	.9478	.8339	.8798	.5977	66.99	2.00	1.019
52	.7279	56.035	.9543	.8365	.8765	.5982	64.16	3.15	1.019
53	.7292	55.855	.9514	.8373	.8801	.6030	65.20	2.46	1.019
54	.7265	55.834	.9557	.8385	.8774	.5975	65.81	1.87	1.019
55	.7080	55.581	.9708	.8372	.8624	.6004	62.88	2.05	1.020
56	.7102	55.243	.9644	.8397	.8707	.6045	64.27	2.09	1.020
57	.7119	55.802	.9730	.8425	.8659	.5992	64.86	1.24	1.020
58	.6891	54.483	.9833	.8503	.8647	.6133	65.86	1.40	1.020
59	.6990	55.117	.9770	.8477	.8676	.6130	63.94	2.00	1.020
60	.7011	54.151	.9591	.8521	.8884	.6258	65.06	2.13	1.020
61	.6912	55.180	.9893	.8530	.8622	.6203	63.97	1.58	1.020
62	.6941	54.958	.9820	.8560	.8717	.6211	64.43	2.51	1.020
63	.6669	54.182	1.0064	.8492	.8438	.6213	63.80	2.60	1.020
64	.6757	53.734	.9870	.8530	.8643	.6364	64.81	2.13	1.020

Table 4. Mid-span Velocity Vectors (IGVs 0°)

Sta.1 Velocities

Point	V1	Alfa1	Phi1	Va1	W1	Beta1
1	227.90	17.24	-3.26	217.31	256.74	32.03
4	216.94	17.27	-4.36	206.56	249.72	33.95
7	216.60	17.46	-3.42	206.25	248.88	33.88
10	208.54	17.46	-3.52	198.56	243.93	35.36
13	201.49	17.46	-3.63	191.82	239.74	36.71
16	196.73	17.47	-3.28	187.35	236.93	37.62
19	207.53	17.46	-3.23	197.65	243.28	35.54
22	190.79	17.46	-3.14	181.73	233.60	38.82
25	190.31	17.47	-3.20	181.25	233.31	38.92
28	189.08	17.47	-3.12	180.09	232.62	39.17
31	185.75	17.47	-3.43	176.86	230.84	39.87
34	183.70	17.47	-2.69	175.04	229.68	40.28
37	181.42	17.47	-3.15	172.79	228.50	40.77
40	179.47	17.47	-2.72	171.00	227.44	41.18
43	176.32	17.47	-3.11	167.94	225.86	41.87
46	175.83	17.46	-2.92	167.52	225.62	41.98
49	174.77	17.48	-2.69	166.51	225.01	42.20
52	174.68	17.46	-2.72	166.44	225.03	42.23
55	171.12	17.46	-3.09	163.00	223.27	43.02
58	168.81	17.47	-2.95	160.81	222.11	43.53
61	167.27	17.47	-2.38	159.42	221.32	43.87
64	162.70	17.47	-2.66	155.03	219.19	44.93

Sta.2 Velocities

Point	V2	Alfa2	Phi2	Va2	W2	Beta2
1	260.92	32.85	.84	219.18	227.78	15.78
4	253.73	33.60	1.20	211.30	220.55	16.62
7	250.83	35.33	.84	204.61	212.81	15.93
10	242.87	35.34	.33	198.12	207.90	17.64
13	236.62	36.08	.40	191.23	201.70	18.54
16	233.23	36.31	.34	186.72	197.29	18.84
19	242.79	35.08	.13	198.69	208.71	17.83
22	226.98	37.83	.15	179.29	190.46	19.72
25	226.91	37.83	.05	179.23	190.42	19.74
28	226.54	37.83	.11	178.93	190.20	19.83
31	222.62	38.32	-.46	174.64	186.50	20.54
34	222.06	38.57	-.37	173.61	185.39	20.53
37	219.67	38.95	-.26	170.84	182.91	20.94
40	218.90	39.32	-.31	169.34	181.30	20.92
43	215.68	39.57	-.75	166.24	178.91	21.67
46	215.69	39.62	-.54	166.15	178.76	21.64
49	215.45	39.82	-.47	165.47	177.97	21.59
52	215.56	39.83	-.30	165.54	178.00	21.56
55	212.01	40.32	-.73	161.63	174.71	22.30
58	209.44	40.81	-.45	158.52	171.95	22.79
61	209.33	40.80	-.40	158.46	171.92	22.82
64	206.08	41.36	-.70	154.67	168.69	23.51

Table 4 (Continued)

Sta.3 Velocities

Point	V3	Alfa3	Phi3	Va3
1	228.24	18.37	-4.43	215.97
4	222.18	18.64	-3.62	210.11
7	217.40	18.64	-3.52	205.61
10	210.05	18.53	-2.68	198.94
13	204.34	20.15	-1.02	191.81
16	201.12	20.16	.42	188.79
19	208.72	20.15	-1.85	195.84
22	196.56	20.15	1.63	184.45
25	195.75	20.15	1.05	183.74
28	194.52	20.15	2.05	182.50
31	191.38	20.15	1.96	179.56
34	187.98	20.15	1.99	176.37
37	188.54	20.16	2.28	176.85
40	187.19	20.15	2.77	175.53
43	183.77	20.15	2.26	172.39
46	181.67	20.15	2.36	170.40
49	183.21	20.15	2.99	171.76
52	182.74	20.15	2.30	171.41
55	172.88	20.15	2.72	162.11
58	166.45	20.16	2.04	156.15
61	164.71	20.16	3.11	151.47
64	147.91	22.10	4.08	136.69

Table 5. Mid-span Pressure Variations with Throttling (IGVs 0°)

Point	P1	P2	P3	Pt1	Pt2	Pt3
1	-11.13	-9.94	-5.52	-.39	5.53	5.27
2	-11.00	-9.98	-5.52	-.22	5.54	5.05
3	-11.08	-9.87	-5.49	-.45	5.48	5.43
4	-11.18	-9.66	-5.22	-1.40	4.91	4.93
5	-11.24	-9.64	-5.21	-1.36	5.00	4.80
6	-11.28	-9.73	-5.23	-1.46	5.10	4.90
7	-11.25	-9.42	-5.02	-1.69	4.71	4.62
8	-11.28	-9.42	-4.99	-1.76	4.78	4.60
9	-11.20	-9.37	-4.95	-1.66	4.57	4.66
10	-11.25	-8.92	-4.61	-2.48	4.29	4.33
11	-11.29	-8.98	-4.59	-2.47	4.39	4.31
12	-11.25	-8.95	-4.59	-2.45	4.28	4.34
13	-11.24	-8.48	-4.24	-3.15	3.99	4.19
14	-11.26	-8.49	-4.23	-3.21	4.06	4.13
15	-11.20	-8.45	-4.17	-3.14	3.94	4.16
16	-11.25	-8.25	-4.00	-3.55	3.83	4.16
17	-11.20	-8.22	-3.97	-3.50	3.84	4.13
18	-11.22	-8.21	-3.98	-3.47	3.84	4.17
19	-11.23	-8.89	-4.53	-2.55	4.30	4.28
20	-11.25	-8.92	-4.57	-2.55	4.29	4.27
21	-11.29	-8.91	-4.54	-2.59	4.35	4.32
22	-11.15	-7.81	-3.69	-3.91	3.62	4.13
23	-11.21	-7.82	-3.72	-3.99	3.66	4.05
24	-11.18	-7.81	-3.68	-3.89	3.67	4.16
25	-11.13	-7.76	-3.63	-3.98	3.61	4.08
26	-11.20	-7.84	-3.71	-3.97	3.63	4.08
27	-11.22	-7.85	-3.68	-3.99	3.61	4.14
28	-11.23	-7.75	-3.64	-4.16	3.59	3.99
29	-11.14	-7.70	-3.54	-4.00	3.59	4.09
30	-11.24	-7.76	-3.62	-4.25	3.55	4.01
31	-11.08	-7.40	-3.38	-4.26	3.52	4.01
32	-11.09	-7.41	-3.36	-4.27	3.53	4.10
33	-11.09	-7.43	-3.32	-4.29	3.56	4.16
34	-11.15	-7.38	-3.39	-4.48	3.44	3.69
35	-11.11	-7.31	-3.27	-4.54	3.48	4.01
36	-11.16	-7.39	-3.33	-4.43	3.48	3.99
37	-10.99	-7.15	-3.17	-4.52	3.43	3.98
38	-10.98	-7.13	-3.18	-4.54	3.47	3.96
39	-11.03	-7.17	-3.17	-4.46	3.47	4.03
40	-11.13	-7.17	-3.21	-4.76	3.37	3.86

Table 5 (Continued)

Point	P1	P2	P3	Pt1	Pt2	Pt3
41	-11.11	-7.15	-3.18	-4.68	3.39	3.85
42	-11.12	-7.09	-3.11	-4.78	3.34	3.92
43	-11.00	-6.89	-3.05	-4.86	3.32	3.76
44	-10.97	-6.88	-3.07	-4.86	3.34	3.72
45	-10.98	-6.89	-3.08	-4.83	3.34	3.74
46	-10.98	-6.84	-3.13	-4.89	3.33	3.50
47	-10.96	-6.86	-3.07	-4.86	3.30	3.62
48	-10.95	-6.84	-3.02	-4.81	3.34	3.76
49	-11.08	-6.92	-3.11	-5.02	3.28	3.66
50	-11.08	-6.89	-3.14	-5.00	3.33	3.50
51	-11.07	-6.91	-3.09	-4.99	3.31	3.66
52	-11.05	-6.88	-3.09	-5.01	3.32	3.64
53	-11.06	-6.86	-3.09	-5.03	3.34	3.61
54	-11.07	-6.89	-3.07	-5.05	3.28	3.62
55	-10.95	-6.68	-3.07	-5.15	3.19	2.96
56	-10.96	-6.68	-3.07	-5.16	3.18	3.09
57	-10.95	-6.65	-3.03	-5.18	3.20	3.12
58	-10.90	-6.51	-3.03	-5.29	3.07	2.53
59	-10.39	-6.51	-3.08	-5.29	3.07	2.18
60	-10.89	-6.51	-3.04	-5.33	3.05	2.45
61	-10.98	-6.56	-3.06	-5.44	3.04	2.41
62	-10.94	-6.52	-3.11	-5.42	3.01	2.12
63	-10.86	-6.31	-3.05	-5.60	2.95	1.32
64	-10.33	-6.30	-3.02	-5.59	2.95	1.40

Table 6. Velocity Vectors at 17 Inches Radius (IGVs 0°)

Sta.1 Velocities

Point	V1	Alfa1	Phi1	Va1	W1	Beta1
1	211.42	22.96	-.31	194.67	250.58	39.02
2	215.94	22.96	-.17	198.84	252.73	38.12
3	206.81	22.95	1.21	190.40	248.51	39.98
4	207.00	22.96	1.36	190.55	248.56	39.93
5	202.65	22.61	1.07	187.04	247.71	40.96
6	199.82	22.62	.89	184.43	246.42	41.54
7	192.19	22.61	1.06	177.38	243.23	43.16
8	194.58	22.61	1.29	179.58	244.23	42.65
9	183.69	22.62	.17	169.56	239.81	45.00
10	183.96	22.61	-.68	169.81	239.96	44.95
11	180.63	22.61	-.21	166.75	238.70	45.69
12	179.57	22.61	-.85	165.75	238.33	45.93
13	149.68	22.09	-.67	138.68	230.37	52.98
14	149.21	22.09	-.91	138.24	230.28	53.10
15	171.00	22.05	-.42	158.49	236.88	48.00
16	169.27	22.05	-.42	156.88	236.29	48.40
17	164.09	22.04	-.62	152.09	234.65	49.59
18	166.34	22.04	-1.05	154.16	235.39	49.08
19	156.84	22.04	.09	145.38	232.46	51.29
20	156.98	22.04	-.07	145.51	232.50	51.26

Sta.2 Velocities

Point	V2	Alfa2	Phi2	Va2	W2	Beta2
1	228.12	34.79	-2.43	187.18	217.35	30.46
2	226.60	34.79	-.59	186.09	216.67	30.81
3	218.43	36.54	-2.83	175.29	207.31	32.16
4	218.85	36.53	-2.89	175.63	207.49	32.05
5	217.64	37.67	-2.21	172.15	202.98	31.92
6	218.78	37.66	-2.06	173.10	203.41	31.62
7	213.47	38.77	-2.27	166.31	197.69	32.65
8	212.29	38.77	-1.90	165.42	197.29	32.97
9	207.63	41.00	-1.32	156.66	188.10	33.58
10	209.49	41.00	-1.23	158.07	188.51	33.04
11	206.40	42.00	-.75	153.38	184.29	33.66
12	205.60	42.00	-1.03	152.77	184.09	33.91
13	188.08	47.71	1.58	126.50	162.00	38.63
14	188.06	47.71	1.71	126.48	162.00	38.64
15	201.22	43.24	-.63	146.59	178.82	34.93
16	200.50	43.23	-.41	146.08	178.69	35.16
17	197.94	44.74	-.19	140.59	173.06	35.67
18	197.66	44.25	.04	141.59	174.70	35.86
19	192.66	46.22	.43	133.29	167.31	37.19
20	192.93	46.23	-.19	133.47	167.34	37.13

Table 6 (Continued)

Sta.3 Velocities

Point	V3	Alfa3	Phi3	Va3
1	187.06	26.16	.55	167.89
2	187.37	26.16	-.01	168.18
3	179.88	26.14	.61	161.47
4	178.19	26.15	1.40	159.90
5	180.69	26.15	1.24	162.16
6	176.95	26.08	1.49	158.87
7	173.43	26.15	2.51	155.53
8	174.01	26.14	3.18	155.97
9	168.04	26.16	2.65	150.66
10	168.75	26.15	2.00	151.38
11	165.66	26.16	4.04	148.32
12	163.89	26.14	2.30	147.01
13	138.95	38.40	2.34	108.81
14	139.49	38.41	2.50	109.20
15	154.65	27.37	-.11	137.34
16	155.57	27.36	1.44	138.12
17	150.22	29.02	1.96	131.28
18	149.02	29.02	1.64	130.25
19	141.84	34.23	3.44	117.06
20	142.32	34.23	3.38	117.46

Table 7. Pressure Variations at 17 Inches Radius (IGVs 0°)

Point	P1	P2	P3	Pt1	Pt2	Pt3
1	-10.40	-8.60	-4.77	-1.19	2.94	2.29
2	-9.97	-8.53	-4.67	-.29	2.89	2.40
3	-10.43	-8.21	-4.56	-1.63	2.25	1.95
4	-10.58	-8.18	-4.54	-2.23	2.32	1.86
5	-10.57	-8.08	-4.39	-2.16	2.32	2.19
6	-10.56	-7.98	-4.32	-2.40	2.55	1.98
7	-10.57	-7.49	-3.86	-3.07	2.48	2.21
8	-10.52	-7.49	-3.87	-2.82	2.38	2.25
9	-10.67	-6.86	-3.33	-3.87	2.57	2.37
10	-10.70	-5.86	-3.32	-3.89	2.76	2.42
11	-10.64	-6.45	-3.00	-4.08	2.88	2.56
12	-10.63	-6.44	-3.01	-4.16	2.81	2.42
13	-9.83	-5.07	-2.08	-5.33	2.64	1.85
14	-9.83	-5.10	-2.12	-5.36	2.61	1.84
15	-10.47	-5.68	-2.54	-4.62	3.17	2.28
16	-10.50	-5.70	-2.53	-4.76	3.09	2.37
17	-10.47	-5.42	-2.39	-5.08	3.13	2.18
18	-10.46	-5.39	-2.39	-4.93	3.14	2.11
19	-10.28	-5.14	-2.30	-5.35	2.95	1.80
20	-10.30	-5.14	-2.32	-5.36	2.96	1.81

Table 8. Performance Parameters (IGVs 4°)

I	Cflow	POWER	Cwork	Cpt3	Etaav	Etats	T	T3-T	Prise
1	.9405	43.608	.5701	.3948	.6926	.0718	63.73	.10	1.009
2	.9389	43.598	.5725	.3859	.6740	.0694	65.10	.39	1.009
3	.9396	43.929	.5743	.3813	.6638	.0562	63.30	1.35	1.009
4	.9011	45.686	.6255	.4617	.7382	.2133	65.52	-.34	1.011
5	.9053	45.783	.6229	.4611	.7404	.2228	64.60	.50	1.011
6	.9018	45.509	.6236	.4629	.7422	.2328	66.39	-.55	1.011
7	.8777	47.003	.6576	.5133	.7807	.3046	63.05	.77	1.012
8	.8778	46.922	.6596	.5203	.7889	.3124	65.59	.57	1.012
9	.8789	46.818	.6566	.5235	.7973	.3063	65.04	.47	1.012
10	.8421	48.369	.7105	.5880	.8276	.3887	66.86	-.01	1.013
11	.8409	48.427	.7103	.6044	.8510	.4108	65.32	.79	1.014
12	.8423	48.586	.7120	.5977	.8395	.4013	65.75	1.27	1.014
13	.7696	50.423	.8105	.7061	.8712	.5108	66.94	.91	1.016
14	.7678	50.551	.8119	.7087	.8728	.5079	65.31	2.27	1.016
15	.7699	50.799	.8143	.7079	.8693	.5093	65.67	1.83	1.016
16	.7443	50.752	.8446	.7417	.8782	.5319	67.64	.75	1.017
17	.7420	50.860	.8466	.7434	.8781	.5290	66.09	1.29	1.017
18	.7436	50.828	.8396	.7343	.8746	.5333	63.14	.63	1.017
19	.7277	51.336	.8695	.7516	.8644	.5406	65.00	1.37	1.017
20	.7295	51.489	.8713	.7543	.8658	.5438	65.78	.51	1.017
21	.7281	50.948	.8635	.7483	.8666	.5487	65.68	1.00	1.017
22	.7064	50.829	.8889	.7749	.8717	.5833	66.18	1.36	1.018
23	.7069	51.384	.8960	.7730	.8626	.5762	65.06	2.33	1.018
24	.7076	51.071	.8883	.7682	.8648	.5793	64.24	2.39	1.018
25	.6877	50.713	.9098	.7880	.8661	.5949	65.54	1.95	1.019
26	.6884	50.550	.9010	.7856	.8720	.5986	62.66	2.60	1.018
27	.6895	50.141	.9002	.7915	.8793	.6025	57.26	1.29	1.018
28	.6735	49.967	.9166	.8048	.8730	.6088	66.28	1.88	1.019
29	.6720	50.163	.9146	.7972	.8717	.6034	61.89	3.02	1.019
30	.6756	50.427	.9206	.8025	.8717	.6037	65.36	1.34	1.019

Table 9. Mid-span Velocity Vectors (IGVs 4°)

Sta.1 Velocities

Point	V1	Alfa1	Phi1	Va1	W1	Beta1
1	224.43	20.81	-3.16	209.46	243.48	30.50
4	219.94	20.80	-3.05	205.31	240.73	31.34
7	210.86	20.83	-2.94	196.82	235.17	33.07
10	203.55	20.82	-2.97	190.00	230.98	34.54
13	188.44	-1147.45	-3.27	72.15	384.64	79.17
16	182.80	20.82	-2.98	170.64	219.86	39.00
19	179.58	20.83	-3.13	167.59	218.23	39.73
22	174.71	20.81	-3.17	163.06	215.95	40.87
25	170.83	20.83	-3.22	159.42	214.09	41.77
28	167.07	20.83	-3.43	155.87	212.40	42.68

Sta.2 Velocities

Point	V2	Alfa2	Phi2	Va2	W2	Beta2
1	243.93	33.31	-.26	203.85	215.27	18.75
4	236.37	34.44	-.49	194.93	206.95	19.62
7	233.13	35.27	-1.75	190.24	202.29	19.80
10	227.69	36.28	-1.16	183.51	195.89	20.45
13	219.03	38.38	-.87	171.68	184.37	21.36
16	216.12	39.26	-1.00	167.31	180.02	21.64
19	213.83	39.98	-.66	163.83	176.54	21.86
22	212.17	41.01	-1.12	160.07	172.40	21.77
25	209.48	41.49	-.82	156.90	169.60	22.30
28	207.63	42.09	-.42	154.07	166.82	22.54

Sta.3 Velocities

Point	V3	Alfa3	Phi3	Va3
1	217.56	18.72	-3.08	205.75
4	210.45	18.71	-2.22	199.18
7	206.52	18.46	-.75	195.88
10	200.62	18.47	1.41	190.23
13	188.81	18.48	3.37	178.76
16	183.06	18.47	4.53	173.09
19	176.81	18.59	4.93	166.96
22	155.82	19.82	4.32	146.17
25	145.63	24.05	1.25	132.95
28	144.31	26.93	-1.73	128.60

Table 10. Mid-span Pressure Variations with Throttling (IGVs 4°)

Point	P1	P2	P3	Pt1	Pt2	Pt3
1	-10.65	-9.50	-5.17	-.21	3.93	4.57
2	-10.59	-9.46	-5.15	-.11	4.00	4.57
3	-10.69	-9.51	-5.17	-.34	3.92	4.77
4	-10.64	-8.94	-4.72	-1.11	3.56	4.32
5	-10.70	-8.95	-4.79	-1.09	3.59	4.23
6	-10.64	-8.95	-4.70	-1.02	3.43	4.26
7	-10.73	-8.65	-4.50	-1.65	3.48	4.21
8	-10.64	-8.65	-4.52	-1.52	3.50	4.11
9	-10.73	-8.64	-4.50	-1.65	3.45	4.08
10	-10.64	-8.18	-4.05	-2.31	3.29	4.12
11	-10.77	-8.18	-4.11	-2.44	3.26	4.14
12	-10.69	-8.18	-4.11	-2.32	3.27	4.15
13	-10.58	-7.26	-3.40	-3.55	3.27	3.79
14	-10.68	-7.34	-3.45	-3.55	3.27	3.78
15	-10.63	-7.30	-3.45	-3.57	3.27	3.74
16	-10.57	-6.96	-3.26	-3.98	3.26	3.49
17	-10.56	-6.98	-3.25	-3.94	3.28	3.52
18	-10.60	-7.00	-3.32	-3.98	3.28	3.45
19	-10.56	-6.82	-3.17	-4.17	3.21	3.15
20	-10.53	-6.82	-3.16	-4.15	3.26	3.05
21	-10.53	-6.81	-3.18	-4.17	3.18	3.15
22	-10.55	-6.59	-3.14	-4.53	3.24	1.75
23	-10.57	-6.59	-3.12	-4.53	3.23	1.99
24	-10.58	-6.57	-3.16	-4.57	3.23	1.79
25	-10.57	-6.35	-3.22	-4.81	3.22	1.05
26	-10.52	-6.36	-3.22	-4.85	3.21	1.03
27	-10.48	-6.36	-3.19	-4.78	3.21	1.02
28	-10.41	-6.16	-3.12	-4.92	3.23	1.04
29	-10.51	-6.23	-3.16	-5.05	3.23	1.04
30	-10.50	-6.23	-3.14	-4.97	3.20	1.06

Table 11. Survey Results, Velocity Vectors (IGVs 0°, S2+4)

Sta.1 Velocities

Radius	V1	Alfa1	Phi1	Va1	W1	Beta1
17.49	156.41	27.15	4.46	138.76	224.26	51.64
16.99	169.07	25.92	.15	152.07	224.89	47.45
16.49	172.62	25.91	-1.58	155.21	220.97	45.36
16.00	185.99	25.10	-1.20	168.39	223.44	41.08
15.51	176.80	24.11	-3.05	161.15	218.10	42.27
15.01	177.81	22.81	-2.82	163.71	217.46	41.09
14.51	178.34	20.78	-3.72	166.38	218.79	40.35
13.99	179.36	19.75	-3.01	168.57	217.36	39.05
13.48	179.93	18.56	-2.45	170.42	216.25	37.93
12.97	180.03	16.76	-2.36	172.24	216.56	37.25
12.46	179.50	15.64	-1.67	172.79	214.72	36.38
11.97	179.56	14.13	-.84	174.11	214.32	35.66
11.47	179.56	12.92	-.25	175.01	213.15	34.81
11.19	181.03	12.92	.33	176.45	211.88	33.62

Sta.2 Velocities

Radius	V2	Alfa2	Phi2	Va2	W2	Beta2
17.49	188.04	48.23	2.78	125.12	164.46	40.39
16.99	199.84	45.98	.98	138.85	168.76	34.63
16.49	208.16	44.99	-.87	147.20	170.21	30.13
16.00	212.46	43.74	-1.50	153.44	172.56	27.18
15.51	214.06	42.76	-1.76	157.09	173.47	25.04
15.01	214.26	41.50	-1.57	160.42	174.98	23.49
14.51	213.94	40.11	-.96	163.61	176.75	22.21
13.99	213.93	38.52	-.47	167.37	179.24	20.96
13.48	214.10	38.03	-.63	168.64	178.40	19.03
12.97	212.45	37.03	.26	169.61	178.29	17.95
12.46	211.92	35.79	1.65	171.84	179.54	16.77
11.97	212.37	34.55	3.69	174.56	181.51	15.48
11.47	213.54	32.33	2.44	180.28	186.63	14.79
11.19	210.05	34.05	3.09	173.79	178.64	13.02

Sta.3 Velocities

Radius	V3	Alfa3	Phi3	Va3
17.49	146.14	40.26	5.91	110.93
16.99	149.38	31.24	3.31	127.51
16.49	158.90	25.22	.16	143.75
16.00	163.69	23.24	.51	150.41
15.51	163.44	23.63	.60	149.73
15.01	160.84	22.54	3.85	148.22
14.51	174.58	20.11	5.55	163.17
13.99	173.09	18.63	3.43	163.72
13.48	177.23	16.58	4.07	169.44
12.97	180.06	14.85	2.97	173.91
12.46	179.66	13.27	1.93	174.76
11.97	177.31	11.72	1.30	173.57
11.47	166.07	10.15	-.36	163.46
11.19	159.32	12.11	-5.01	155.18

Table 12. Performance Parameters (IGVs 3°)

I	Cflow	POWER	Cwork	Cpt3	Etaav	Etats	T	T3-T	Prise
1	.9520	45.132	.5842	.3923	.6715	.0551	64.01	.36	1.009
2	.9518	44.889	.5844	.3969	.6791	.0623	66.99	-.75	1.009
3	.9109	47.409	.6427	.4788	.7451	.2035	65.13	.91	1.011
4	.9116	47.184	.6408	.4717	.7362	.1948	66.41	.15	1.011
5	.8872	48.568	.6773	.5443	.8036	.3115	66.12	.85	1.012
6	.8872	48.310	.6721	.5290	.7870	.2968	64.90	-.70	1.012
7	.8460	49.880	.7295	.6100	.8361	.3970	66.17	1.17	1.014
8	.8496	49.836	.7247	.6044	.8340	.3897	65.41	1.10	1.014
9	.7733	51.773	.8261	.7106	.8602	.5049	64.72	2.45	1.016
10	.7754	51.110	.8165	.7117	.8717	.5120	66.73	2.37	1.016
11	.7197	51.743	.8913	.7583	.8508	.5168	67.19	1.30	1.017
12	.7528	52.306	.8551	.7515	.8789	.5362	63.34	2.65	1.017
13	.7230	51.892	.8870	.7708	.8691	.5450	65.55	3.16	1.018
14	.7316	51.859	.8787	.7740	.8809	.5534	67.14	2.21	1.018
15	.7045	51.614	.9020	.7827	.8677	.5757	63.57	1.91	1.018
16	.7145	51.586	.8930	.7870	.8813	.5863	65.96	.97	1.018
17	.7048	52.307	.9144	.7821	.8553	.5636	63.92	1.77	1.018
18	.7119	52.406	.9039	.7795	.8623	.5707	62.13	2.50	1.018
19	.6874	51.733	.9259	.7931	.8565	.5924	63.21	2.45	1.018
20	.6898	51.750	.9207	.7886	.8565	.5926	61.94	1.87	1.018
21	.6785	51.030	.9291	.8041	.8655	.6066	64.34	1.65	1.019
22	.6810	50.907	.9239	.8044	.8706	.6092	65.60	1.68	1.019

Table 13. Mid-span Velocity Vectors (IGVs 3°)

Sta.1 Velocities

Point	V1	Alfa1	Phi1	Va1	W1	Beta1
1	226.28	20.08	-3.07	212.22	246.84	30.57
3	218.47	20.24	-2.98	204.70	241.50	31.92
5	212.22	20.07	-3.00	199.06	238.23	33.20
7	204.54	20.07	-2.81	191.89	233.69	34.70
9	189.10	20.08	-2.62	177.42	225.10	37.91
11	182.83	20.09	-2.83	171.50	221.82	39.28
13	179.35	20.07	-2.43	168.31	220.11	40.06
15	174.79	20.07	-2.91	163.97	217.91	41.11
17	175.69	20.08	-2.87	164.80	218.31	40.90
19	170.52	20.09	-2.89	159.94	215.83	42.10
21	168.23	20.06	-3.09	157.79	214.89	42.66

Sta.2 Velocities

Point	V2	Alfa2	Phi2	Va2	W2	Beta2
1	246.50	33.29	-.71	206.04	216.92	18.21
3	239.52	34.28	-1.82	197.82	209.35	19.02
5	234.48	35.02	-.82	192.01	203.89	19.64
7	230.02	36.01	-.84	186.05	198.06	20.04
9	219.60	38.37	-.89	172.15	184.67	21.20
11	216.25	39.12	-1.02	167.74	180.52	21.66
13	214.24	39.50	-1.04	165.23	178.30	22.01
15	211.37	40.24	-.88	161.33	174.53	22.42
17	211.95	40.23	-1.17	161.78	174.83	22.25
19	209.09	41.23	-.99	157.22	170.26	22.55
21	207.42	41.61	-.67	155.07	168.30	22.86

Sta.3 Velocities

Point	V3	Alfa3	Phi3	Va3
1	221.95	18.25	-3.11	210.47
3	209.73	20.30	-2.71	196.49
5	205.16	20.30	-2.47	192.23
7	197.44	20.30	-1.82	185.08
9	186.13	20.67	-.82	174.13
11	182.82	21.34	-1.23	170.25
13	181.27	22.12	.82	167.91
15	179.51	22.13	2.47	166.13
17	179.60	23.23	1.98	164.95
19	177.87	24.31	2.75	161.91
21	176.90	24.96	3.19	160.13

Table 14. Mid-span Pressure Variations with Throtting (IGVs 3°)

Point	P1	P2	P3	Pt1	Pt2	Pt3
1	-10.85	-9.63	-5.34	-.23	4.08	4.83
2	-10.91	-9.57	-5.27	-.65	4.17	4.74
3	-10.76	-9.08	-4.92	-.97	3.73	4.02
4	-10.85	-9.11	-4.98	-1.35	3.79	4.09
5	-10.73	-8.73	-4.70	-1.58	3.51	3.81
6	-10.80	-8.81	-4.74	-1.66	3.50	3.72
7	-10.78	-8.32	-4.27	-2.35	3.40	3.57
8	-10.82	-8.35	-4.32	-2.37	3.34	3.50
9	-10.73	-7.35	-3.43	-3.60	3.26	3.51
10	-10.69	-7.35	-3.43	-3.60	3.24	3.53
11	-10.65	-6.98	-3.17	-4.05	3.24	3.50
12	-10.65	-7.01	-3.19	-4.01	3.32	3.54
13	-10.64	-6.78	-3.05	-4.26	3.23	3.53
14	-10.65	-6.79	-3.07	-4.24	3.21	3.50
15	-10.69	-6.63	-3.03	-4.63	3.17	3.48
16	-10.65	-6.58	-2.99	-4.60	3.17	3.47
17	-10.74	-6.67	-3.03	-4.62	3.17	3.48
18	-10.75	-6.68	-3.03	-4.59	3.20	3.49
19	-10.63	-6.41	-2.95	-4.86	3.15	3.44
20	-10.69	-6.43	-2.96	-4.91	3.16	3.43
21	-10.61	-6.25	-2.92	-5.02	3.14	3.39
22	-10.60	-6.25	-2.92	-5.05	3.13	3.38

Table 15. Survey Results, Velocity Vectors (IGVs 3°, S2+4)

Sta.1 Velocities

Radius	V1	Alfa1	Phi1	Va1	W1	Beta1
17.49	158.27	26.43	4.20	141.35	226.53	51.27
16.99	169.05	24.96	-.19	153.26	227.61	47.67
16.49	173.24	24.97	-1.47	156.99	223.86	45.45
16.00	175.90	24.22	-2.25	160.30	222.13	43.77
15.51	177.37	23.02	-2.96	163.02	221.41	42.50
15.01	178.64	21.67	-3.54	165.70	221.11	41.34
14.51	179.38	20.74	-3.03	167.52	219.31	40.10
14.00	180.73	19.16	-2.78	170.51	219.66	39.00
13.48	180.68	17.67	-2.34	172.02	219.00	38.18
12.97	180.72	16.24	-1.97	173.41	218.26	37.35
12.46	180.16	15.00	-1.36	173.97	216.67	36.57
11.97	180.31	13.49	-.91	175.32	216.33	35.85
11.47	180.87	11.57	-.14	177.19	217.14	35.31

Sta.2 Velocities

Radius	V2	Alfa2	Phi2	Va2	W2	Beta2
17.49	187.36	48.22	2.65	124.69	164.45	40.62
16.99	199.56	44.72	.72	141.79	173.05	34.98
16.49	207.64	44.92	-.97	147.02	170.34	30.32
16.00	212.01	43.22	-1.90	154.41	174.24	27.54
15.51	213.66	42.23	-1.99	158.11	175.16	25.42
15.01	213.34	40.76	-2.09	161.48	177.10	24.16
14.51	214.23	39.48	-1.29	165.30	178.93	22.47
14.00	214.60	38.26	-.59	168.50	180.42	20.94
13.48	214.62	37.77	-.56	169.65	179.50	19.06
12.97	213.31	36.52	.68	171.41	180.31	18.07
12.46	212.08	35.78	2.23	171.92	179.66	16.73
11.97	213.26	34.78	3.37	174.76	181.40	15.08
11.47	213.64	32.30	2.22	180.45	186.77	14.78

Sta.3 Velocities

Radius	V3	Alfa3	Phi3	Va3
17.49	137.45	31.76	1.72	116.82
16.99	160.80	29.16	2.85	140.25
16.49	175.82	28.42	.61	154.63
16.00	180.71	28.14	.48	159.34
15.51	184.01	26.94	1.35	163.99
15.01	184.77	25.85	1.22	149.20
14.51	181.03	22.17	.90	167.63
14.00	180.86	20.13	.47	169.80
13.48	178.37	18.16	-.05	169.48
12.97	175.37	16.60	.21	168.06
12.46	172.81	14.39	-.23	167.39
11.97	170.33	12.38	-.23	166.37
11.47	162.37	8.91	-1.33	160.37

Table 16. Survey Results, Velocity Vectors (IGVs 3°, S1+4)

Sta.1 Velocities

Radius	V1	Alfa1	Phi1	Va1	W1	Beta1
17.74	150.11	29.79	6.94	129.32	219.69	53.63
17.48	160.27	25.42	3.62	144.47	229.51	50.90
16.99	174.36	24.92	-.21	158.12	229.36	46.42
16.50	187.69	24.91	-.73	170.21	229.31	42.07
16.00	179.37	24.10	-2.20	163.61	223.77	42.97
15.31	181.55	22.82	-2.94	167.12	221.88	41.04
14.40	183.19	20.01	-3.02	171.90	222.22	39.23
13.47	183.89	17.67	-2.21	175.08	220.75	37.47
12.71	183.59	15.59	-1.67	176.76	219.42	36.30
11.96	183.50	13.01	-.83	178.77	219.50	35.46
11.46	184.15	12.26	-.36	179.95	217.71	34.25
11.18	185.23	11.60	.23	181.45	217.73	33.56

Sta.2 Velocities

Radius	V2	Alfa2	Phi2	Va2	W2	Beta2
17.74	186.30	53.33	4.24	110.96	150.29	42.24
17.48	190.52	47.12	3.74	129.37	168.21	39.58
16.99	202.43	44.14	.71	145.27	175.60	34.18
16.50	208.64	44.64	-.93	148.45	171.63	30.11
16.00	211.30	43.38	-.91	153.92	173.57	27.52
15.31	213.29	41.78	-1.58	158.99	175.35	24.90
14.40	214.37	39.42	-.37	165.98	178.84	21.86
13.47	215.54	37.93	.10	170.01	179.47	18.69
12.71	212.78	36.20	2.31	171.57	179.86	17.32
11.96	213.31	34.71	4.04	175.32	181.93	14.97
11.46	215.58	31.49	3.16	183.55	190.27	14.95
11.13	211.45	32.88	3.47	177.25	182.68	13.57

Sta.3 Velocities

Radius	V3	Alfa3	Phi3	Va3
17.74	145.58	19.97	6.12	136.05
17.48	146.36	31.78	1.33	124.78
16.99	167.54	29.33	1.48	146.01
16.50	178.93	29.32	1.05	155.98
16.00	181.84	27.36	.45	161.50
15.31	186.26	25.78	.91	167.70
14.40	132.53	19.98	-.27	171.54
13.47	179.53	18.93	-.59	169.81
12.71	175.76	15.15	-.70	169.64
11.96	173.32	13.08	-.91	168.80
11.46	165.16	9.26	-1.12	162.98
11.18	141.64	9.26	-9.25	137.97

Table 17. Survey Results, Velocity Vectors (IGVs 3°, S1+2+4)

Sta.1 Velocities

Radius	V1	Alfa1	Phi1	Va1	W1	Beta1
17.74	141.78	30.15	6.47	121.82	217.91	55.76
17.49	153.22	25.36	4.44	138.04	228.35	52.68
16.99	165.78	24.59	3.14	150.52	227.88	48.59
16.49	181.85	24.59	-.43	165.35	227.92	43.49
16.01	171.80	24.47	-2.07	156.27	219.93	44.68
15.31	174.19	22.55	-2.91	160.67	219.49	42.87
14.40	176.21	20.19	-2.38	165.24	218.24	40.73
13.47	176.37	17.41	-2.32	168.15	217.20	39.21
12.71	175.87	15.10	-1.55	169.74	215.95	38.16
11.96	175.72	13.58	-.29	170.80	213.07	36.71
11.47	176.29	11.95	.03	172.47	213.14	35.98
11.18	177.42	11.65	.41	173.76	212.18	35.02

Sta.2 Velocities

Radius	V2	Alfa2	Phi2	Va2	W2	Beta2
17.74	180.58	55.54	2.47	102.08	143.97	44.79
17.49	185.28	49.00	2.58	121.43	161.90	41.34
16.99	194.00	46.04	.67	134.65	167.73	36.59
16.49	202.55	45.68	.26	141.51	166.44	31.76
16.01	208.17	44.55	-.90	148.32	168.39	28.25
15.31	210.44	43.08	-1.90	153.62	169.24	25.17
14.40	209.71	40.60	-.72	159.21	172.60	22.71
13.47	209.73	38.72	.52	163.62	173.87	19.76
12.71	207.88	37.43	1.40	165.03	173.33	17.76
11.96	208.05	35.69	3.52	168.65	175.47	15.65
11.47	208.20	32.98	2.18	174.52	181.24	15.50
11.18	205.29	34.70	3.24	168.51	173.65	13.59

Sta.3 Velocities

Radius	V3	Alfa3	Phi3	Va3
17.74	127.83	38.31	2.98	100.17
17.49	132.23	32.40	.38	111.65
16.99	154.74	28.95	3.10	135.20
16.49	173.06	29.43	.32	150.73
16.01	177.38	28.22	.72	156.28
15.31	181.59	26.37	1.60	162.63
14.40	178.93	23.35	1.43	164.22
13.47	174.95	19.91	.90	164.47
12.71	172.46	16.64	.28	165.23
11.96	165.68	12.87	-.32	161.50
11.47	157.05	8.61	-1.75	155.21
11.18	131.38	12.11	-9.05	126.86

Table 18. Performance Parameters (IGVs 2°)

I	Cflow	POWER	Cwork	Cpt3	Etaav	Etats	T	T3-T	Prise
1	.9594	47.594	.6156	.4951	.8043	.1031	70.28	.16	1.011
2	.9646	47.754	.6144	.4826	.7855	.0807	70.31	.22	1.011
3	.9621	47.749	.6157	.4741	.7701	.0582	70.08	.21	1.011
4	.9019	51.105	.7015	.5889	.8396	.2797	69.01	.76	1.013
5	.8989	51.185	.7049	.5822	.8259	.2816	68.98	.87	1.013
6	.8562	52.957	.7650	.6493	.8488	.3926	68.46	.66	1.015
7	.8610	52.692	.7589	.6328	.8338	.3900	69.93	.66	1.014
8	.7821	54.681	.8674	.7256	.8365	.4877	70.17	2.77	1.017
9	.7856	54.475	.8591	.7190	.8369	.4842	69.43	.00	1.016
10	.7513	54.742	.9027	.7570	.8386	.5082	69.40	1.76	1.017
11	.7589	54.753	.8947	.7572	.8463	.5154	69.91	1.24	1.017
12	.7416	54.672	.9135	.7783	.8520	.5301	69.51	2.05	1.018
13	.7412	54.554	.9126	.7764	.8508	.5288	69.87	2.00	1.018
14	.7183	54.585	.9410	.7976	.8476	.5568	69.10	2.09	1.018
15	.7184	54.587	.9412	.7968	.8465	.5513	69.34	2.27	1.018
16	.7185	54.552	.9408	.7995	.8499	.5613	69.51	1.61	1.018
17	.7136	54.640	.9459	.7959	.8415	.5559	67.91	2.32	1.018
18	.7190	54.714	.9442	.7991	.8463	.5598	70.24	1.39	1.018
19	.6961	54.390	.9612	.8041	.8365	.5763	65.67	3.10	1.019
20	.6996	54.267	.9586	.8113	.8464	.5841	68.07	2.51	1.019
21	.6836	53.903	.9718	.8167	.8404	.5926	66.65	2.25	1.019
22	.6934	53.896	.9560	.8221	.8599	54.0936	65.61	2.31	.898

Table 19. Mid-span Velocity Vectors (IGVs 2°)

Sta.1 Velocities

Point	V1	Alfa1	Phi1	Va1	W1	Beta1
3	227.26	19.31	-2.94	214.19	249.83	30.86
5	213.72	19.54	-1.25	201.36	240.63	33.17
7	205.37	19.54	-2.20	193.40	235.70	34.80
9	190.04	19.54	-2.56	178.91	227.12	37.95
11	183.25	19.55	-2.58	172.51	223.53	39.42
13	180.79	19.54	-2.78	170.18	222.31	39.97
15	175.51	19.54	-3.20	165.15	219.73	41.17
17	174.19	19.53	-2.89	163.95	219.07	41.47
19	170.28	19.54	-3.13	160.24	217.21	42.37
21	167.78	19.54	-3.24	157.86	826.50	78.97

Sta.2 Velocities

Point	V2	Alfa2	Phi2	Va2	W2	Beta2
3	251.68	32.66	-1.39	211.81	222.31	17.62
5	238.27	-363.52	-2.81	237.54	322.63	42.51
7	230.73	35.63	-2.75	187.32	199.76	20.14
9	220.55	37.84	-2.46	174.01	186.93	21.29
11	217.52	-83.30	-2.26	25.34	420.23	86.54
13	215.67	39.07	-2.19	167.33	180.45	21.88
15	212.35	40.08	-2.39	162.33	175.54	22.24
17	211.48	40.08	-2.62	161.64	175.14	22.50
19	209.07	40.82	-2.62	158.05	171.63	22.80
21	201.41	42.80	-2.58	147.63	744.77	78.56

Sta.3 Velocities

Point	V3	Alfa3	Phi3	Va3
3	221.70	19.34	-1.97	209.06
5	208.05	19.74	-1.74	195.74
7	199.84	298.23	-2.12	62.47
9	186.93	20.63	-1.21	174.90
11	184.06	21.37	-.48	171.40
13	182.81	21.37	-.07	170.24
15	179.95	22.66	1.23	166.03
17	179.60	22.82	.77	165.53
19	178.15	23.94	2.20	162.70
21	176.77	24.63	2.73	160.50

Table 20. Mid-span Pressure Variations with Throttling (IGVs 2°)

Point	P1	P2	P3	Pt1	Pt2	Pt3
1	-10.92	-9.47	-5.58	-.54	4.35	4.43
2	-10.84	-9.57	-5.54	-.34	4.19	4.52
3	-10.78	-9.52	-5.59	-.19	4.63	4.43
4	-10.93	-8.30	-4.91	-1.75	3.62	3.88
5	-10.88	-8.88	-4.89	-1.61	3.66	3.83
6	-10.98	-8.40	-4.52	-2.49	3.39	3.53
7	-10.91	-8.34	-4.44	-2.46	3.33	3.55
8	-10.77	-7.37	-3.59	-3.69	3.16	3.35
9	-10.84	-7.43	-3.62	-3.70	3.18	3.35
10	-10.74	-7.03	-3.31	-4.08	3.25	3.41
11	-10.76	-7.01	-3.31	-4.15	3.25	3.43
12	-10.70	-6.78	-3.19	-4.31	3.22	3.42
13	-10.72	-6.78	-3.16	-4.30	3.28	3.49
14	-10.70	-6.54	-3.06	-4.62	3.18	3.40
15	-10.71	-6.53	-3.05	-4.67	3.19	3.40
16	-10.70	-6.48	-3.03	-4.73	3.20	3.40
17	-10.68	-6.48	-3.06	-4.72	3.17	3.38
18	-10.67	-6.52	-3.02	-4.69	3.16	3.40
19	-10.75	-6.31	-2.98	-5.03	3.13	3.39
20	-10.68	-5.66	-2.98	-4.97	3.12	3.35
21	-10.67	-5.64	-2.95	-5.14	3.08	3.32
22	-10.65	-5.61	-2.95	-5.09	3.08	3.34

Table 21. Survey Results, Velocity Vectors (IGVs 2°, S2+4)

Sta.1 Velocities

Radius	V1	Alfa1	Phi1	Va1	W1	Beta1
17.75	146.98	30.33	6.25	126.11	217.91	54.40
17.50	157.16	24.47	3.00	142.85	231.49	51.83
17.00	171.90	24.48	.15	156.45	229.97	47.13
16.50	181.87	24.46	-.39	165.55	228.45	43.56
16.01	176.83	22.76	-2.23	162.94	226.74	44.01
15.32	177.99	21.52	-3.19	165.33	224.13	42.37
14.42	179.98	19.29	-2.51	169.71	222.69	40.28
13.49	180.29	16.77	-1.75	172.54	221.16	38.69
12.75	180.79	25.76	-.97	162.79	191.70	31.86
11.98	179.98	12.49	-.04	175.72	218.58	36.49
11.48	180.65	11.13	.65	177.24	218.08	35.63
11.19	181.64	10.72	.22	178.47	217.34	34.80

Sta.2 Velocities

Radius	V2	Alfa2	Phi2	Va2	W2	Beta2
17.75	179.30	55.89	2.36	100.46	143.20	45.40
17.50	184.12	49.21	.11	120.28	161.29	41.77
17.00	195.66	46.22	-1.99	135.28	167.44	36.06
16.50	202.52	45.74	-2.85	141.17	166.39	31.85
16.01	207.37	44.98	-4.10	146.30	166.81	28.45
15.32	208.60	43.75	-3.89	150.34	167.01	25.55
14.42	209.68	41.29	-2.80	157.36	170.44	22.43
13.49	209.87	39.56	-2.00	161.70	171.41	19.28
12.75	207.08	38.08	.04	163.00	171.11	17.71
11.98	208.98	36.35	2.05	168.21	174.25	15.00
11.48	210.15	32.88	.92	176.47	182.86	15.17
11.19	206.13	34.37	1.38	170.09	175.13	13.70

Sta.3 Velocities

Radius	V3	Alfa3	Phi3	Va3
17.75	132.19	36.71	4.42	105.66
17.50	143.54	30.51	.97	123.65
17.00	167.03	29.42	1.32	145.45
16.50	179.01	28.53	.26	157.27
16.01	184.16	27.56	.22	163.26
15.32	187.04	25.76	1.25	168.41
14.42	182.08	20.62	.16	170.41
13.49	178.66	18.14	-.34	169.78
12.75	175.81	15.01	-1.10	169.78
11.98	173.04	12.50	-.91	168.92
11.48	165.41	8.52	-1.03	163.55
11.19	141.96	10.97	-8.02	138.00

Table 22. Survey Results, Velocity Vectors (IGVs 2°, S1+4)

Sta.1 Velocities

Radius	V1	Alfa1	Phi1	Va1	W1	Beta1
17.75	149.93	28.18	5.69	131.51	223.65	53.78
17.50	161.00	24.51	4.29	146.09	232.50	50.94
17.01	171.04	24.42	.11	155.74	229.90	47.36
16.51	185.64	24.40	-.27	169.05	230.12	42.72
16.02	179.34	22.77	-1.94	165.27	227.75	43.44
15.33	181.36	21.67	-2.43	168.39	225.20	41.55
14.42	182.96	19.34	-1.60	172.57	224.08	39.61
13.50	183.29	16.79	-1.67	175.40	222.92	38.08
12.74	183.26	14.47	-.42	177.44	222.26	37.03
12.74	183.18	14.46	-.94	177.35	222.24	37.05
11.99	182.25	12.25	-.11	178.10	220.76	36.22
11.50	182.65	10.98	.55	179.30	219.93	35.38
11.21	184.01	10.85	1.08	180.68	218.86	34.34

Sta.2 Velocities

Radius	V2	Alfa2	Phi2	Va2	W2	Beta2
17.75	181.20	54.93	3.89	103.88	145.95	44.49
17.50	186.66	48.46	.95	123.77	163.70	40.87
17.01	197.09	46.22	-2.33	136.26	167.70	35.59
16.51	204.25	45.72	-2.88	142.43	166.90	31.30
16.02	207.19	44.97	-3.27	146.34	166.81	28.51
15.33	209.24	43.22	-3.89	152.13	169.09	25.61
14.42	211.15	41.37	-2.98	158.24	170.87	21.97
13.50	210.98	39.24	-2.11	163.30	173.05	19.22
12.74	208.29	37.76	.16	164.67	172.71	17.55
12.74	208.88	37.77	.21	165.11	173.02	17.39
11.99	210.13	34.62	2.21	172.80	179.94	16.05
11.50	211.96	32.54	1.56	178.62	185.06	15.08
11.21	208.10	33.79	1.23	172.91	178.06	13.76

Sta.3 Velocities

Radius	V3	Alfa3	Phi3	Va3
17.75	138.55	35.60	3.73	112.42
17.50	150.66	30.21	1.00	130.18
17.01	169.78	29.26	1.21	148.08
16.51	181.57	28.27	.53	159.90
16.02	185.54	27.68	.58	164.29
15.33	188.58	26.48	.65	168.79
14.42	184.03	20.54	-.39	172.33
13.50	180.25	18.53	-1.04	170.83
12.74	178.20	14.86	-1.05	172.21
12.74	178.16	14.85	-1.32	172.16
11.99	175.59	12.43	-.76	171.46
11.50	167.92	11.58	-1.22	164.46
11.21	146.20	11.16	-7.69	142.15

Table 23. Performance Parameters (IGVs 0°)

I	Cflow	POWER	Cwork	Cpt3	Etaav	Etats	T	T3-T	Prise
1	.9900	50.898	.6308	.5964	.9455	.1597	62.63	.74	1.014
2	.9871	51.213	.6345	.6040	.9518	.1856	60.95	1.08	1.014
3	.9898	50.995	.6319	.5813	.9200	.1451	62.44	1.31	1.013
4	.9276	53.852	.7132	.6805	.9542	.3539	63.24	.41	1.016
5	.9264	53.929	.7155	.6707	.9374	.3498	63.57	.52	1.015
6	.9289	53.818	.7137	.6808	.9539	.3574	64.72	.23	1.016
7	.8846	54.367	.7655	.7120	.9301	.4333	65.73	1.21	1.016
8	.8832	55.118	.7678	.7100	.9247	.4298	64.10	1.52	1.016
9	.8831	55.026	.7673	.7036	.9169	.4153	64.56	1.58	1.016
10	.8337	56.152	.8304	.7703	.9276	.5158	65.17	1.65	1.018
11	.8360	56.257	.8288	.7644	.9223	.5176	64.65	2.97	1.018
12	.8355	56.123	.8274	.7641	.9235	.5148	64.66	.75	1.018
13	.8083	56.401	.8588	.7861	.9153	.5435	64.23	1.58	1.018
14	.8073	56.252	.8626	.7880	.9135	.5383	67.32	2.12	1.018
15	.8095	56.321	.8601	.7842	.9118	.5301	66.59	.58	1.018
16	.7810	56.694	.8973	.8147	.9079	.5653	66.47	1.51	1.019
17	.7841	56.721	.8959	.8106	.9047	.5631	67.53	3.00	1.019
18	.7810	56.521	.8932	.8073	.9038	.5618	65.72	.86	1.019
19	.7500	56.656	.9318	.8237	.8840	.5652	65.44	2.49	1.019
20	.7648	56.678	.9138	.8276	.9057	.5781	65.26	.77	1.019
21	.7664	56.368	.9145	.8263	.9036	.5794	64.96	2.16	1.019
22	.7316	56.289	.9504	.8457	.8898	.5886	66.17	2.34	1.020
23	.7442	56.414	.9356	.8485	.9069	.5975	65.73	2.50	1.020
24	.7439	56.348	.9342	.8446	.9041	.5976	65.36	1.32	1.020
25	.7131	55.675	.9637	.8685	.9012	.6178	65.78	2.14	1.020
26	.7140	55.735	.9642	.8547	.8864	.6097	66.18	1.47	1.020
27	.7163	55.734	.9568	.8648	.9019	.6184	64.92	2.00	1.020
28	.7015	55.368	.9740	.8681	.8913	.6253	65.64	2.82	1.020
29	.7056	55.332	.9649	.8657	.8973	.6311	64.10	2.95	1.020
30	.7021	55.306	.9702	.8635	.8900	.6237	64.55	3.16	1.020
31	.6449	52.961	1.0113	.8742	.8645	.6261	64.49	2.41	1.020
32	.6467	52.871	1.0080	.8799	.8729	.6275	65.17	2.23	1.020
33	.6447	52.710	1.0084	.8808	.8734	.6294	65.39	2.20	1.020

Table 24. Mid-span Velocity Vectors (IGVs 0°)

Sta.1 Velocities

Point	V1	Alfa1	Phi1	Va1	W1	Beta1
1	230.53	17.67	-4.25	219.05	257.06	31.30
4	213.17	17.26	-4.66	202.90	247.26	34.58
7	208.60	17.27	-4.52	198.58	244.43	35.42
10	198.53	17.25	-4.63	188.98	238.52	37.35
13	192.95	17.24	-4.76	183.64	235.39	38.48
16	187.06	17.63	-4.56	177.72	231.01	39.49
19	183.44	17.63	-4.40	174.31	229.05	40.25
22	179.03	17.36	-4.34	170.38	227.46	41.30
25	173.58	17.37	-4.08	165.25	224.62	42.48
28	170.51	17.36	-4.12	162.33	223.12	43.16
31	158.22	17.36	-4.70	150.51	217.41	46.01

Sta.2 Velocities

Point	V2	Alfa2	Phi2	Va2	W2	Beta2
1	259.64	34.31	-1.14	214.42	221.86	14.93
4	250.07	35.75	-1.07	202.92	210.82	15.70
7	241.22	36.99	-1.20	192.63	201.22	16.76
10	231.32	38.25	-1.46	181.60	191.29	18.26
13	227.11	38.99	-1.59	176.46	186.54	18.85
16	222.07	50.45	-1.65	141.35	144.96	12.70
19	219.38	49.84	-1.84	141.42	145.87	14.07
22	215.64	51.73	-1.67	133.51	137.78	14.22
25	212.00	51.45	-1.93	132.05	137.30	15.78
28	210.19	51.45	-1.89	130.92	136.60	16.48
31	205.37	51.86	-1.98	126.77	133.50	18.15

Sta.3 Velocities

Point	V3	Alfa3	Phi3	Va3
1	226.92	23.19	-2.28	208.42
4	214.30	20.35	-2.95	200.65
7	204.76	20.35	-3.10	191.70
10	194.50	20.33	-3.40	182.06
13	189.47	20.34	-2.70	177.45
16	185.85	21.29	-1.67	173.09
19	183.05	21.77	-1.61	169.93
22	181.44	22.31	-.11	167.86
25	179.45	23.12	.39	165.04
28	178.30	23.44	.77	163.57
31	174.86	24.36	1.21	159.26

Table 25. Survey Results, Velocity Vectors (IGVs 0°, S1+4)

Sta.1 Velocities

Radius	V1	Alfa1	Phi1	Va1	W1	Beta1
17.90	143.47	35.43	11.85	114.41	209.29	56.04
17.80	150.42	28.15	8.17	131.28	225.57	53.99
17.65	157.55	24.23	6.49	142.75	235.01	52.31
17.49	163.74	22.67	1.98	151.00	238.33	50.66
17.25	172.79	23.01	.45	159.04	237.47	47.95
17.00	176.44	21.86	-1.39	163.70	239.42	46.85
16.75	179.10	22.37	-2.56	165.45	236.48	45.54
16.50	180.65	22.20	-2.92	167.04	235.12	44.65
16.50	180.85	22.20	-2.97	167.22	235.22	44.61
16.01	184.12	21.04	-3.58	171.51	235.19	43.06
15.32	185.01	19.78	-4.78	173.48	232.78	41.59
14.41	186.34	17.07	-4.46	177.59	232.55	40.01
13.49	187.30	14.71	-3.76	180.77	231.05	38.36
12.72	186.82	12.66	-3.11	182.01	229.30	37.35
11.98	186.80	10.72	-2.17	183.40	227.64	36.27
11.48	186.48	9.13	-1.83	183.99	226.88	35.77
11.19	189.57	8.58	-1.11	187.41	228.09	34.73

Sta.2 Velocities

Radius	V2	Alfa2	Phi2	Va2	W2	Beta2
17.90	184.33	57.03	6.56	99.65	141.01	44.66
17.80	184.03	54.42	3.09	106.92	148.00	43.66
17.65	186.23	49.69	.75	120.47	161.48	41.75
17.49	190.47	46.29	1.06	131.60	171.31	39.79
17.25	197.39	44.50	-.43	140.78	175.89	36.83
17.00	204.62	43.96	-.97	147.27	176.92	33.64
16.75	207.83	43.97	-1.61	149.53	175.60	31.58
16.50	211.30	43.76	-2.53	152.47	175.38	29.52
16.50	212.65	43.71	-2.13	153.61	175.93	29.11
16.01	217.82	42.49	-1.32	160.58	178.63	25.95
15.32	220.22	41.00	-1.20	166.16	180.89	23.25
14.41	223.08	39.17	-1.24	172.91	183.91	19.89
13.49	226.00	37.28	-.96	179.81	461.87	67.09
12.72	226.43	35.93	-.90	183.33	189.44	14.57
11.98	226.41	33.79	-.52	188.16	193.29	13.22
11.48	224.36	32.55	-.78	189.11	196.83	16.09
11.19	223.58	33.29	-.44	186.99	193.08	14.55

Table 25 (Continued)

Sta.3 Velocities

Radius	V3	Alfa3	Phi3	Va3
17.90	132.04	37.01	6.61	104.73
17.80	138.80	35.33	4.48	112.89
17.65	150.71	33.39	1.86	125.77
17.49	155.27	31.01	.95	133.06
17.25	162.81	29.85	.90	141.20
17.00	173.51	29.49	1.40	150.98
16.75	182.20	29.02	.08	159.33
16.50	185.68	28.94	.84	162.48
16.50	186.47	28.95	-.18	163.17
16.01	186.73	27.01	1.31	166.33
15.32	188.15	25.39	.75	169.96
14.41	184.83	20.85	.58	172.72
13.49	179.22	16.74	.09	171.63
12.72	179.41	14.95	.42	173.33
11.98	181.12	12.64	-.41	176.72
11.48	169.56	7.88	.24	167.96
11.19	157.18	10.29	-6.86	153.54

Table 26. Survey Results, Velocity Vectors (IGVs 0°, S4)

Sta.1 Velocities

Radius	V1	Alfa1	Phi1	Va1	W1	Beta1
17.89	143.51	34.73	11.62	115.52	210.80	55.98
17.79	156.57	28.84	8.90	135.53	224.72	52.39
17.64	164.88	23.63	6.96	149.94	238.52	50.71
17.49	169.99	22.61	4.62	156.41	240.64	49.30
17.24	179.41	22.50	3.80	165.39	241.37	46.63
16.99	182.29	22.50	-1.43	168.36	239.62	45.35
16.74	185.16	22.21	-2.07	171.31	239.14	44.21
16.49	187.07	21.94	-3.16	173.26	238.42	43.30
16.00	188.56	20.99	-3.56	175.71	237.23	42.09
15.31	191.14	19.69	-4.54	179.40	235.92	40.29
14.40	191.90	17.53	-4.35	182.45	234.19	38.62
13.48	193.19	14.93	-3.82	186.25	233.97	37.08
12.71	193.27	12.88	-3.26	188.10	232.85	35.99
11.97	194.49	10.86	-2.06	190.88	232.53	34.77
11.47	193.82	9.52	-1.73	191.07	231.26	34.25
11.19	194.58	8.71	-1.87	192.23	231.44	33.79

Sta.2 Velocities

Radius	V2	Alfa2	Phi2	Va2	W2	Beta2
17.89	189.46	55.13	5.30	107.85	145.99	42.10
17.79	189.19	51.91	3.53	116.49	155.49	41.36
17.64	190.31	47.42	2.32	128.65	168.88	40.32
17.49	194.72	44.21	.60	139.57	178.59	38.60
17.24	201.41	42.85	-.06	147.66	182.21	35.86
16.99	209.26	42.21	-1.07	154.97	184.23	32.72
16.74	213.40	42.05	-1.45	158.41	184.10	30.60
16.49	216.81	41.85	-2.26	161.38	184.19	28.74
16.00	220.89	41.22	-2.35	166.01	184.75	25.93
15.31	224.82	40.24	-1.80	171.52	185.82	22.55
14.40	227.93	38.24	-1.20	178.98	189.61	19.24
13.48	231.80	36.76	-1.33	185.66	192.80	15.59
12.71	233.28	35.02	-.77	191.03	196.47	13.49
11.97	233.84	33.29	-.30	195.46	199.68	11.80
11.47	231.02	32.04	-.32	195.83	199.80	11.43
11.19	228.93	32.78	-.82	192.45	195.48	10.07

Table 26 (Continued)

Sta.3 Velocities

Radius	V3	Alfa3	Phi3	Va3
17.89	131.69	35.49	7.18	106.39
17.79	144.29	33.57	4.65	119.83
17.64	150.35	33.32	2.47	125.52
17.49	157.44	31.68	1.92	133.90
17.24	159.07	30.21	1.62	137.42
16.99	176.33	29.81	.21	153.00
16.74	185.05	28.90	.50	162.00
16.49	189.84	28.81	-.73	166.33
16.00	189.30	26.69	-1.41	169.08
15.31	191.97	23.78	-1.76	175.59
14.40	183.56	20.19	-2.63	172.10
13.48	190.62	17.61	-2.26	181.54
12.71	191.06	14.88	-.67	184.64
11.97	188.12	12.00	-.12	184.01
11.47	177.98	8.07	.75	176.21
11.19	165.37	9.81	-3.34	163.17

Table 27. Survey Results, Velocity Vectors (IGVs 0°, S2+3)

Sta.1 Velocities

Radius	V1	Alfa1	Phi1	Va1	W1	Beta1
17.87	150.32	35.32	9.60	120.93	208.10	53.89
17.77	158.71	28.62	7.11	138.26	224.89	51.72
17.62	168.05	24.10	3.02	153.19	237.03	49.67
17.46	174.09	22.72	1.67	160.51	241.00	48.22
17.22	181.17	23.20	-.20	166.52	239.46	45.94
16.97	187.62	22.55	-1.37	173.23	241.37	44.12
16.72	187.68	22.90	-2.91	172.66	237.98	43.41
16.47	190.12	22.27	-3.11	175.68	238.52	42.47
15.98	194.36	21.55	-3.45	180.44	238.03	40.58
15.29	195.53	20.29	-4.57	182.32	236.19	39.06
14.38	198.81	17.81	-4.27	188.76	237.18	37.05
13.46	199.66	15.48	-4.03	191.94	236.37	35.51
12.69	201.61	13.19	-3.08	196.01	237.44	34.24
11.95	200.08	10.96	-2.70	196.21	236.10	33.70
11.45	198.61	9.58	-1.56	195.77	234.44	33.35
11.16	201.22	8.88	-1.42	198.75	235.80	32.53

Sta.2 Velocities

Radius	V2	Alfa2	Phi2	Va2	W2	Beta2
17.87	187.79	54.44	8.38	108.05	148.74	42.75
17.77	188.23	51.47	4.30	116.93	156.89	41.64
17.62	191.50	47.60	2.68	128.99	168.19	39.85
17.46	196.29	44.33	.23	140.42	178.21	38.01
17.22	201.42	42.74	-.36	147.93	182.43	35.82
16.97	209.76	42.56	-1.44	154.46	183.02	32.41
16.72	212.93	41.99	-1.07	158.23	184.04	30.69
16.47	218.05	41.99	-1.17	162.03	183.94	28.23
15.98	224.97	40.25	-1.20	171.67	189.69	25.15
15.29	228.79	39.25	-1.16	177.14	191.03	21.96
14.38	233.09	37.76	-1.14	184.24	193.98	18.21
13.46	235.25	36.25	-.82	189.70	196.49	15.09
12.69	236.94	34.52	-.70	195.21	200.37	13.02
11.95	237.86	32.97	-.32	199.55	203.41	11.18
11.45	235.93	31.37	-.62	201.43	205.20	10.98
11.16	235.57	32.05	-.57	199.66	202.34	9.33

Table 27 (Continued)

Sta.3 Velocities

Radius	V3	Alfa3	Phi3	Va3
17.87	125.69	33.41	9.26	103.55
17.77	144.16	32.25	7.36	120.92
17.62	158.74	32.81	2.89	133.25
17.46	166.21	31.48	-.59	141.74
17.22	169.89	30.36	-.42	146.58
16.97	177.87	29.95	-.30	154.11
16.72	187.41	29.07	.75	163.78
16.47	191.59	28.77	.22	167.93
15.98	192.64	25.40	.06	174.02
15.29	193.87	24.21	-.82	176.80
14.38	192.33	20.26	-1.26	180.39
13.46	193.81	16.88	.46	185.45
12.69	195.11	14.55	.60	188.84
11.95	194.39	11.67	1.09	190.34
11.45	188.24	8.31	.28	186.26
11.16	178.15	8.66	-2.85	175.90

Table 28. Off Design Survey Velocity Vectors (IGVs 0°, S1)

Sta.1 Velocities

Radius	V1	Alfa1	Phi1	Va1	W1	Beta1
17.70	183.81	26.63	6.96	163.10	235.82	45.83
17.45	193.34	22.96	1.34	177.97	247.09	43.91
16.96	206.38	22.93	-1.33	190.03	248.04	39.97
16.46	209.71	22.54	-4.24	193.16	246.65	38.25
15.97	213.02	21.49	-3.57	197.83	247.37	36.75
15.28	216.41	20.01	-4.13	202.82	248.19	34.98
14.37	221.91	17.35	-4.62	211.12	252.46	32.96
13.44	223.80	15.15	-3.79	215.55	253.06	31.39
12.67	224.41	13.13	-3.44	218.15	253.48	30.44
11.93	224.23	10.87	-2.48	220.00	253.98	29.89
11.44	225.87	9.43	-2.19	222.66	255.37	29.24
11.15	226.97	8.83	-2.18	224.11	255.70	28.70

Sta.2 Velocities

Radius	V2	Alfa2	Phi2	Va2	W2	Beta2
17.70	199.90	44.51	5.01	142.01	180.42	37.80
17.45	208.59	38.89	1.50	162.30	199.42	35.50
16.96	224.38	37.38	-.61	178.28	206.16	30.14
16.46	233.48	36.64	-1.31	187.29	209.32	26.49
15.97	242.98	36.40	-.98	195.55	211.91	22.64
15.28	247.52	35.89	-.66	200.51	212.68	19.47
14.37	254.76	34.42	-.80	210.13	218.31	15.71
13.44	262.06	33.16	-.24	219.38	224.29	12.01
12.67	266.60	31.10	-.65	228.26	232.00	10.29
11.93	270.32	29.68	-.01	234.86	237.43	8.44
11.44	272.86	28.69	-.01	239.36	241.32	7.30
11.15	260.75	28.44	-.01	229.28	231.70	8.29

Sta.3 Velocities

Radius	V3	Alfa3	Phi3	Va3
17.70	161.84	29.16	5.00	140.79
17.45	179.14	31.82	1.57	152.15
16.96	190.52	28.40	-1.03	167.57
16.46	202.88	26.14	-.38	182.12
15.97	206.67	23.72	-2.39	189.04
15.28	211.81	22.47	-.73	195.71
14.37	221.50	19.91	.35	208.26
13.44	225.39	17.35	.59	215.60
12.67	230.37	14.75	1.24	222.73
11.93	230.76	10.10	1.41	227.11
11.44	218.77	9.19	.69	215.94
11.15	202.30	6.40	.25	201.04

Table 29. Off Design Survey Velocity Vectors (IGVs 0°, S2+3+4)

Sta.1 Velocities

Radius	V1	Alfa1	Phi1	Va1	W1	Beta1
17.70	138.29	26.94	8.19	122.03	226.13	56.96
17.45	150.31	22.74	4.46	138.21	234.56	53.77
16.96	160.17	22.31	2.43	148.05	232.42	50.39
16.46	164.97	22.43	-3.03	152.27	228.33	48.10
15.97	168.01	21.08	-3.60	156.46	228.06	46.57
15.28	169.36	20.00	-4.52	158.65	224.65	44.89
14.37	170.42	17.72	-4.53	161.83	222.20	43.06
13.44	169.94	15.08	-3.33	163.82	219.71	41.68
12.67	170.86	13.32	-3.18	166.00	217.37	40.10
12.68	169.97	13.22	-3.46	165.16	217.13	40.35
11.93	170.03	10.92	-2.48	166.30	215.67	39.28
11.43	169.63	9.57	-1.75	167.19	214.01	38.59
11.15	170.95	9.57	-1.69	168.50	212.41	37.47

Sta.2 Velocities

Radius	V2	Alfa2	Phi2	Va2	W2	Beta2
17.70	182.34	56.78	1.05	99.88	139.77	44.38
17.45	183.51	48.55	1.19	121.45	163.35	41.96
16.96	195.72	45.83	-.86	136.36	168.71	36.06
16.46	202.46	45.33	-1.19	142.30	167.71	31.93
15.97	207.66	44.34	-1.56	148.46	168.99	28.49
15.28	210.73	42.85	-1.53	154.43	170.73	25.20
14.37	213.58	40.99	-2.29	161.08	173.11	21.36
13.44	214.58	39.62	-2.09	165.17	173.65	17.86
12.67	213.90	37.38	-1.47	169.92	176.99	16.19
12.68	214.02	37.40	-1.52	169.96	177.00	16.15
11.93	211.70	35.64	-1.32	172.01	177.91	14.75
11.43	208.94	34.07	-1.45	173.03	178.74	14.45
11.15	206.60	35.14	.23	168.94	173.31	12.89

Sta.3 Velocities

Radius	V3	Alfa3	Phi3	Va3
17.70	123.32	39.55	2.32	95.01
17.45	126.31	33.72	.79	105.05
16.96	148.87	23.83	3.22	130.21
16.46	170.36	28.85	1.66	149.16
15.97	177.27	27.60	1.45	157.05
15.28	181.36	26.13	1.46	162.77
14.37	178.59	21.62	1.84	165.94
13.44	173.80	18.26	.81	165.02
12.67	173.44	19.19	1.05	163.77
12.68	169.87	16.49	.37	162.38
11.93	161.99	12.42	-.94	158.18
11.43	153.53	8.82	-.64	151.71
11.15	128.16	12.60	-7.36	124.04

Table 30. Velocity Vectors at Station One at Three Survey Locations

Sta.1 Velocities Port 7

Radius	V1	Alfa1	Phi1	Va1	W1	Beta1
17.74	146.73	31.23	7.42	124.42	215.81	54.45
17.49	155.59	25.75	3.84	139.82	227.70	52.02
16.99	169.35	24.69	.43	153.87	228.47	47.66
16.49	185.22	25.38	-.59	167.34	226.90	42.48
16.00	174.40	24.19	-2.43	158.94	221.68	44.14
15.31	176.19	22.66	-2.86	162.38	220.03	42.36
14.40	178.68	20.30	-2.79	167.39	219.21	40.14
13.47	178.84	17.69	-2.36	170.24	217.87	38.55
12.71	178.65	15.36	-1.46	172.21	216.96	37.44
11.96	179.16	13.26	-.51	174.38	216.10	36.20
11.47	179.14	12.11	.05	175.15	214.68	35.33
11.18	180.29	12.12	.38	176.27	213.11	34.20

Sta.1 Velocities Port 8

Radius	V1	Alfa1	Phi1	Va1	W1	Beta1
17.74	140.41	29.95	9.74	119.90	219.49	56.34
17.49	148.84	29.16	5.12	129.46	217.86	53.37
16.99	158.40	28.90	1.61	138.62	214.07	49.62
16.49	181.51	28.37	-.79	159.69	216.63	42.50
16.01	170.01	27.22	-2.80	151.00	211.67	44.42
15.32	171.11	24.57	-4.67	155.10	212.93	43.04
14.40	173.99	21.24	-5.03	161.55	214.65	40.93
13.47	175.57	18.31	-4.26	166.22	214.64	39.05
12.70	176.29	16.12	-3.26	169.08	213.75	37.60
11.97	177.12	13.83	-1.74	171.90	213.49	36.33
11.47	177.90	12.10	-1.77	173.86	213.92	35.60
11.18	178.71	11.93	-1.02	174.33	212.47	34.62

Sta.1 Velocities Port 9

Radius	V1	Alfa1	Phi1	Va1	W1	Beta1
17.74	150.31	31.66	6.12	127.21	214.60	53.40
17.49	162.40	26.61	.25	145.20	226.56	50.14
17.00	173.48	24.59	-.52	157.74	230.12	46.72
16.50	177.68	24.57	-1.67	161.52	226.59	44.51
16.01	181.85	24.58	-1.40	165.32	223.36	42.23
15.32	180.79	23.67	-1.68	165.51	219.10	40.91
14.41	181.13	21.54	-1.35	168.44	217.01	39.07
13.49	181.81	18.82	-1.45	172.04	216.64	37.40
12.72	181.66	17.08	.02	173.65	214.56	35.97
11.97	180.38	14.68	-.01	174.49	213.56	35.21
11.48	180.21	12.90	.70	175.65	213.71	34.72
11.19	181.91	12.17	.28	177.82	214.22	33.89

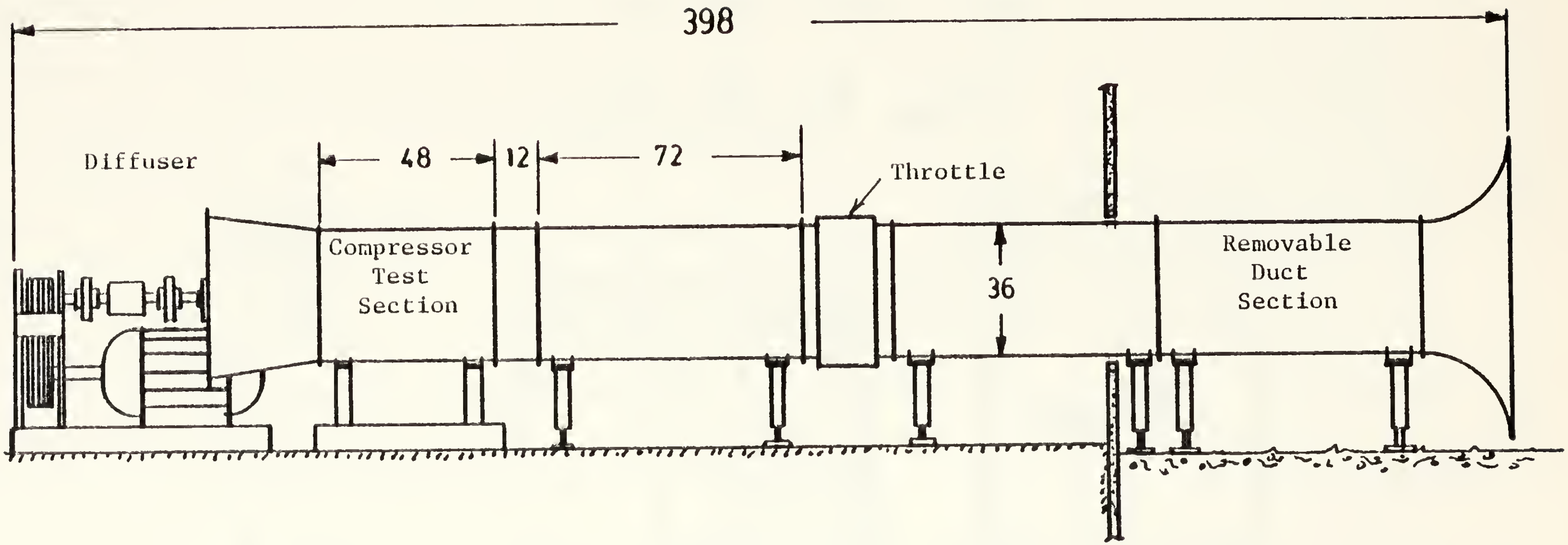

Figure 1. Compressor Schematic

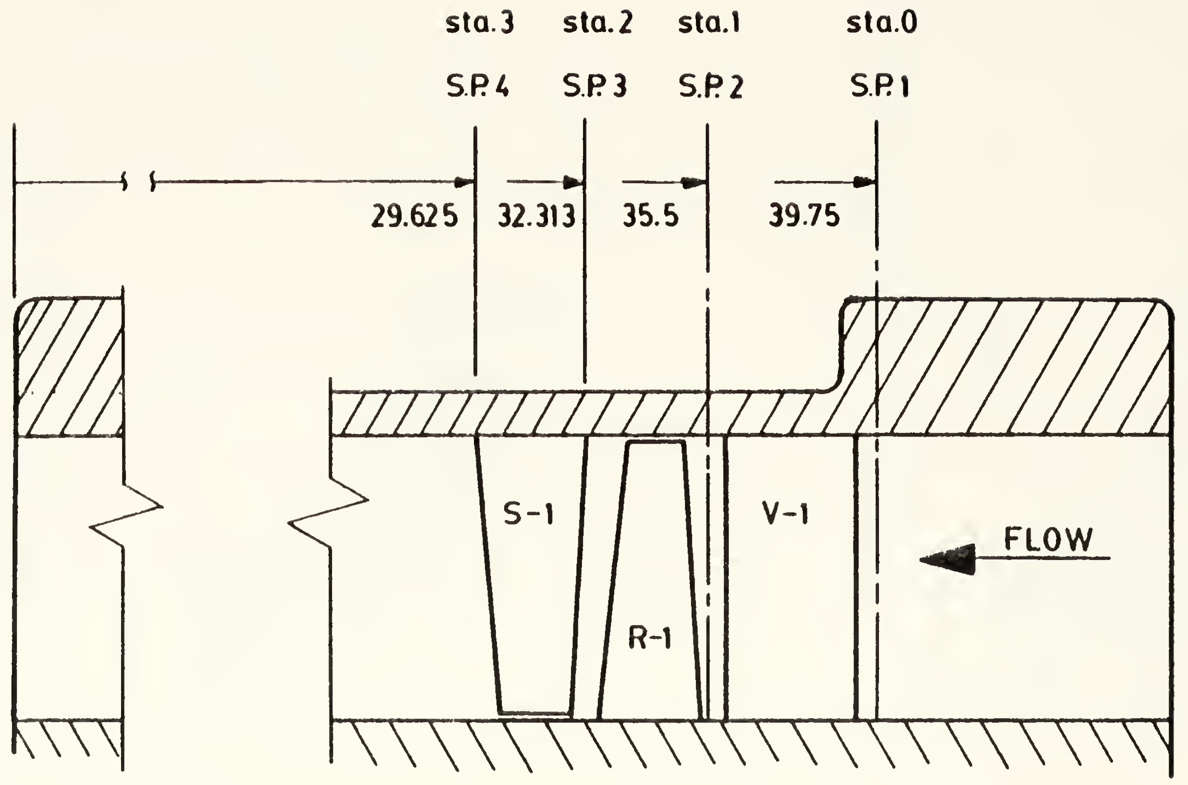

Figure 2. Measurement Planes for Installed Stage

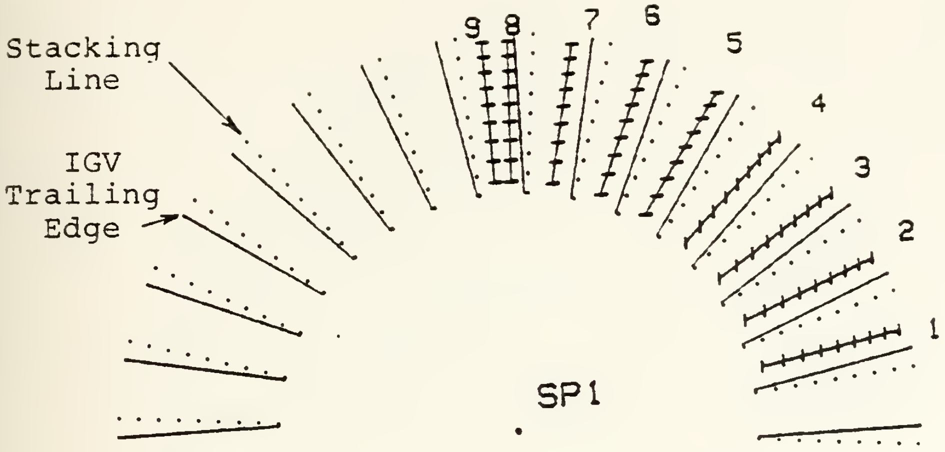

a. Survey Plane 1 IGV Inlet

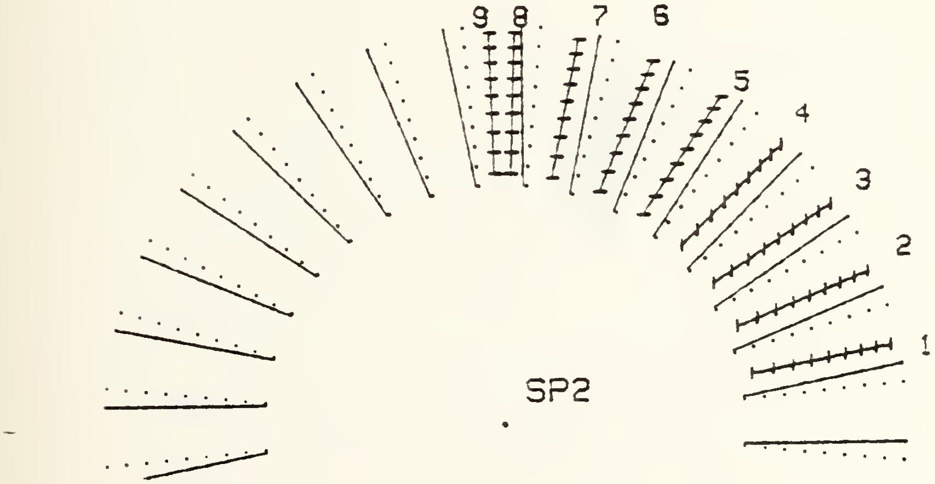

b. Survey Plane 2 IGV Exit

Figure 3. Locations of Survey Ports

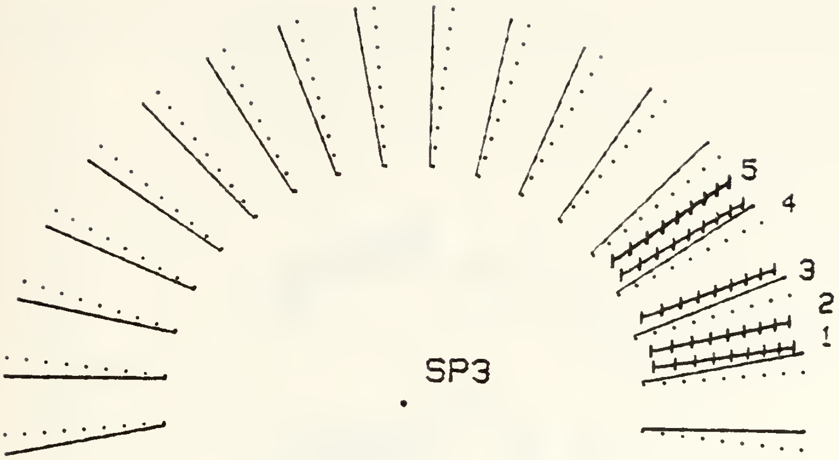

c. Survey Plane 3 Rotor Exit

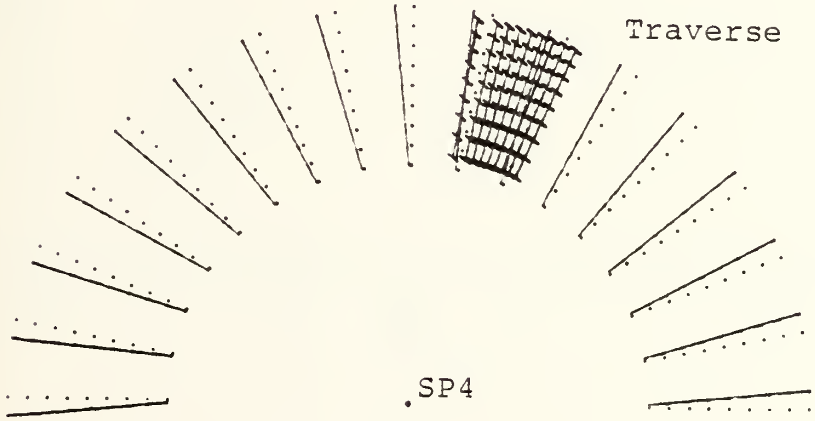

d. Survey Plane 4 Stator Exit

Figure 3 (Continued)

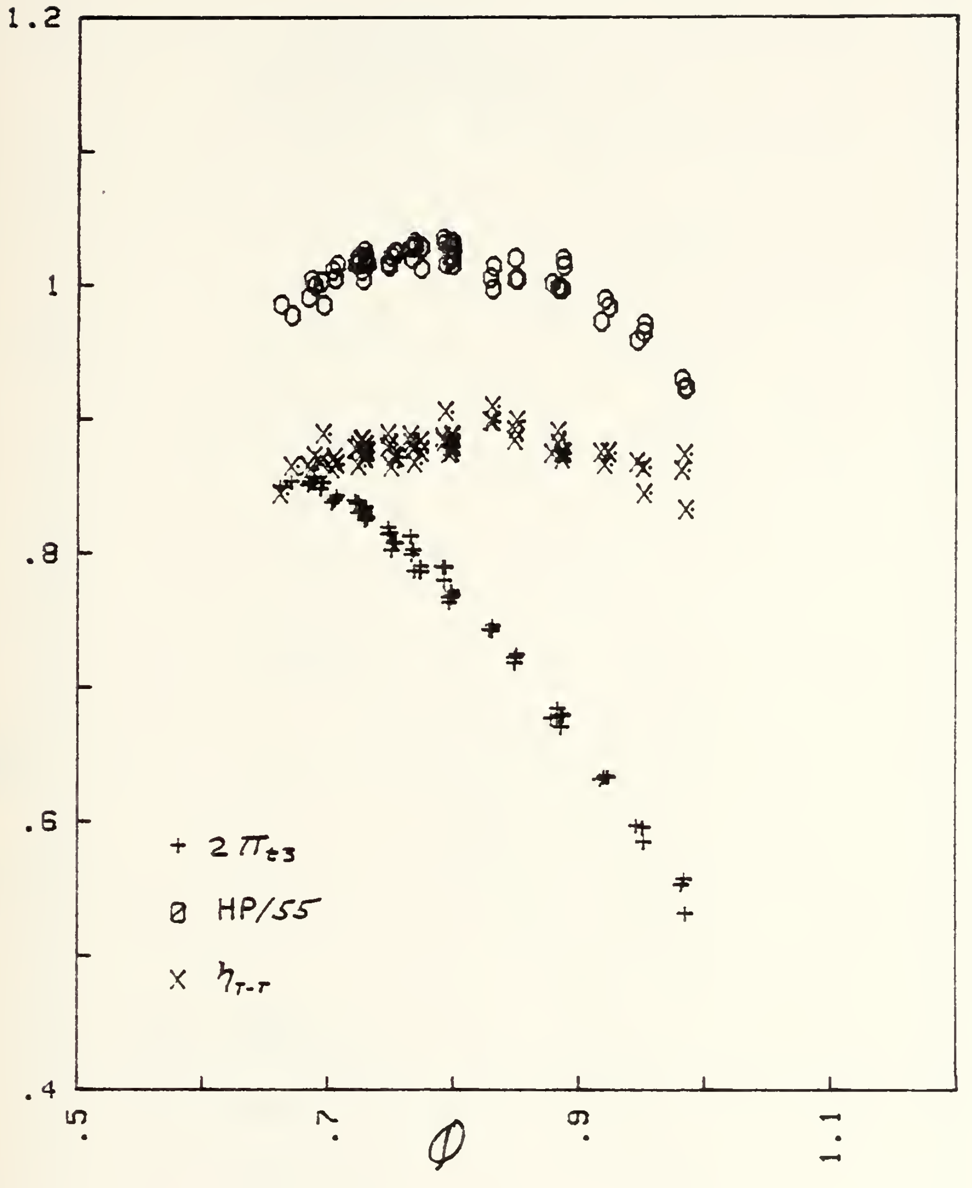

Figure 4. Performance Parameters vs Flow Rate (IGVs 0°)

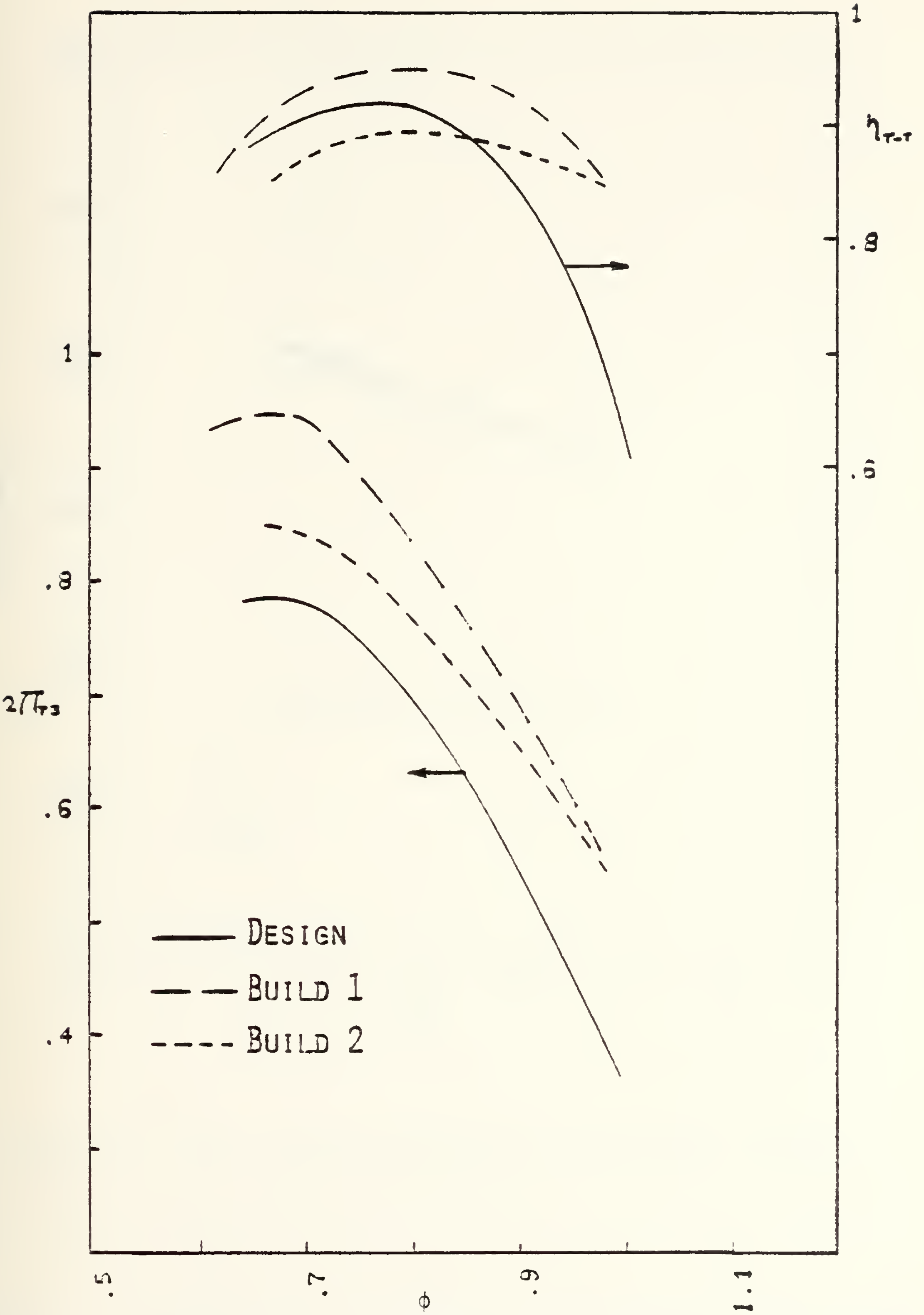

Figure 5. Comparison of Measured Performance with Design Values and Build One Measurements

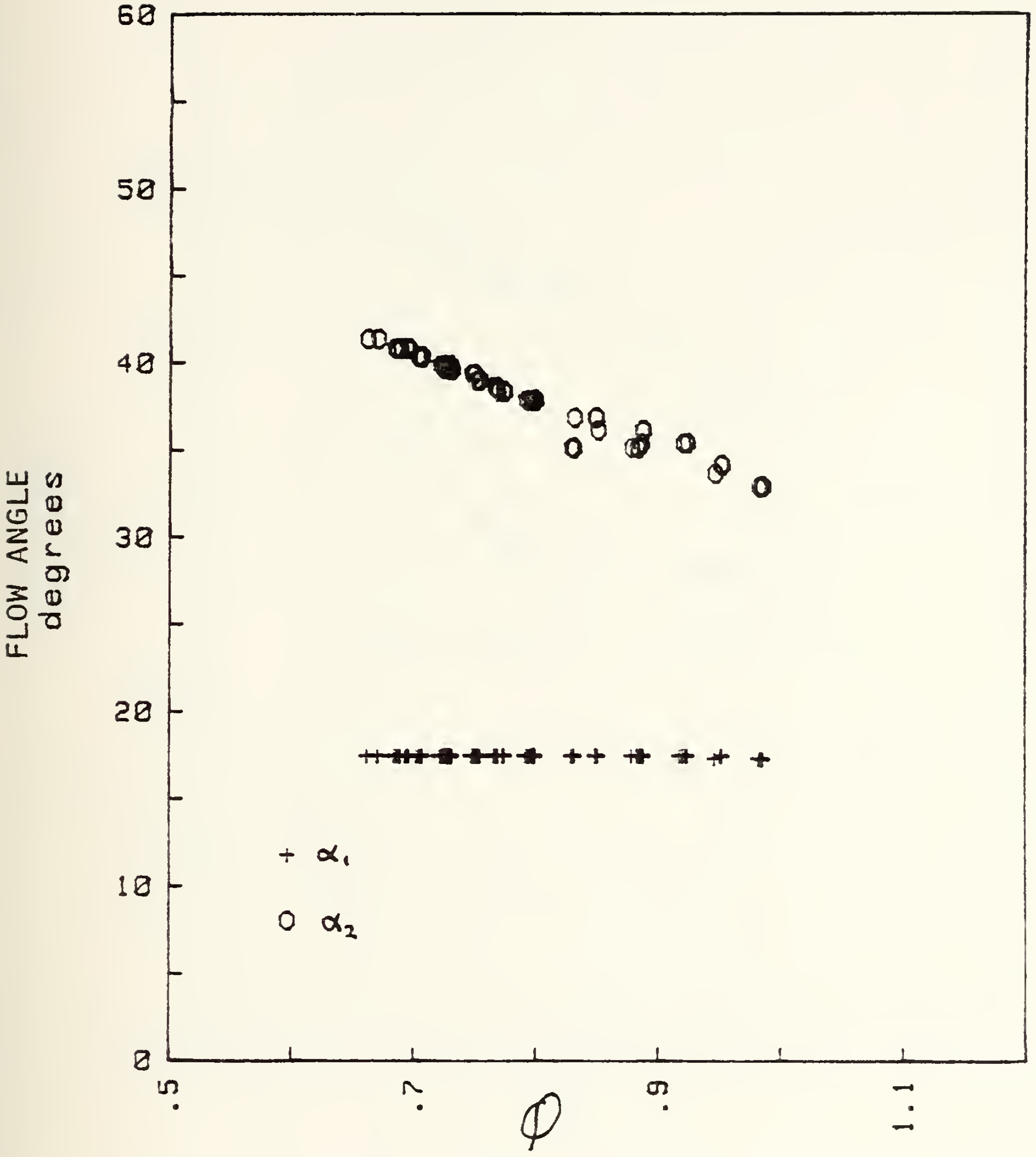

Figure 6. Mid-span Flow Angles vs Flow Rate (IGVs 0°)

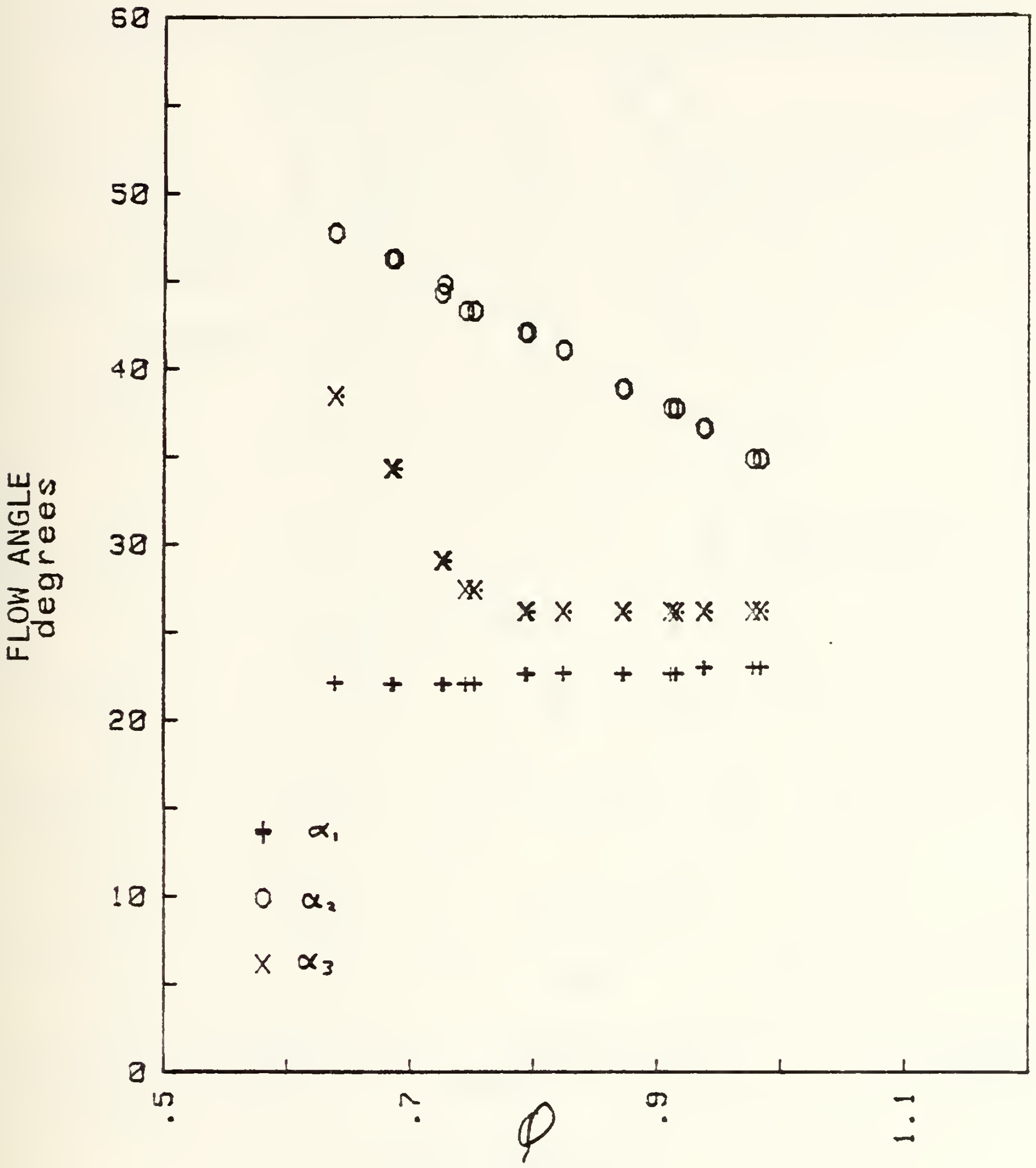

Figure 7. Flow Angles at 17 Inches Radius vs Flow Rate (IGVs 0°)

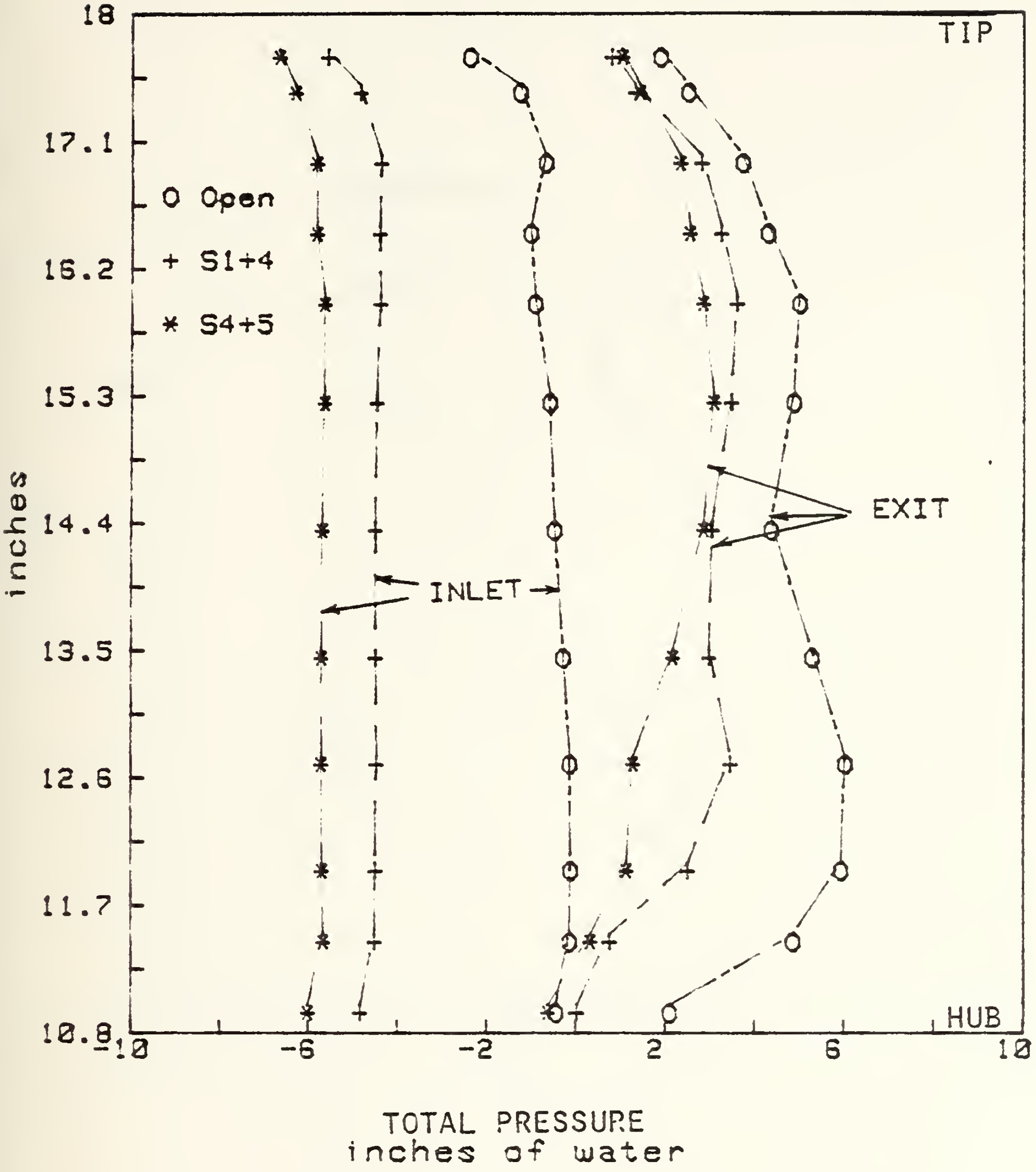

Figure 8. Inlet and Exit Pressure Distributions vs Radius at Three Throttle Settings (IGVs 0°)

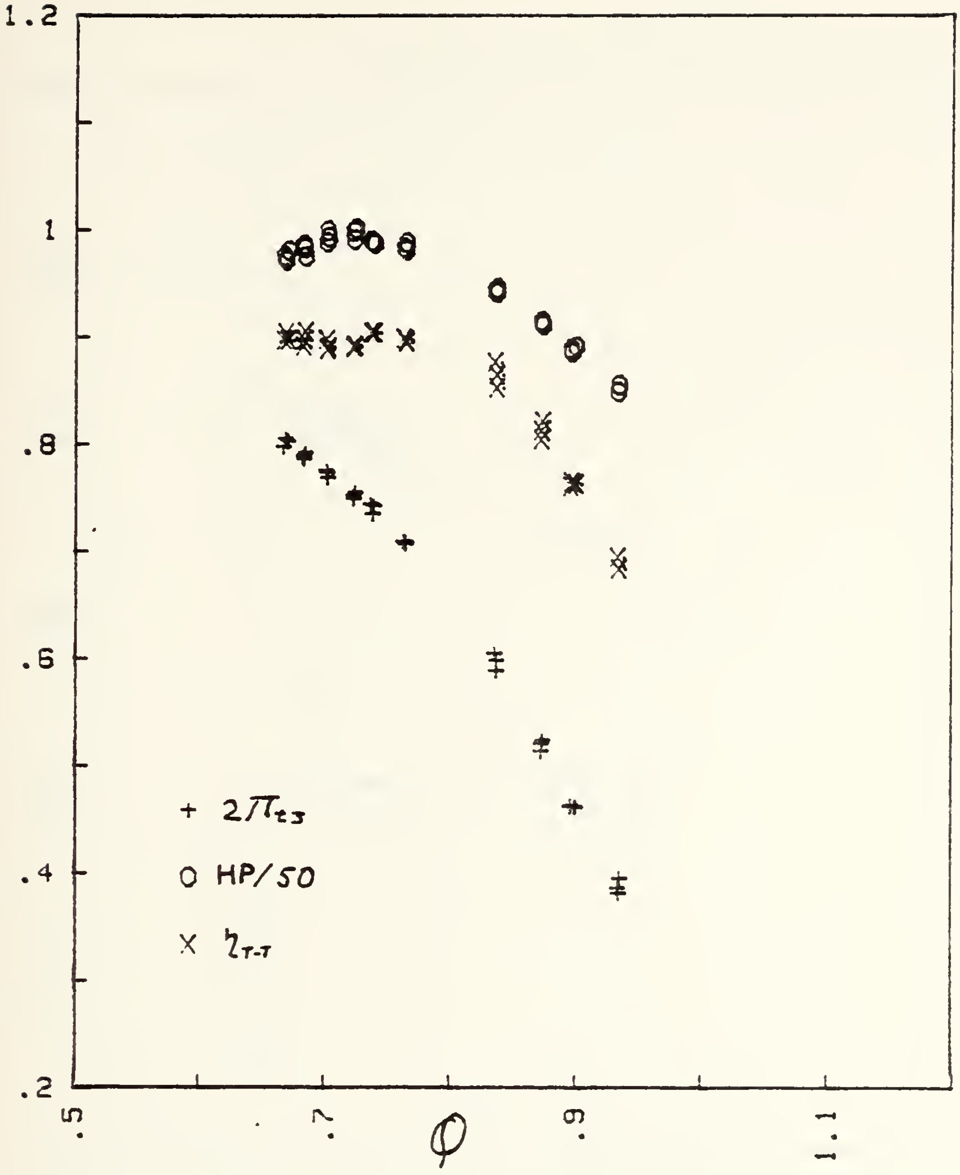

Figure 9. Performance Parameters vs Flow Rate (IGVs 4°)

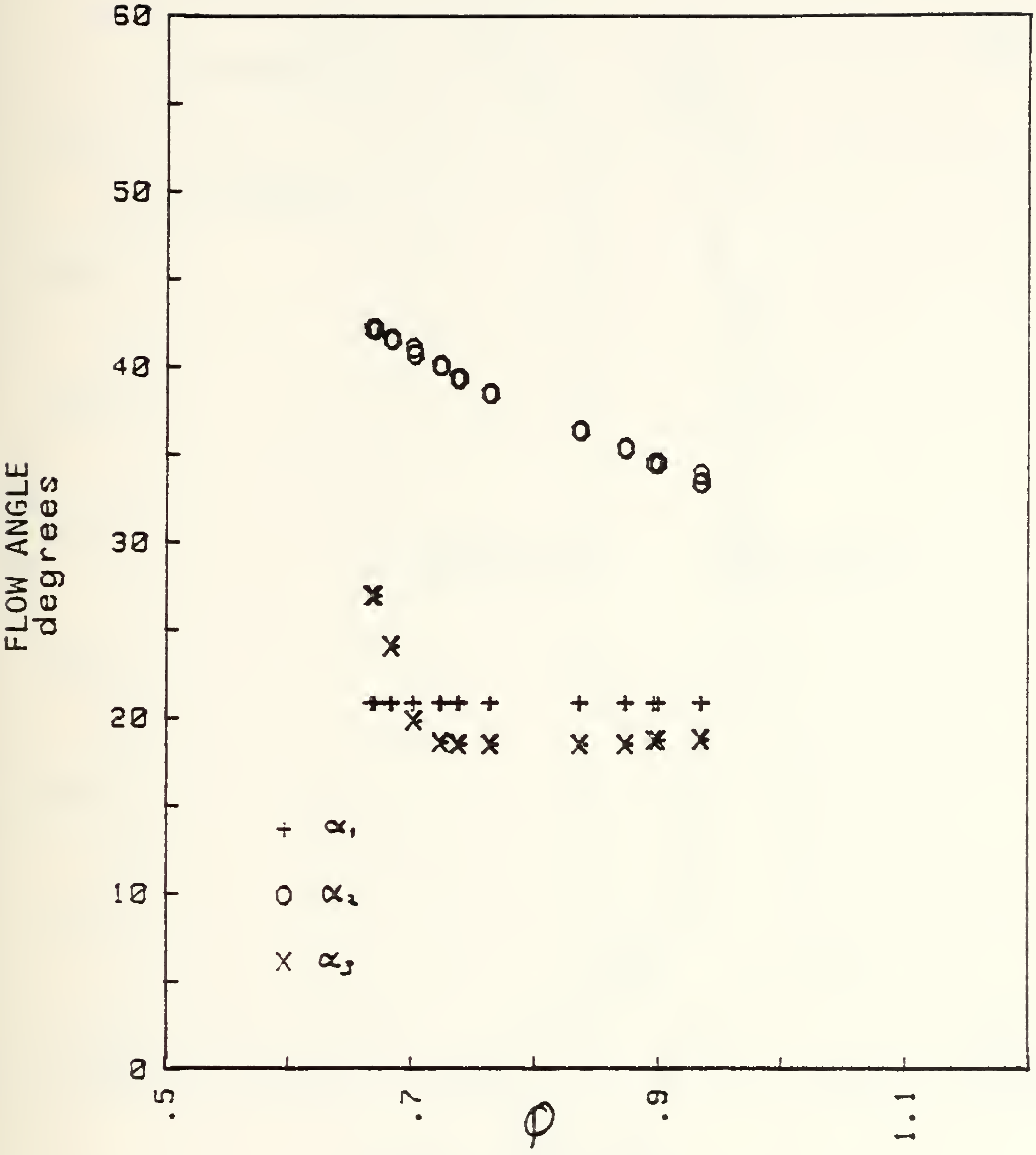

Figure 10. Mid-span Flow Angles vs Flow Rate (IGVs 4°)

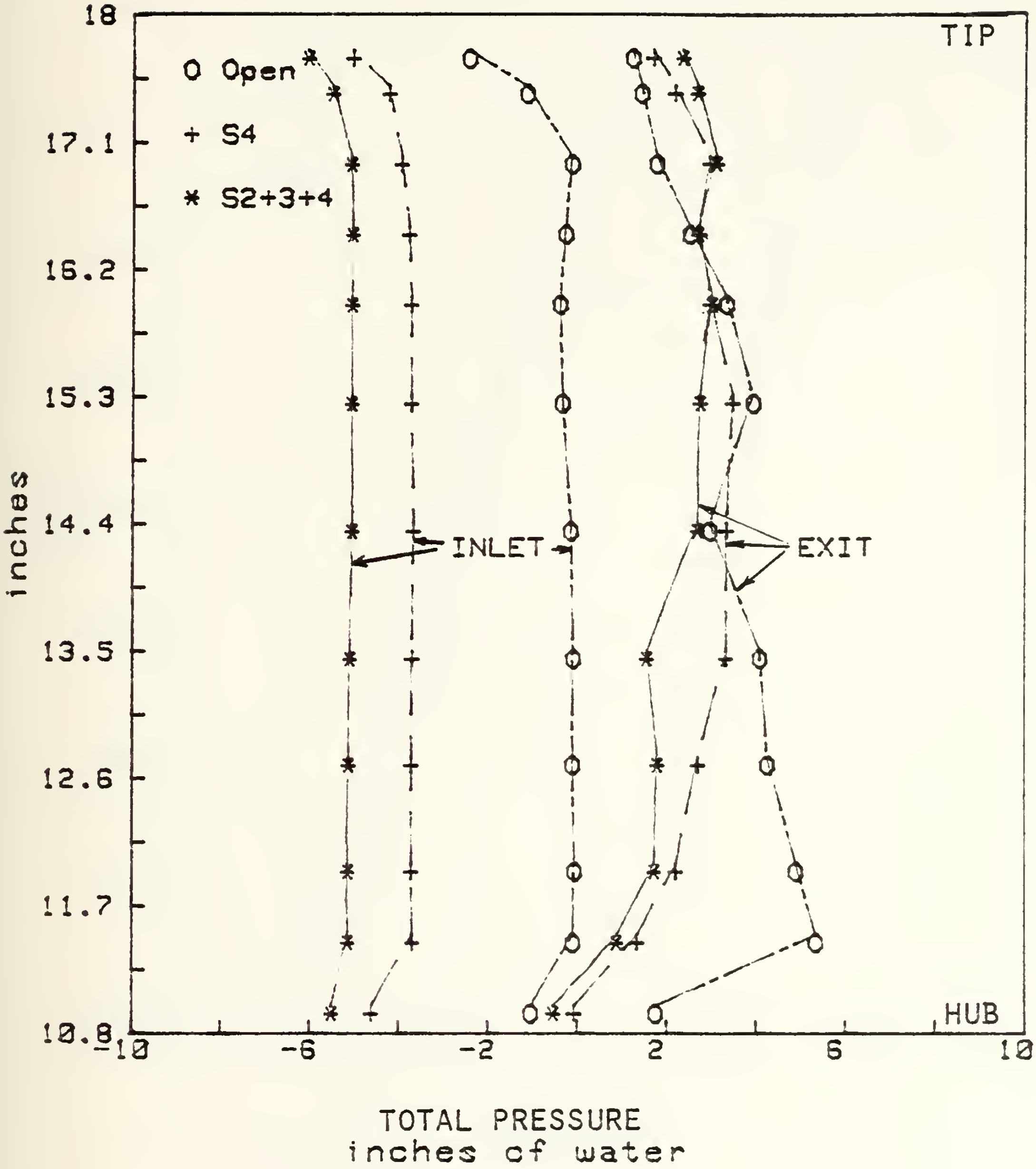

Figure 11. Inlet and Exit Pressure Distributions vs Radius at Three Throttle Settings (IGVs 4°)

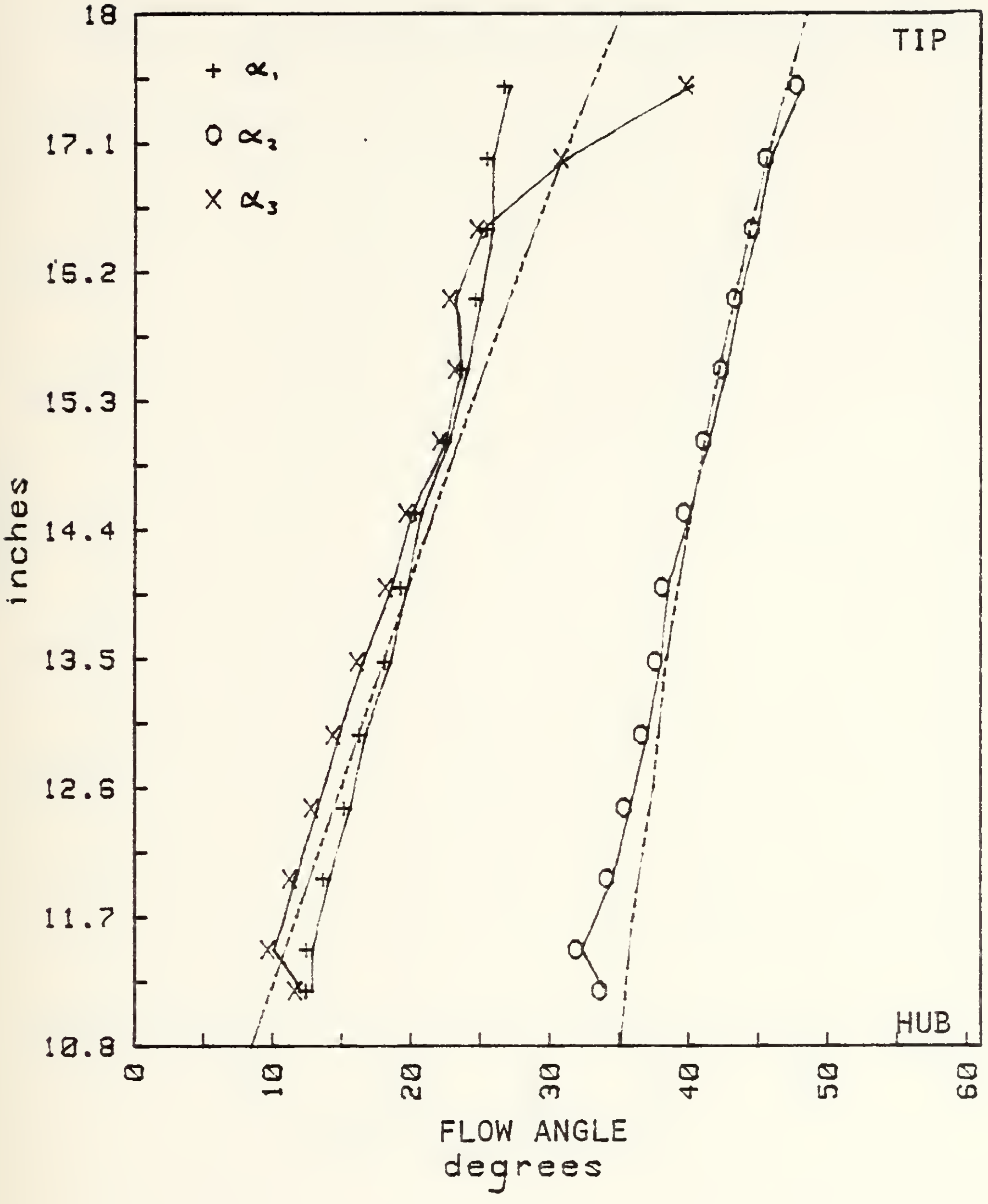

Figure 12. Measured Flow Angle Radial Distribution at Moderate Throttling (IGVs 4°, S2+S4; — – – — Design)

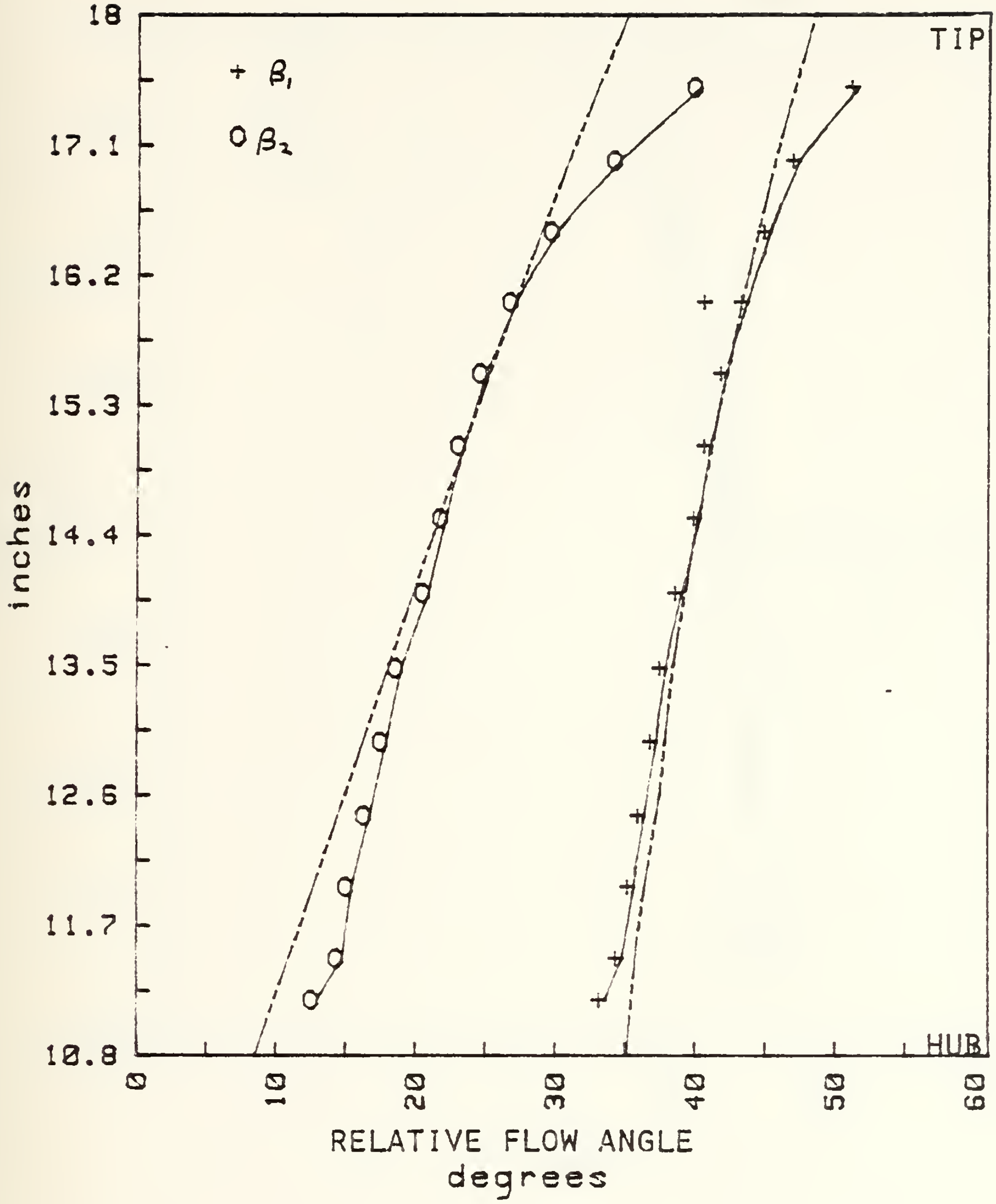

Figure 13. Relative Flow Angle Radial Distribution at Moderate Throttling (IGVs 4°, S2+S4; — - - — Design)

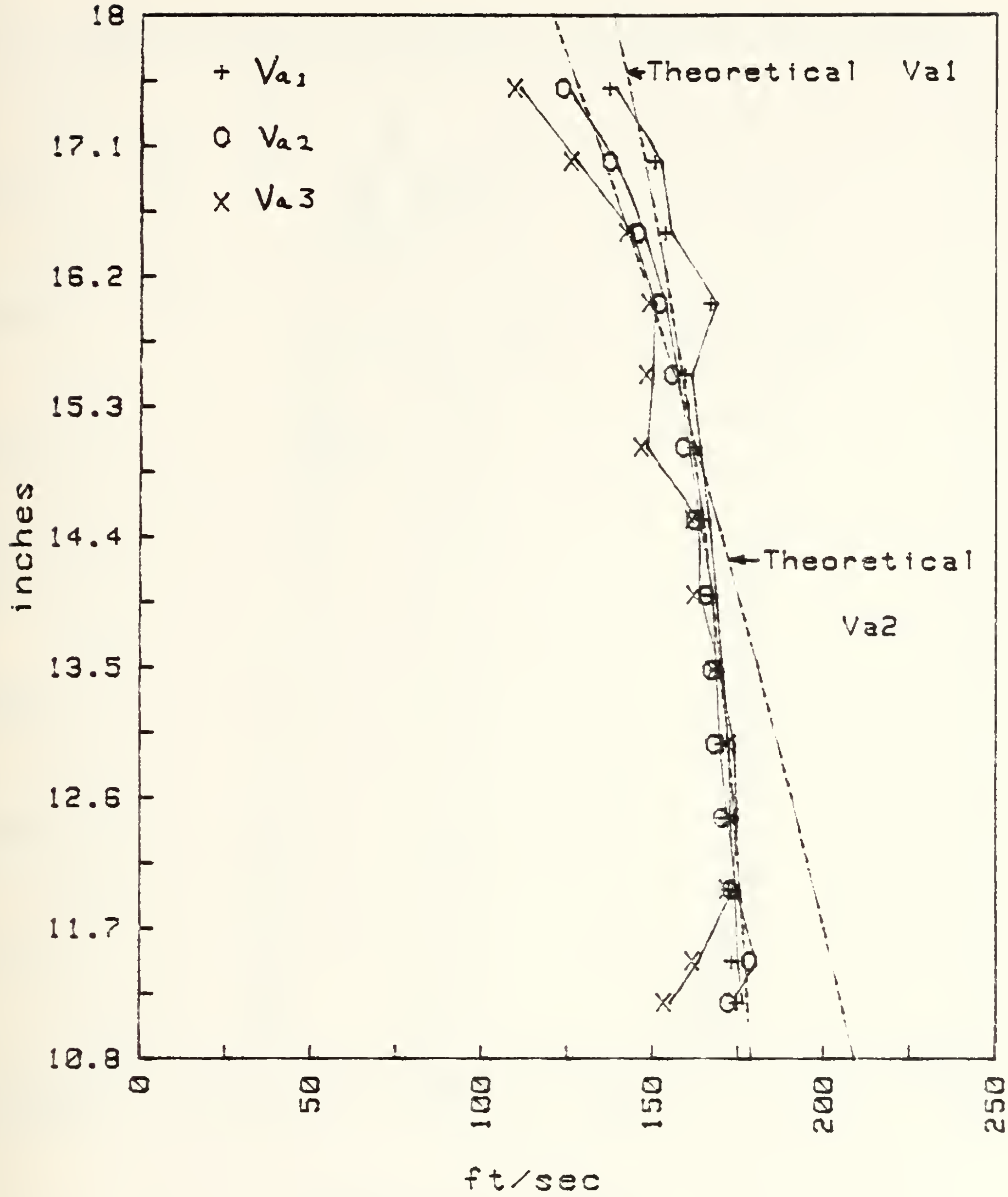

Figure 14. Axial Velocity Radial Distribution at Moderate Throttling (IGVs 4°, S2+S4)

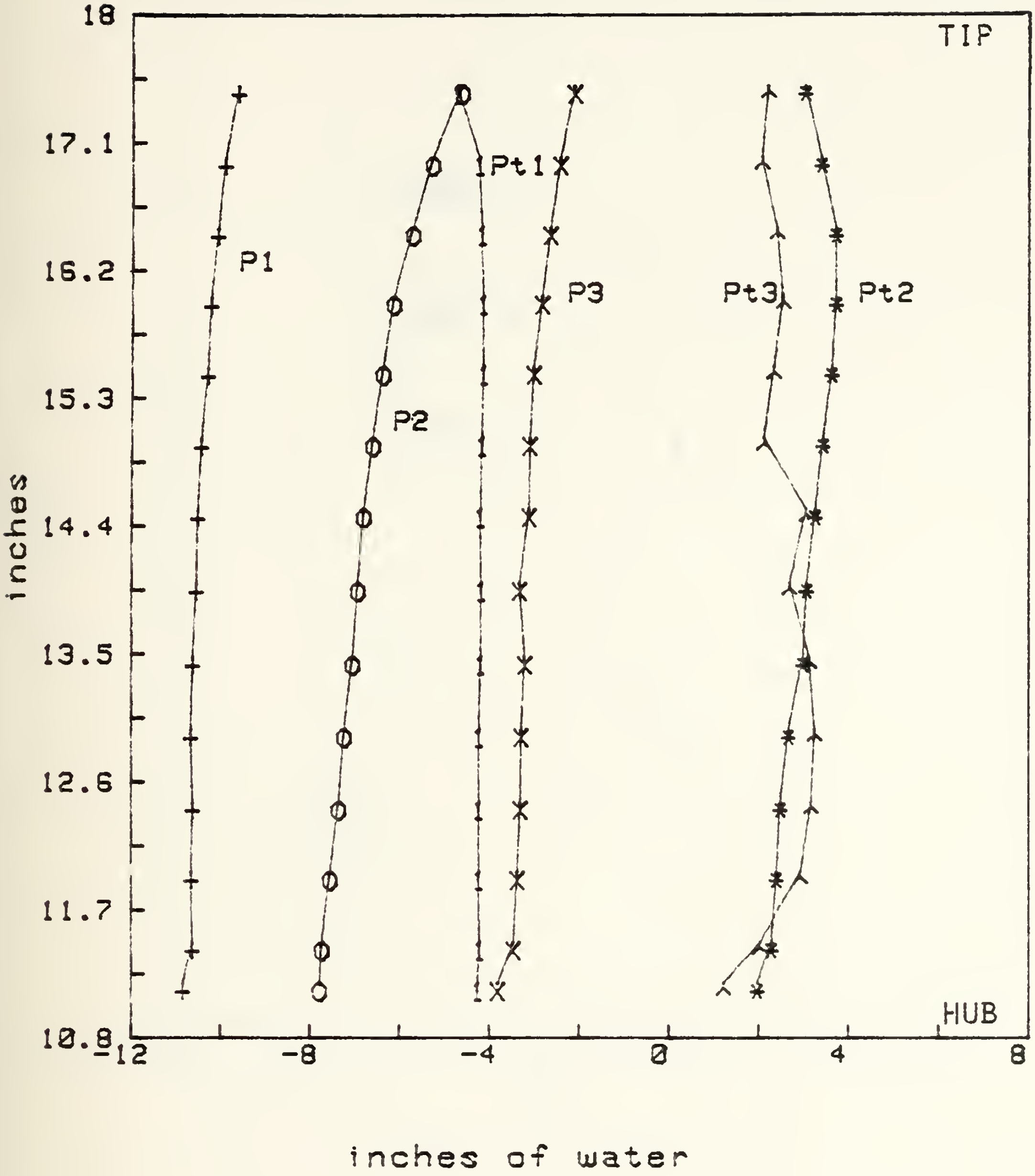

Figure 15. Intrastage Pressure Radial Distributions at Moderate Throttling (IGVs 4°, S2+S4)

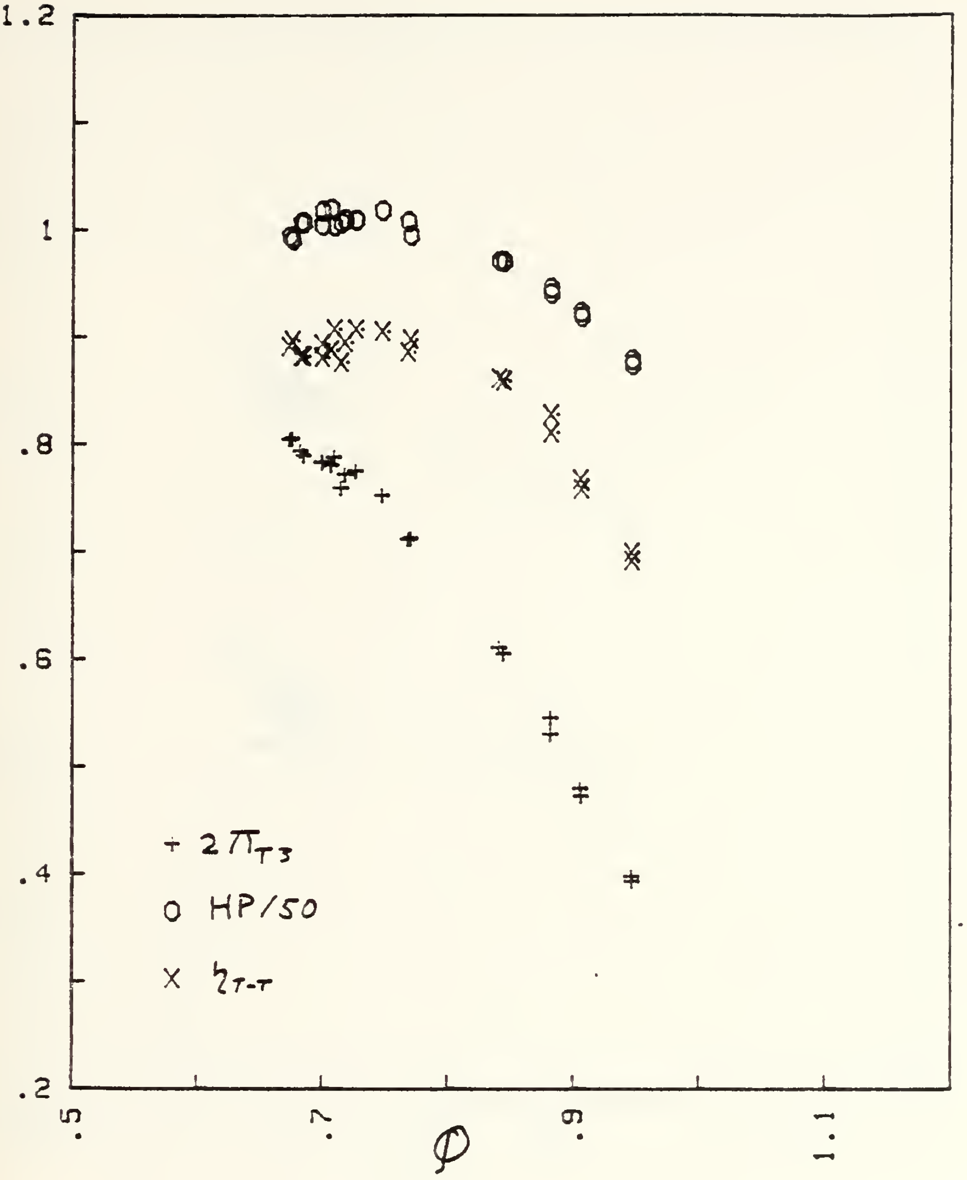

Figure 16. Performance Parameters vs Flow Rate (IGVs 3°)

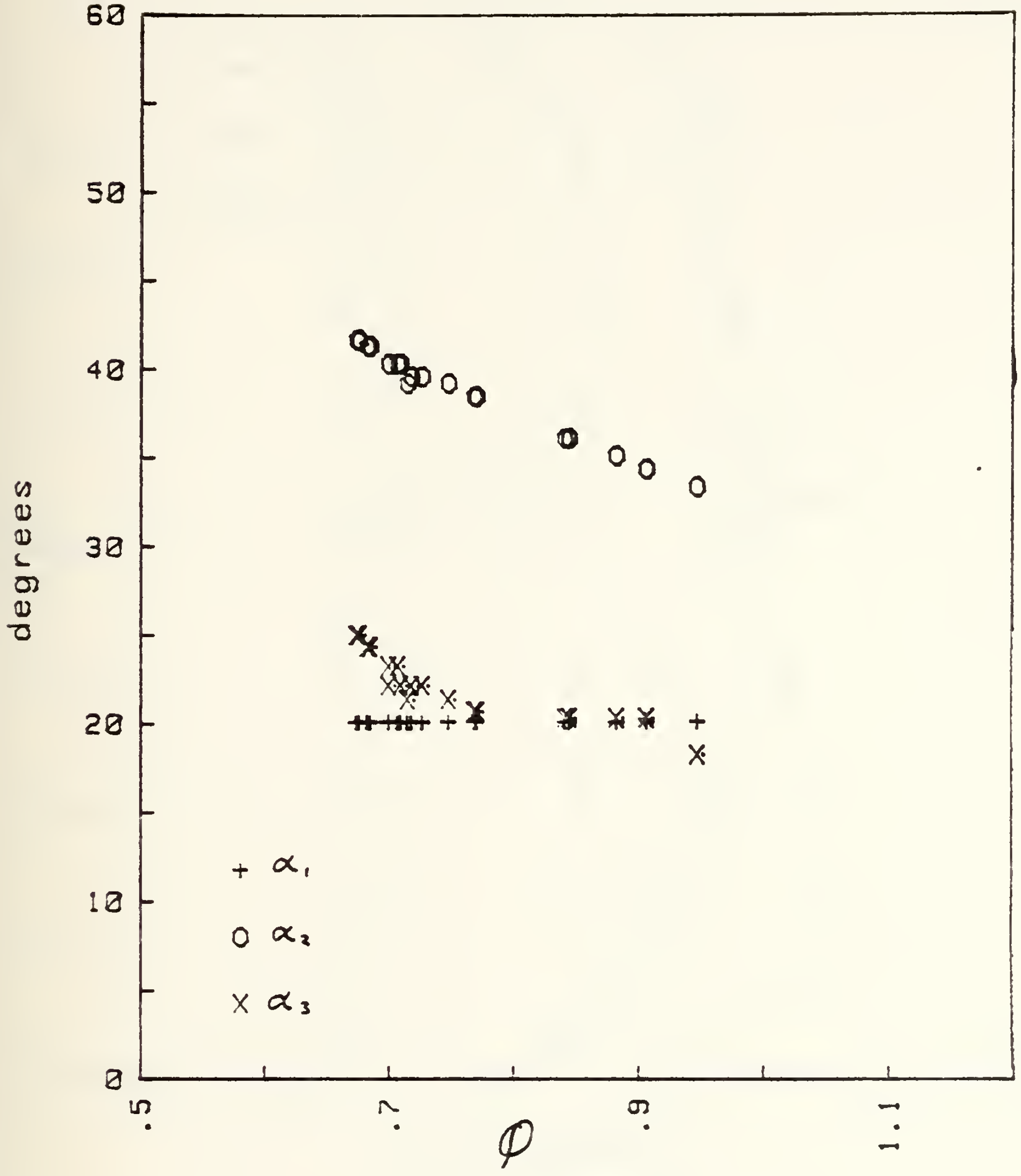

Figure 17. Mid-span Flow Angles vs Flow Rate (IGVs 3°)

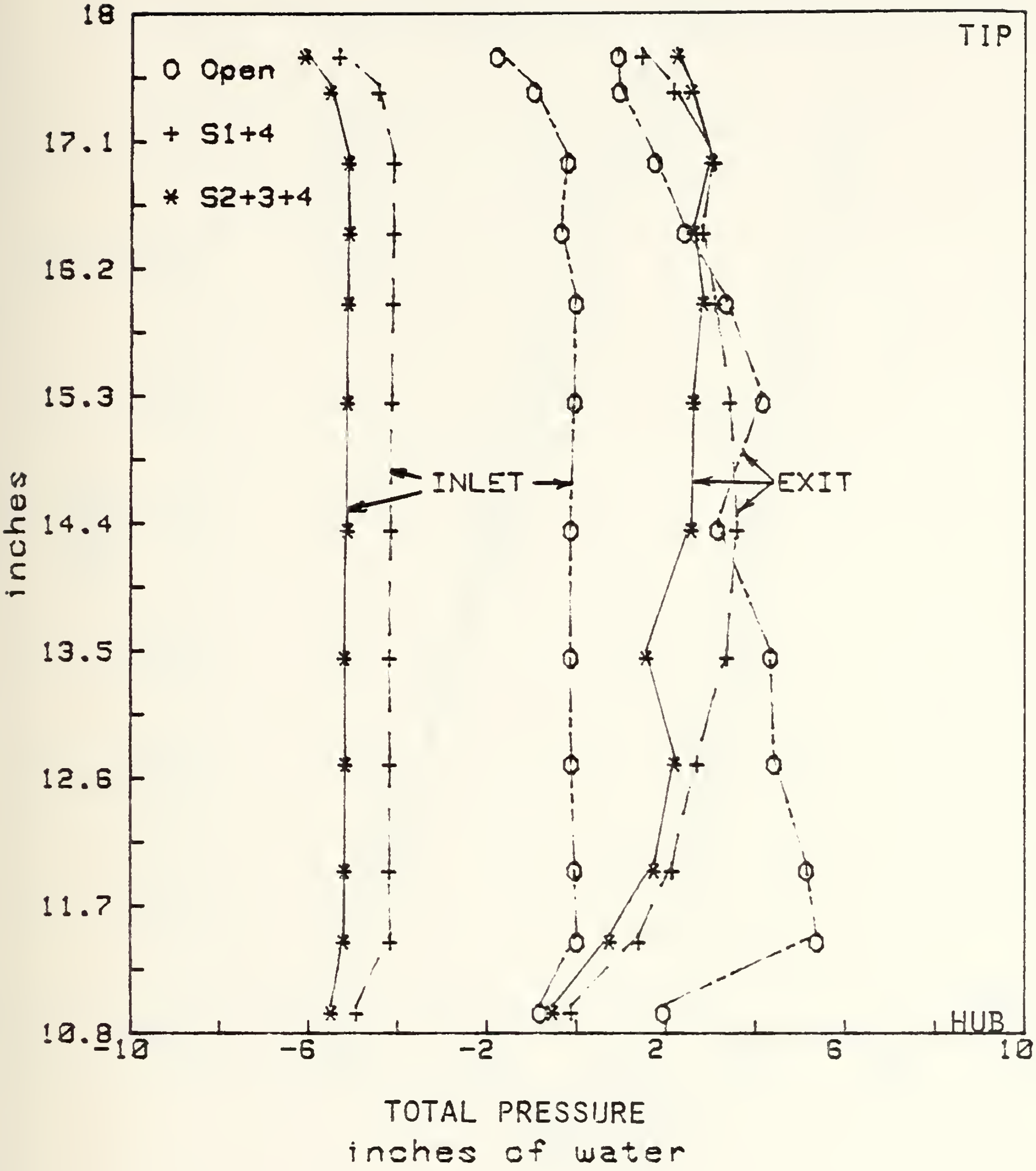

Figure 18. Inlet and Exit Pressure Distributions vs Radius at Three Throttle Settings (IGVs 3°)

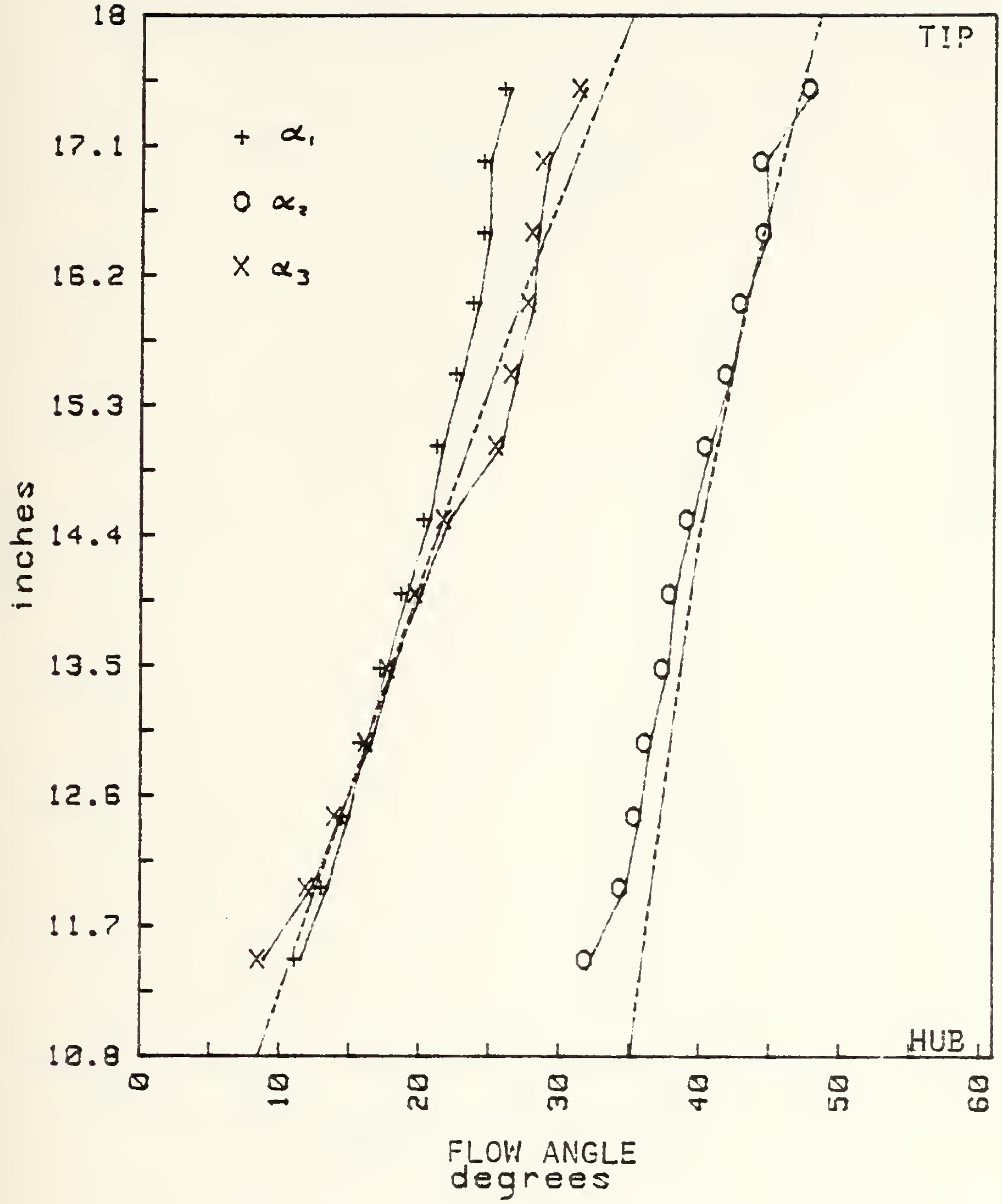

Figure 19. Measured Flow Angle Radial Distribution at Moderate Throttling (IGVs 3°, S2+S4)

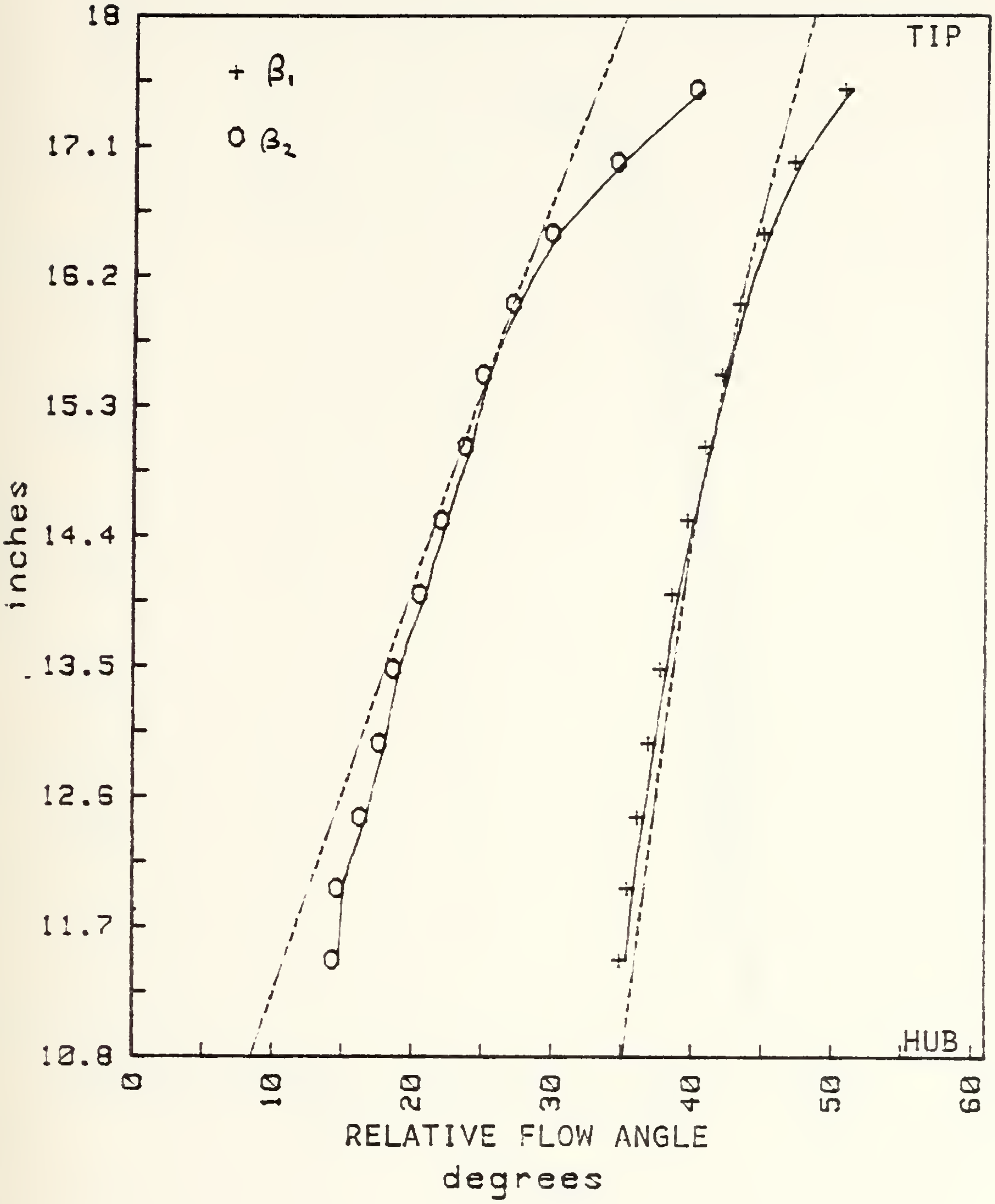

Figure 20. Relative Flow Angle Radial Distribution at Moderate Throttling (IGVs 3°, S2+4)

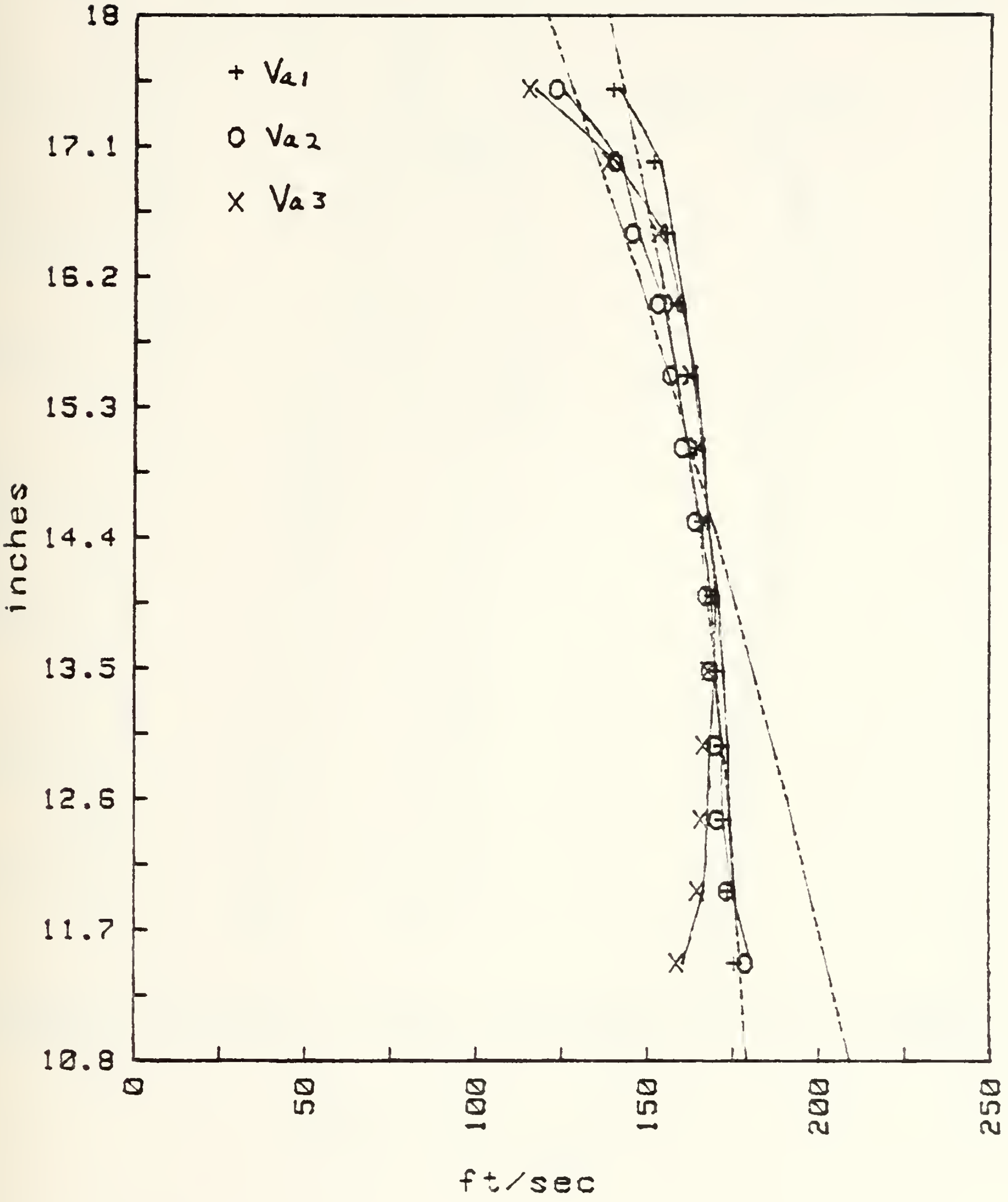

Figure 21. Axial Velocity Radial Distribution at Moderate Throttling (IGVs 3°, S2+4)

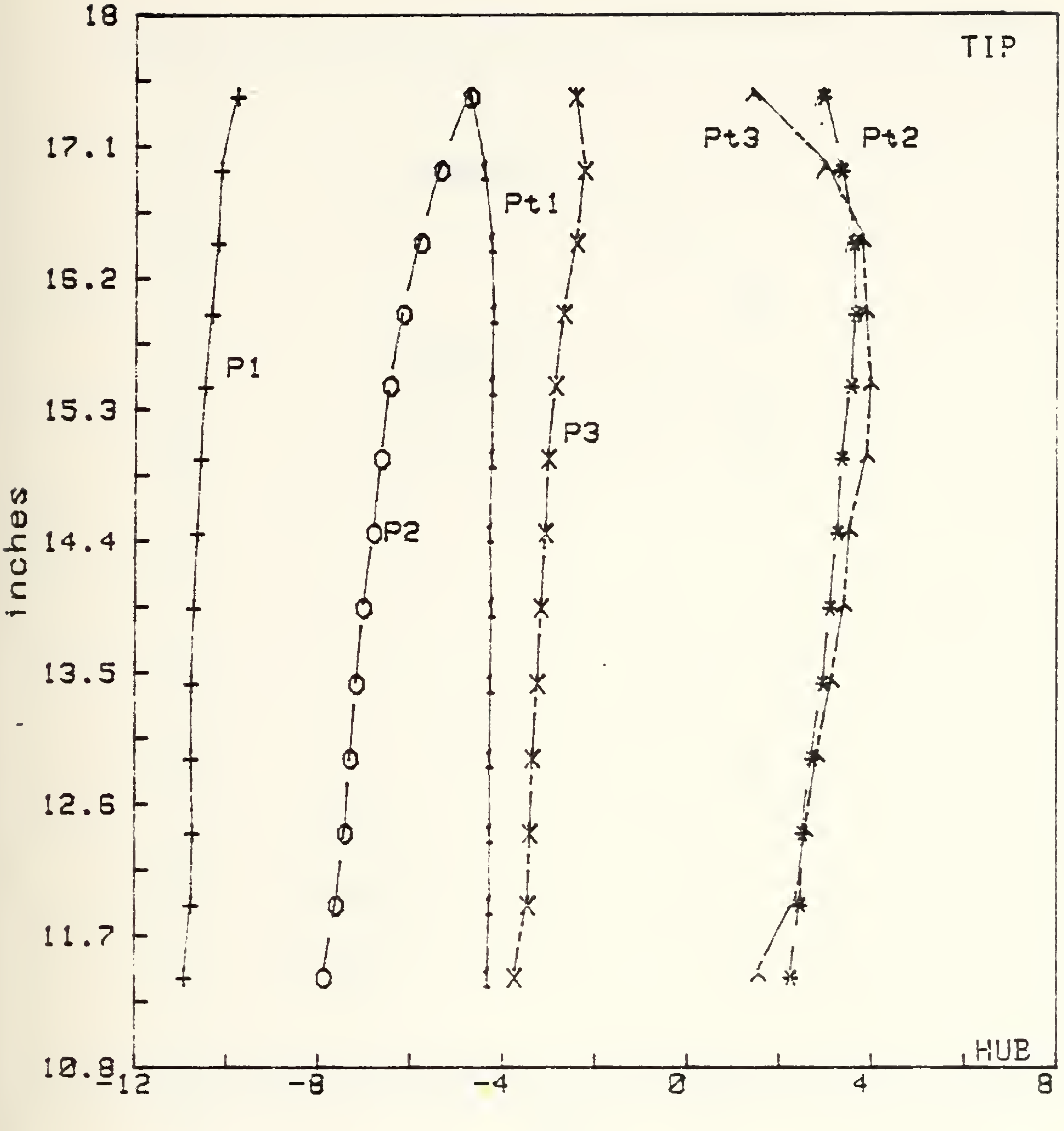

Figure 22. Intrastage Pressure Radial Distributions at Moderate Throttling (IGVs 3°, S2+4)

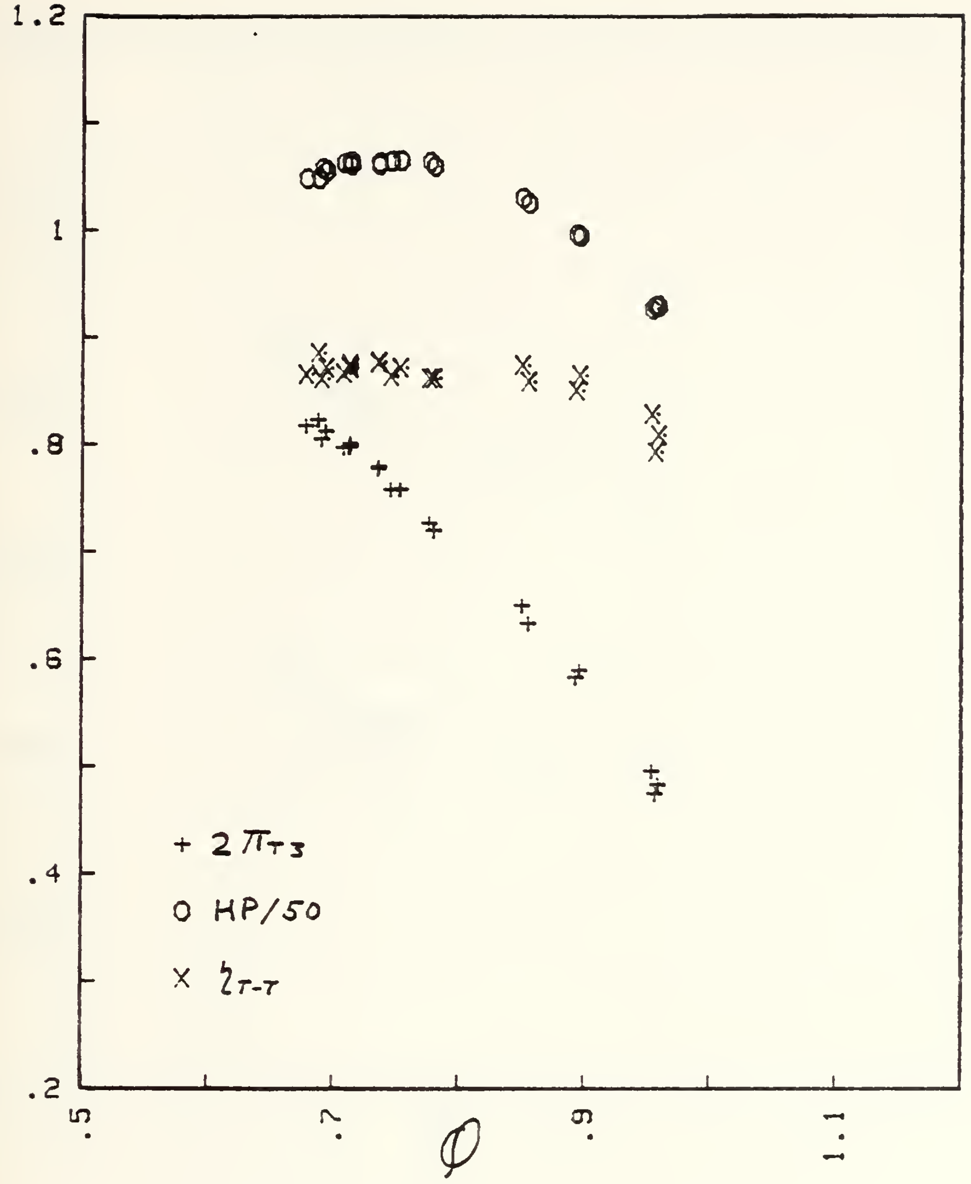

Figure 23. Performance Parameters vs Flow Rate (IGVs 2°)

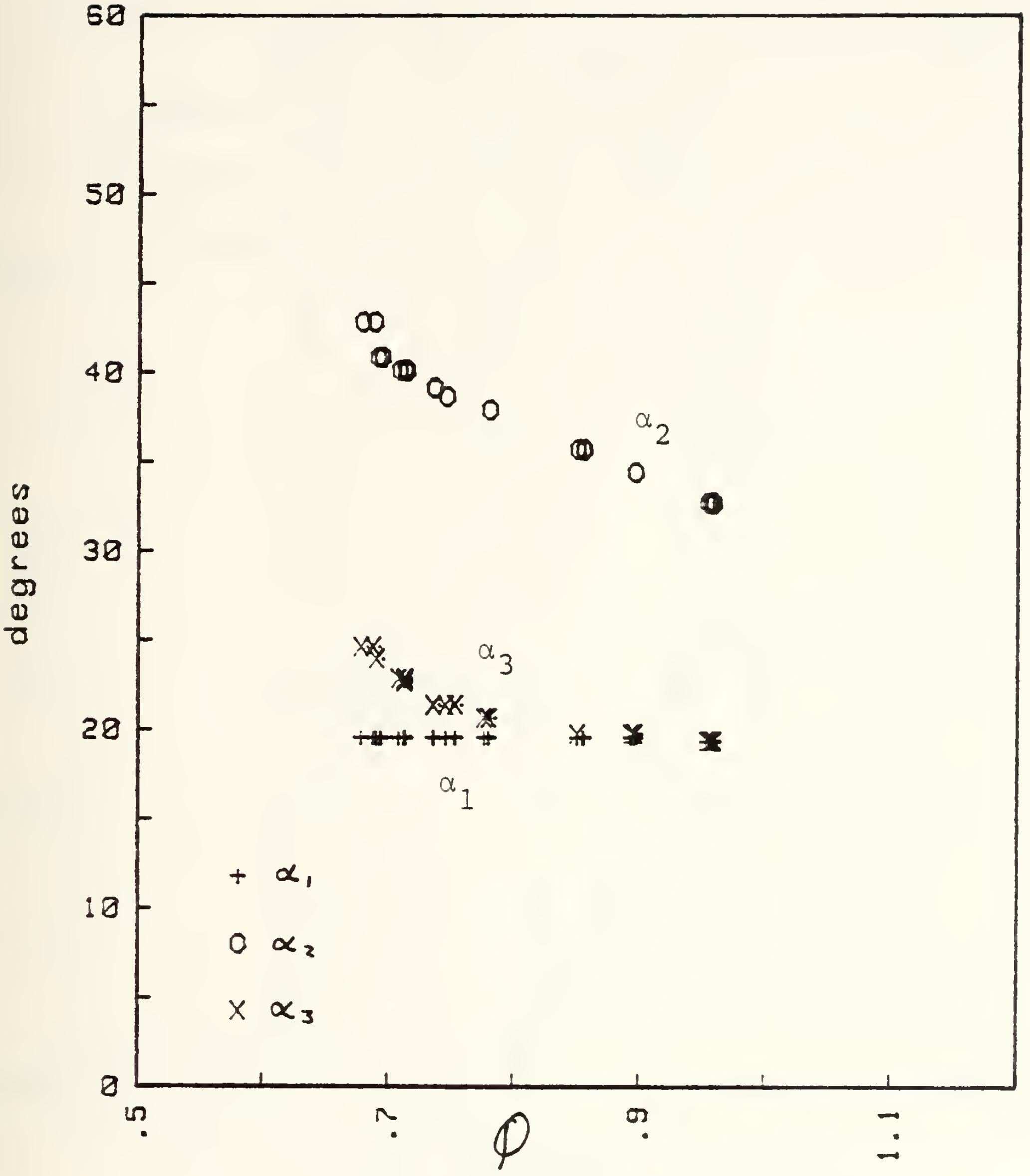

Figure 24. Mid-span Flow Angles vs Flow Rate (IGVs 2°)

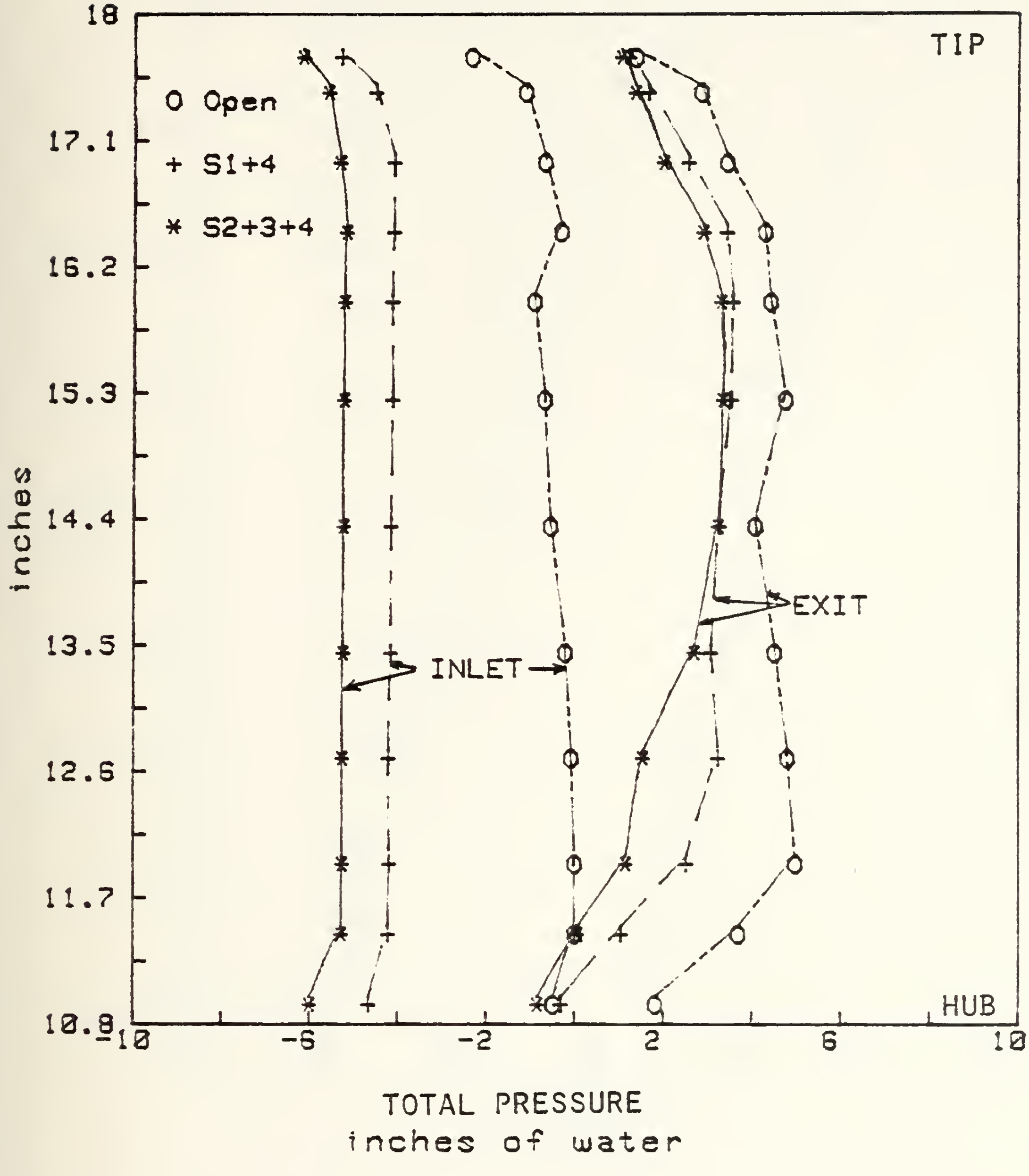

Figure 25. Inlet and Exit Pressure Radial Distributions at Three Throttle Settings (IGVs 2°)

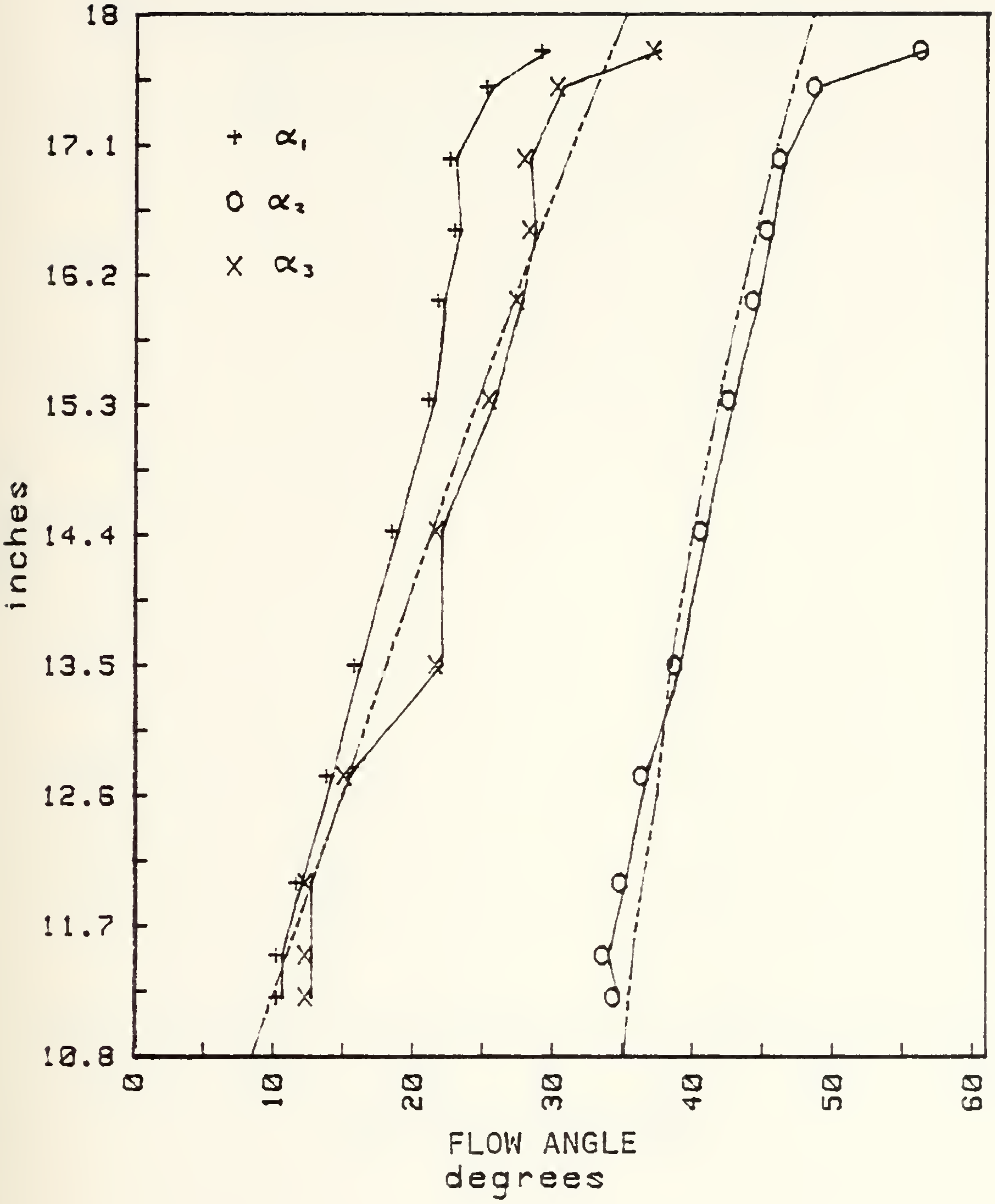

Figure 26. Measured Flow Angle Radius Distributions at Moderate Throttling (IGVs 2°, S2+4)

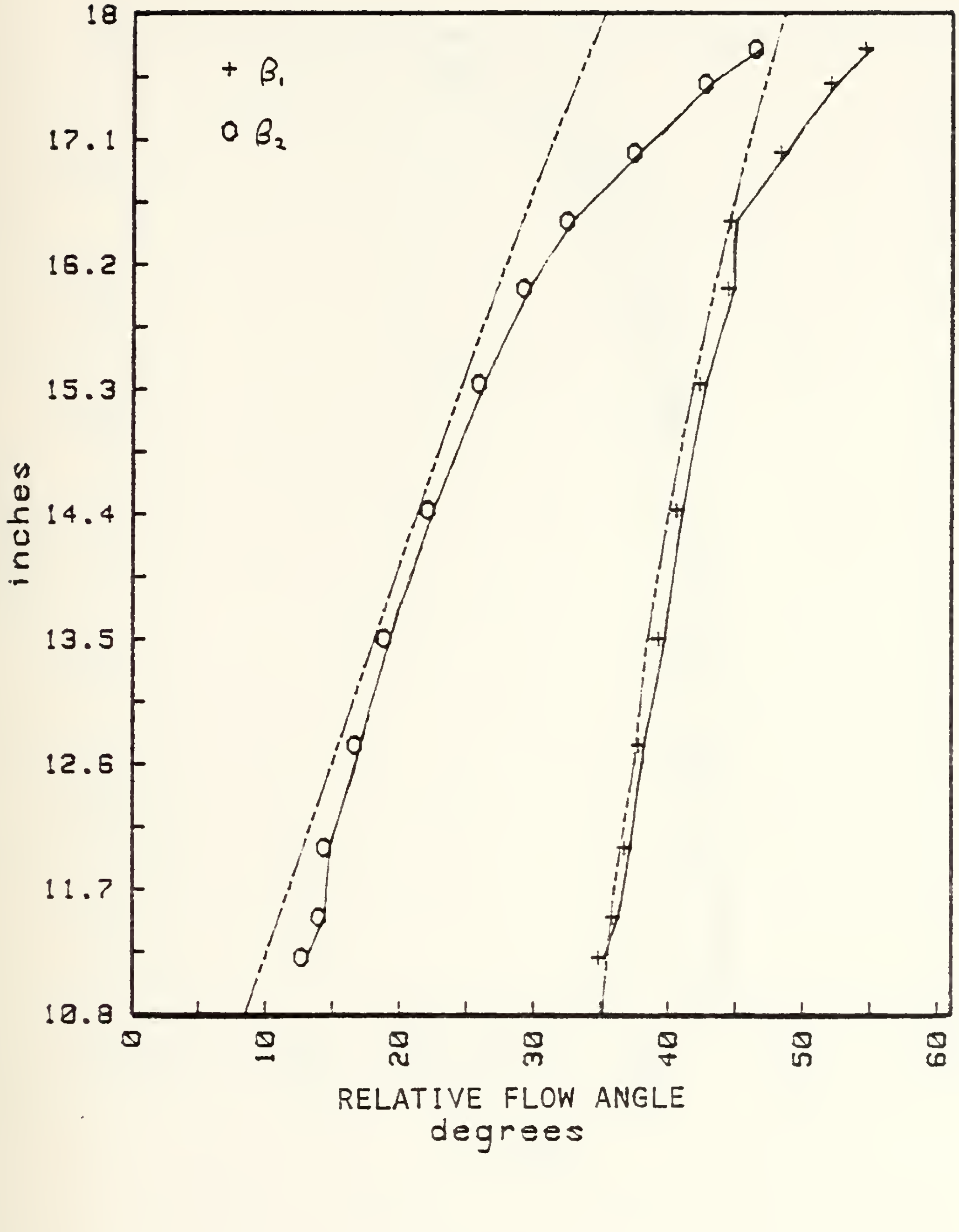

Figure 27. Relative Flow Angle Radius Distributions at Moderate Throttling (IGVs 2°, S2+4)

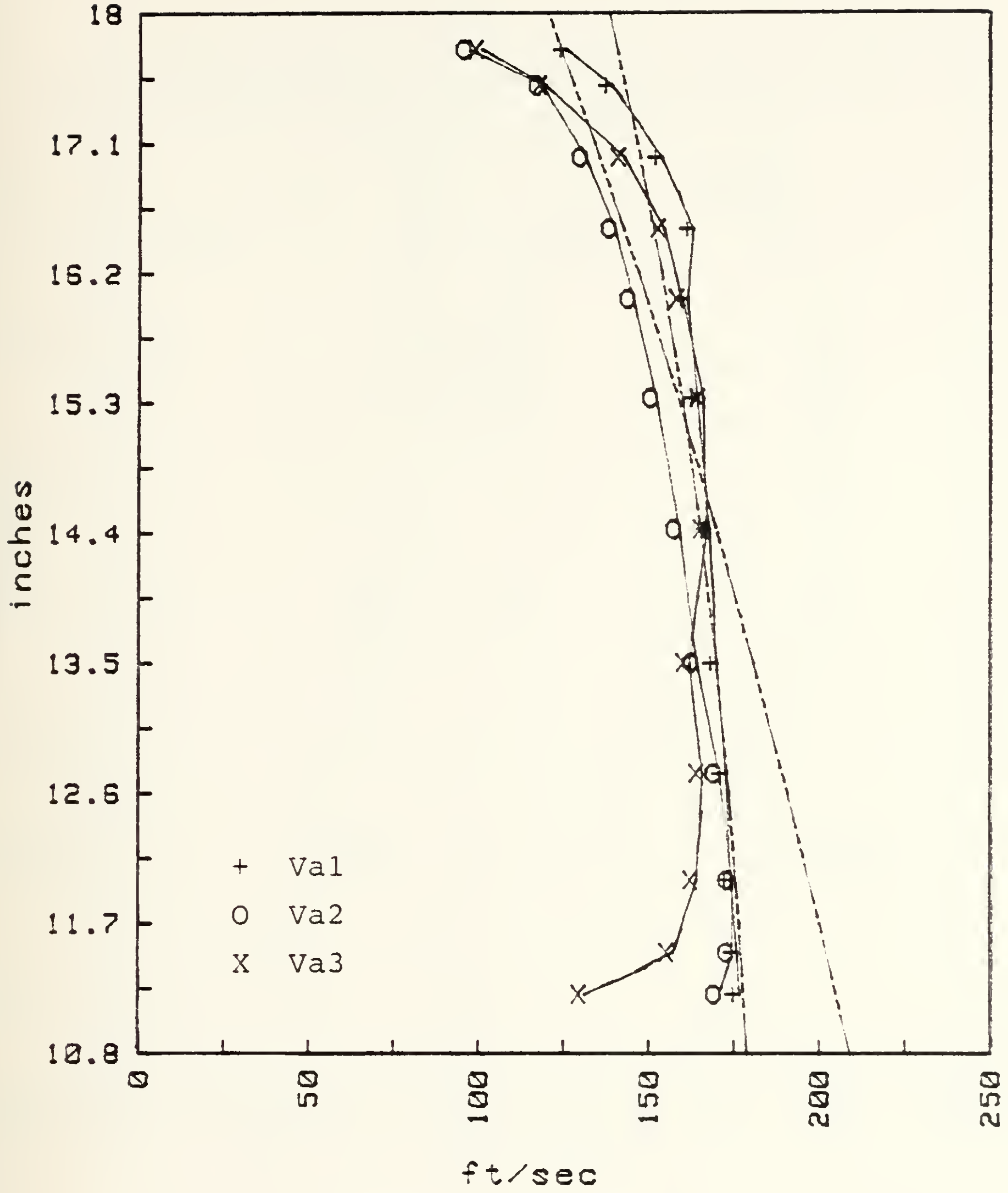

Figure 28. Axial Velocity Radial Distributions at Moderate Throttling (IGVs 2°, S2+4)

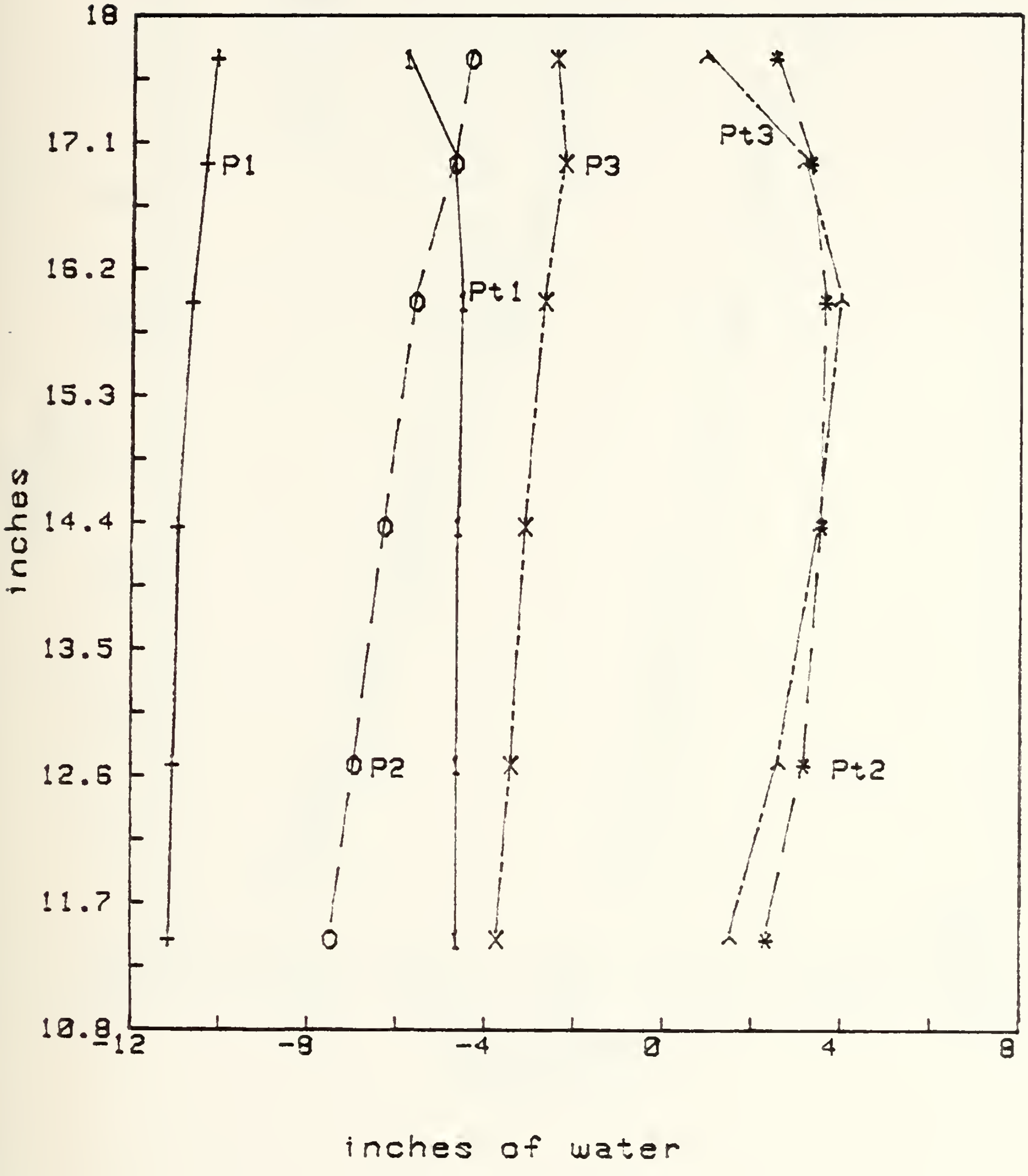

Figure 29. Intrastage Pressure Radial Distributions at Moderate Throttling (IGVs 2°, S2+4)

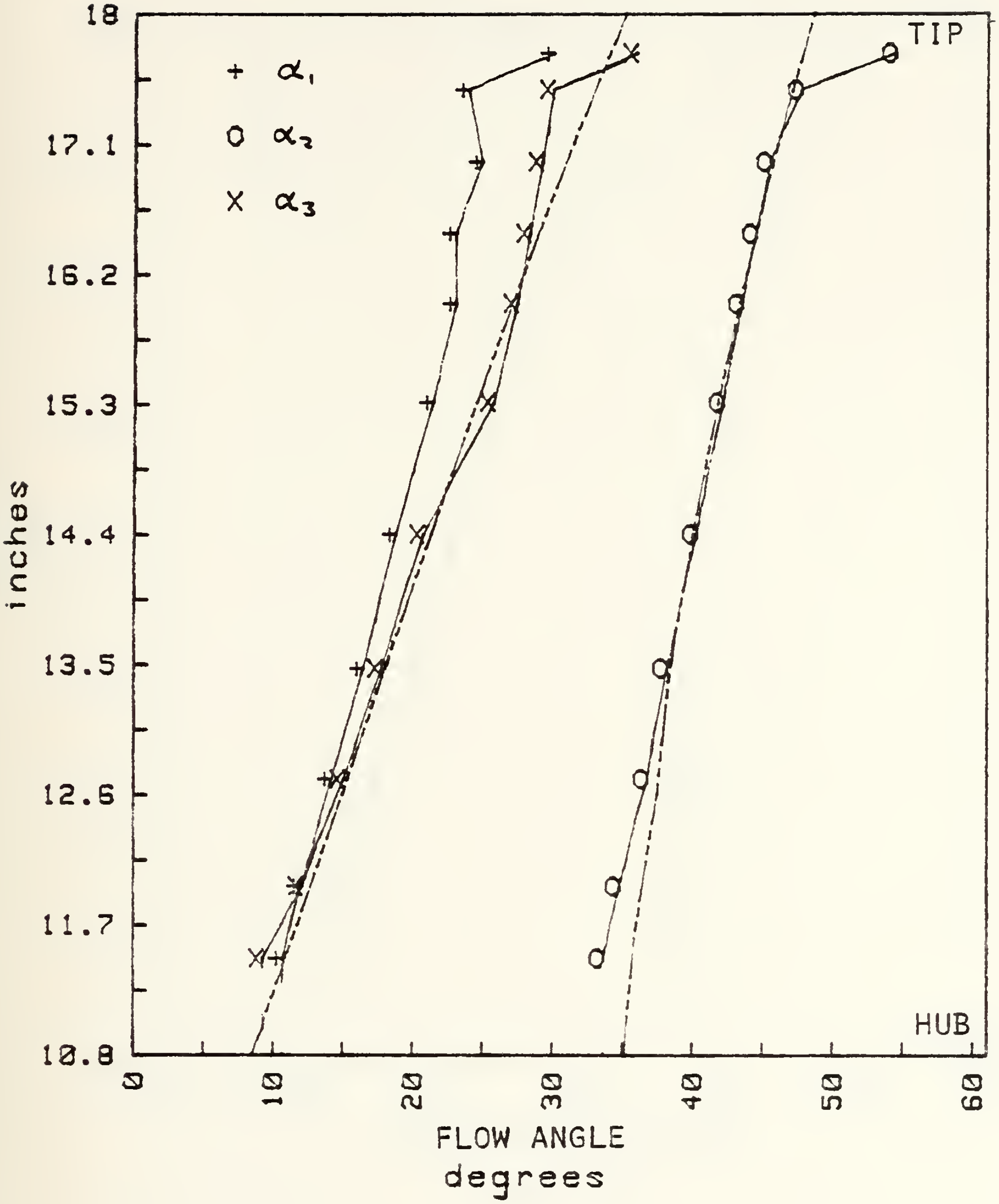

Figure 30. Measured Flow Angle Radial Distributions at Moderate Throttling (IGVs 2°, S1+4)

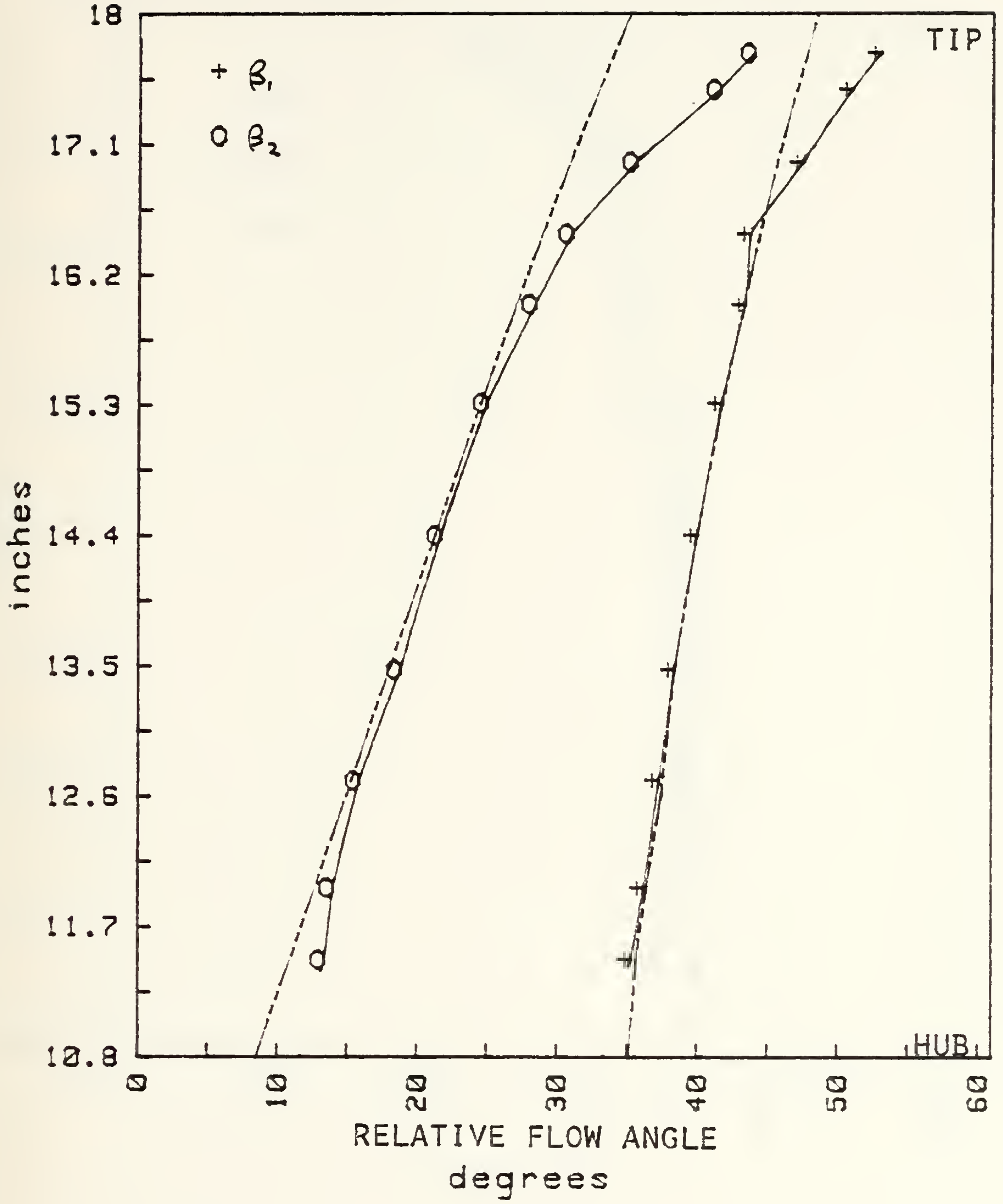

Figure 31. Relative Flow Angle Radial Distributions at Moderate Throttling (IGVs 2°, S1+4)

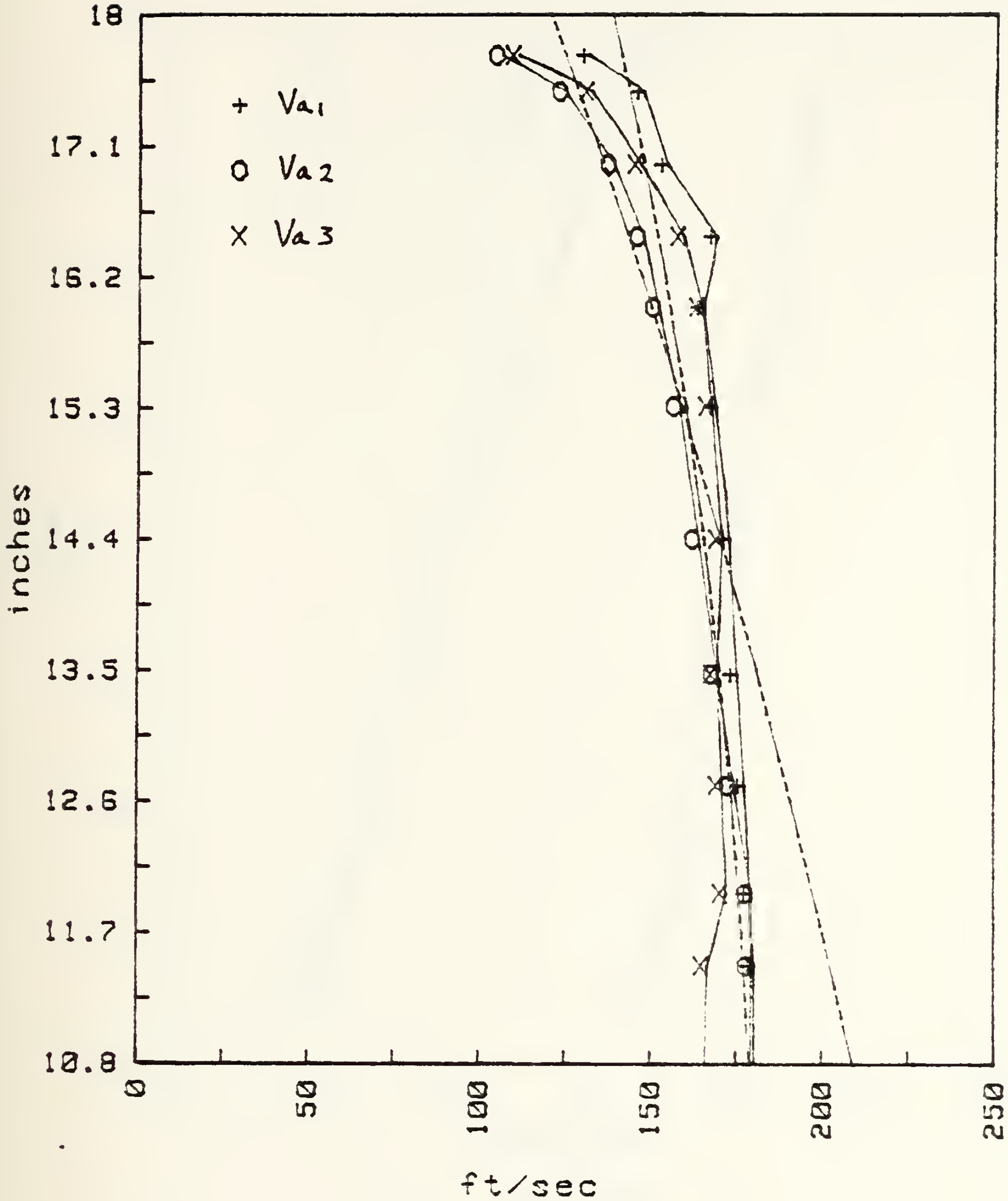

Figure 32. Axial Velocity Radial Distribution at Moderate Throttling (IGVs 2°, S1+4)

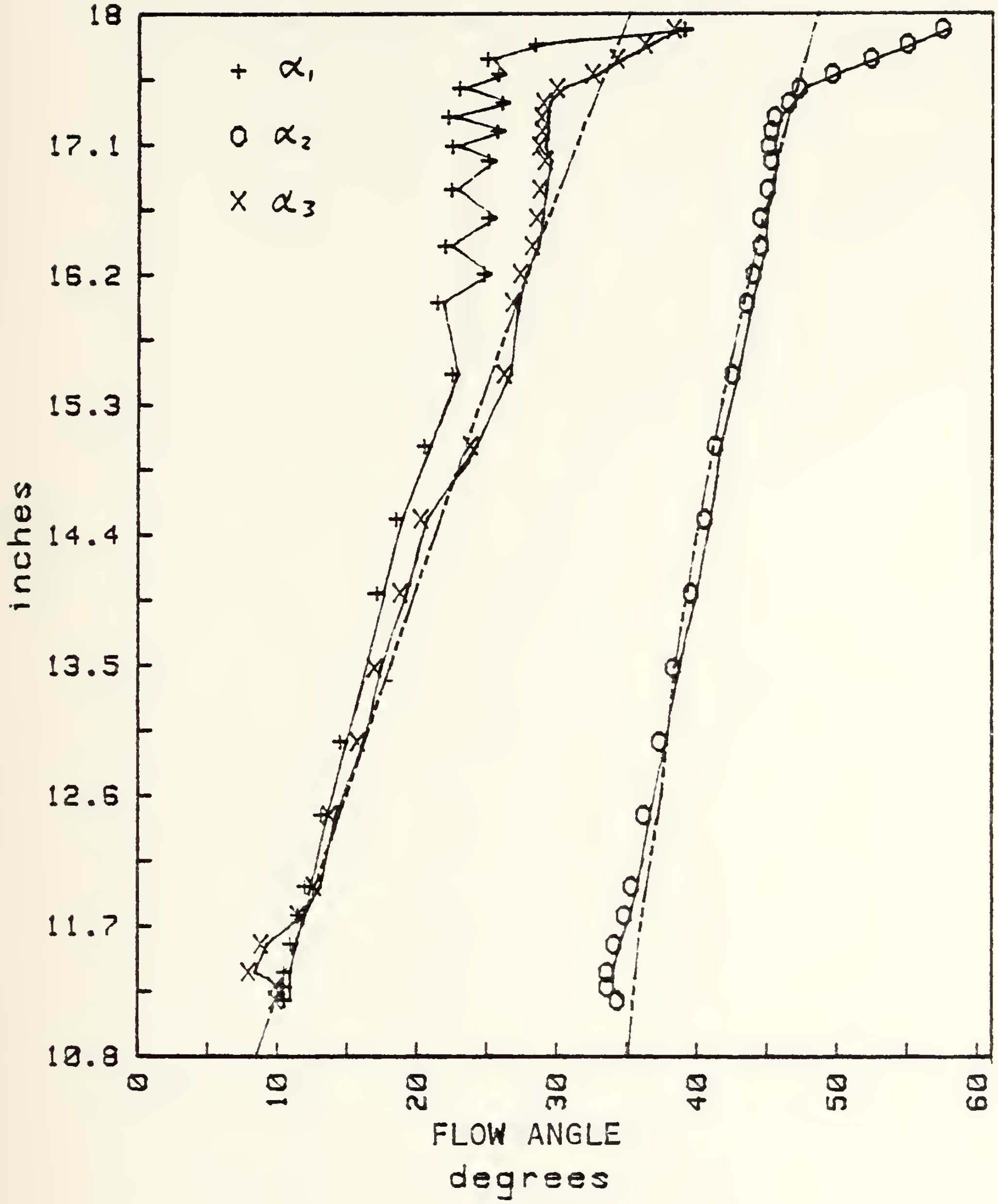

Figure 33. Measured Flow Angle Radial Distributions with Closely Spaced Data Points (IGV 2°, S1+4)

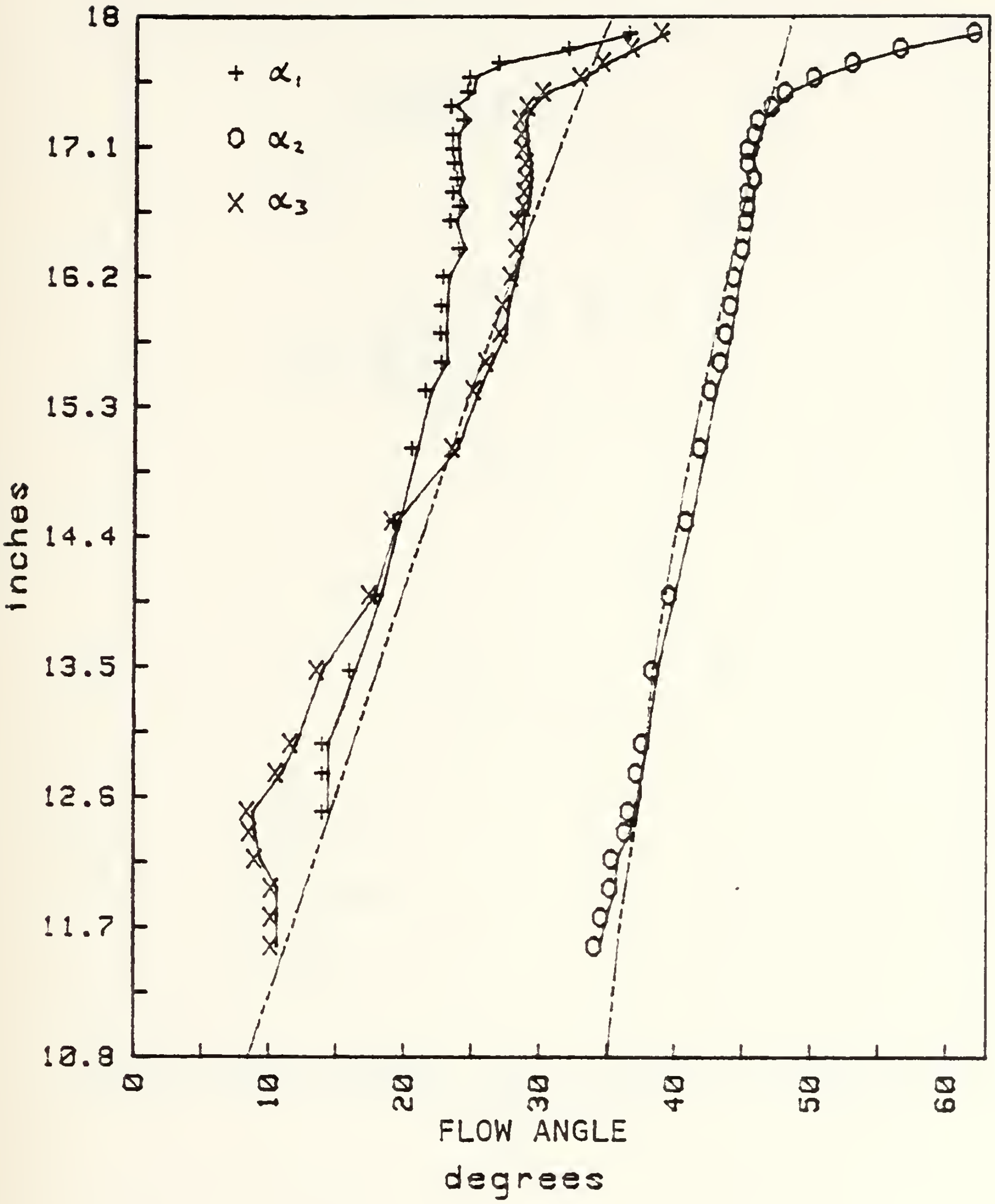

Figure 34. Measured Flow Angle Radial Distributions Measured by Yaw Probe

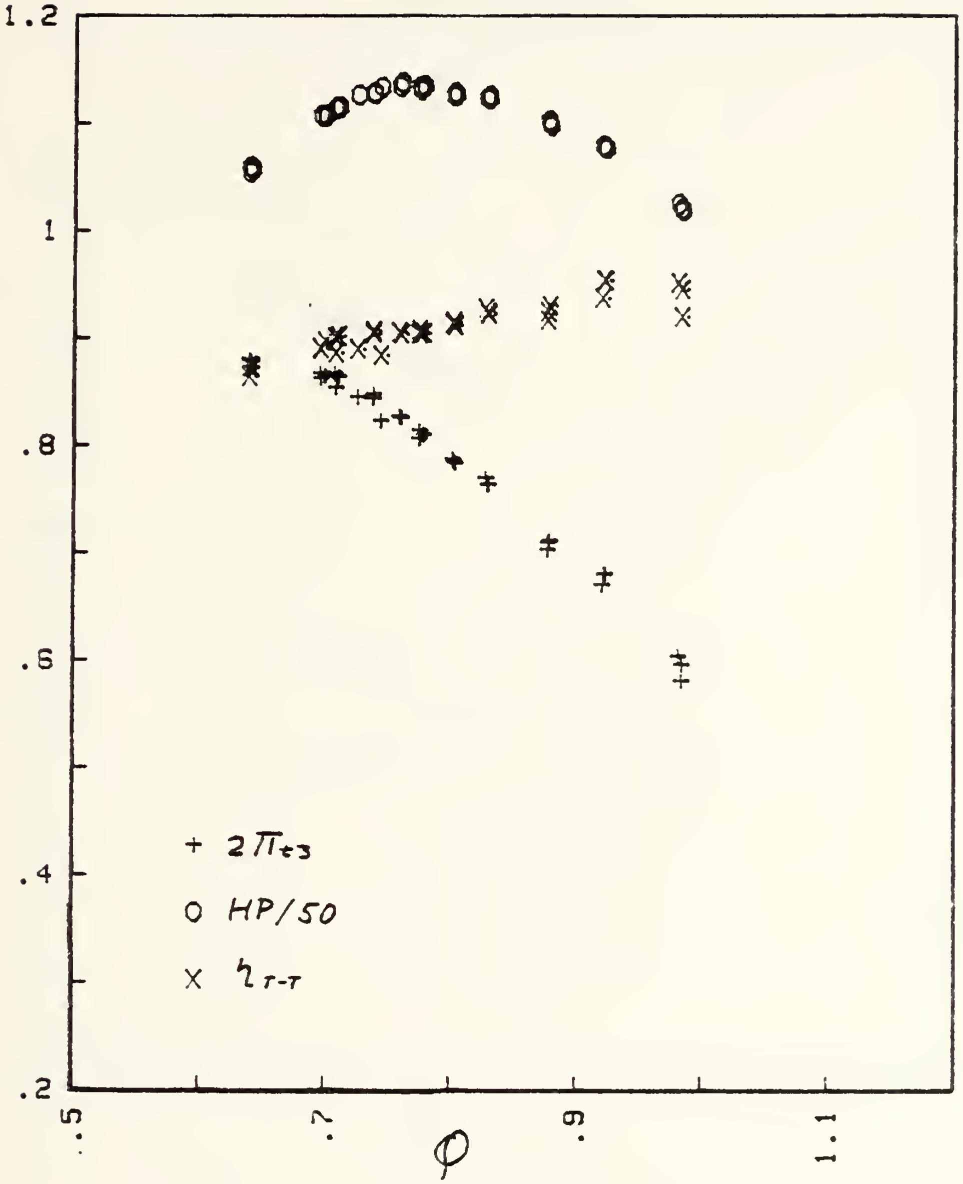

Figure 35. Performance Parameters vs Flow Rate (IGVs 0°)

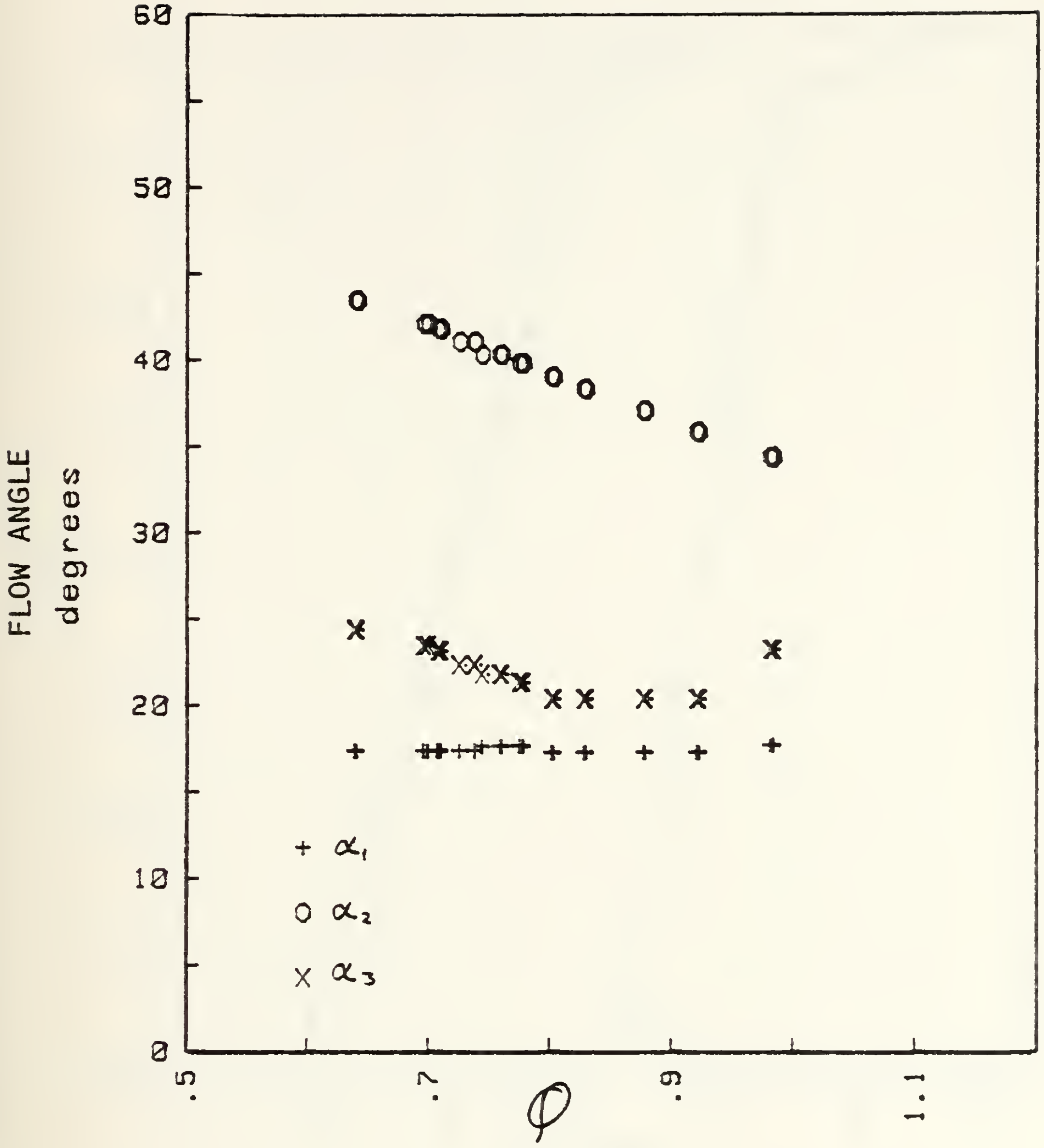

Figure 36. Mid-span Flow Angles vs Flow Rate (IGVs 0°)

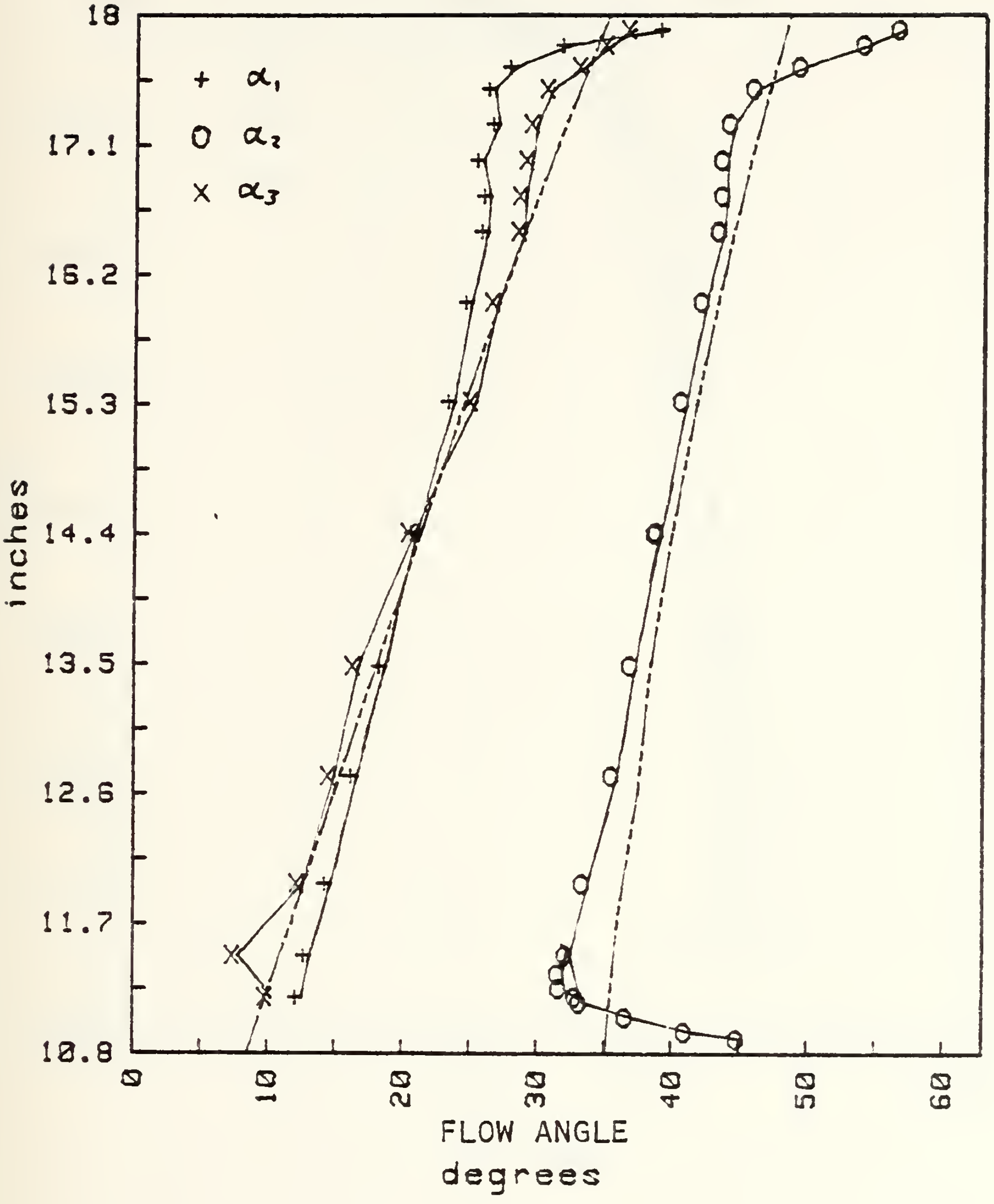

Figure 37. Measured Flow Angle Radial Distribution at Moderate Throttling (IGVs 0°, S1+4)

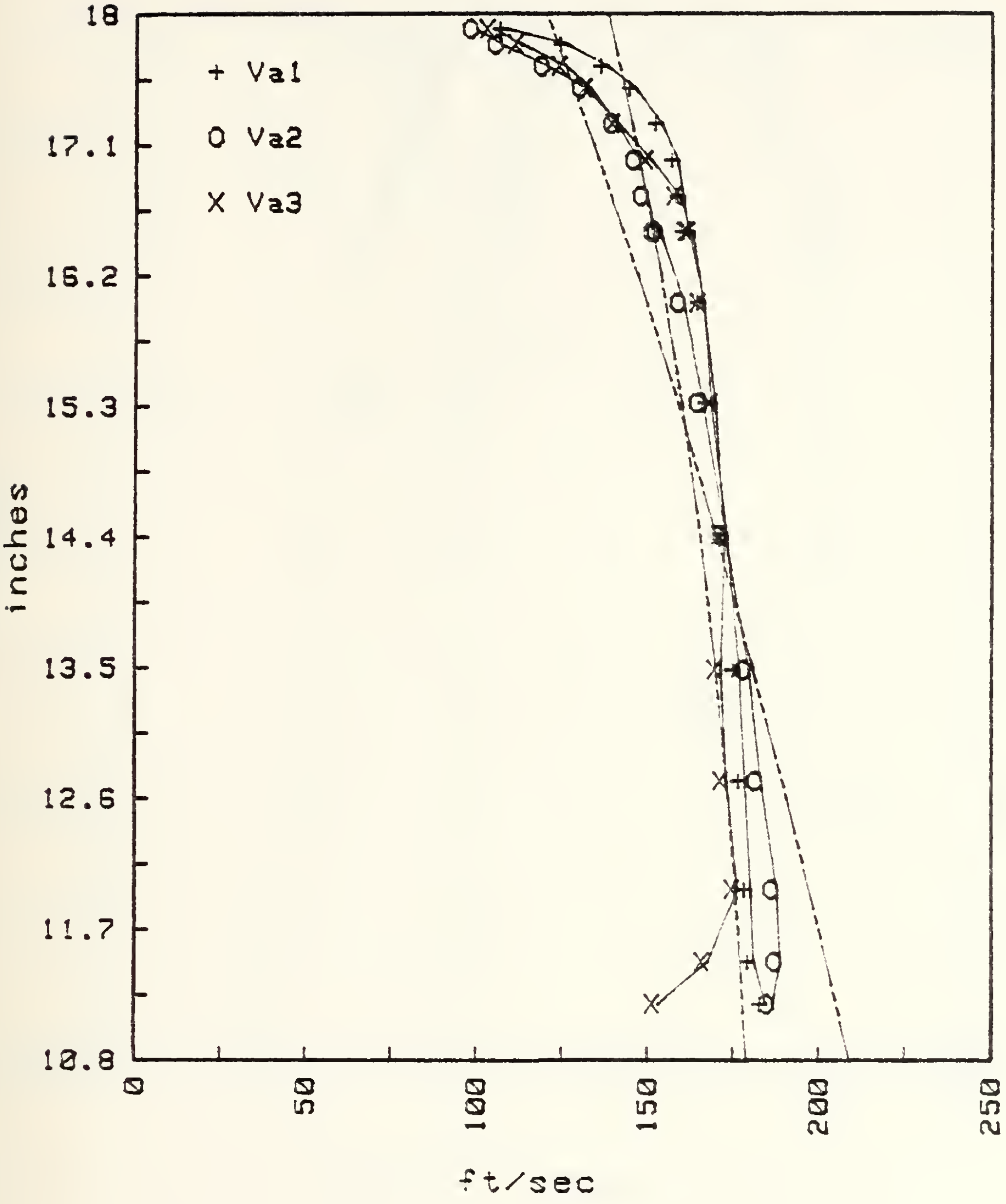

Figure 38. Axial Velocity Radial Distribution at Moderate Throttling (IGVs 0°, S1+4)

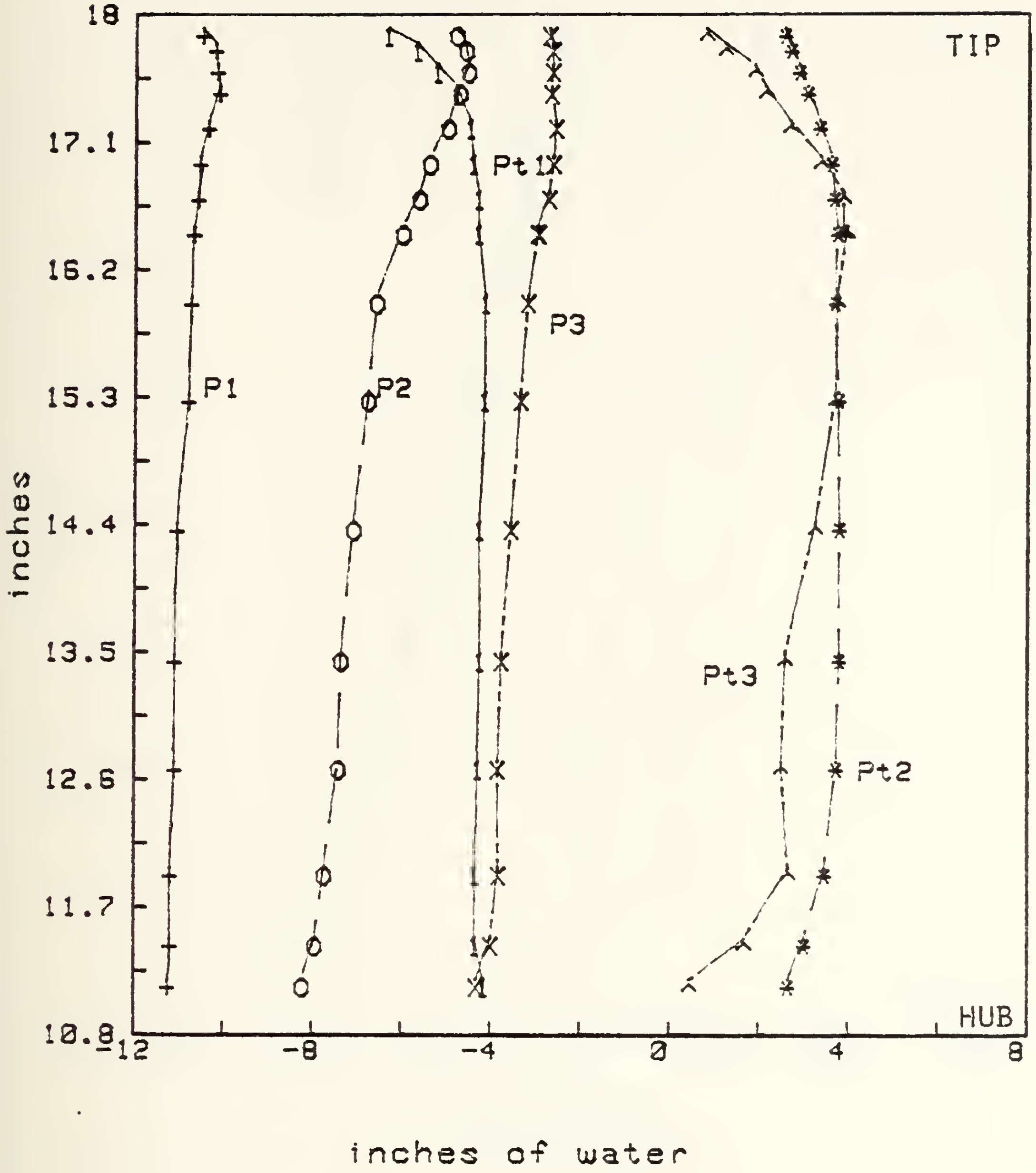

Figure 39. Intrastage Pressure Radial Distribution at Moderate Throttling (IGVs 0°, S1+4)

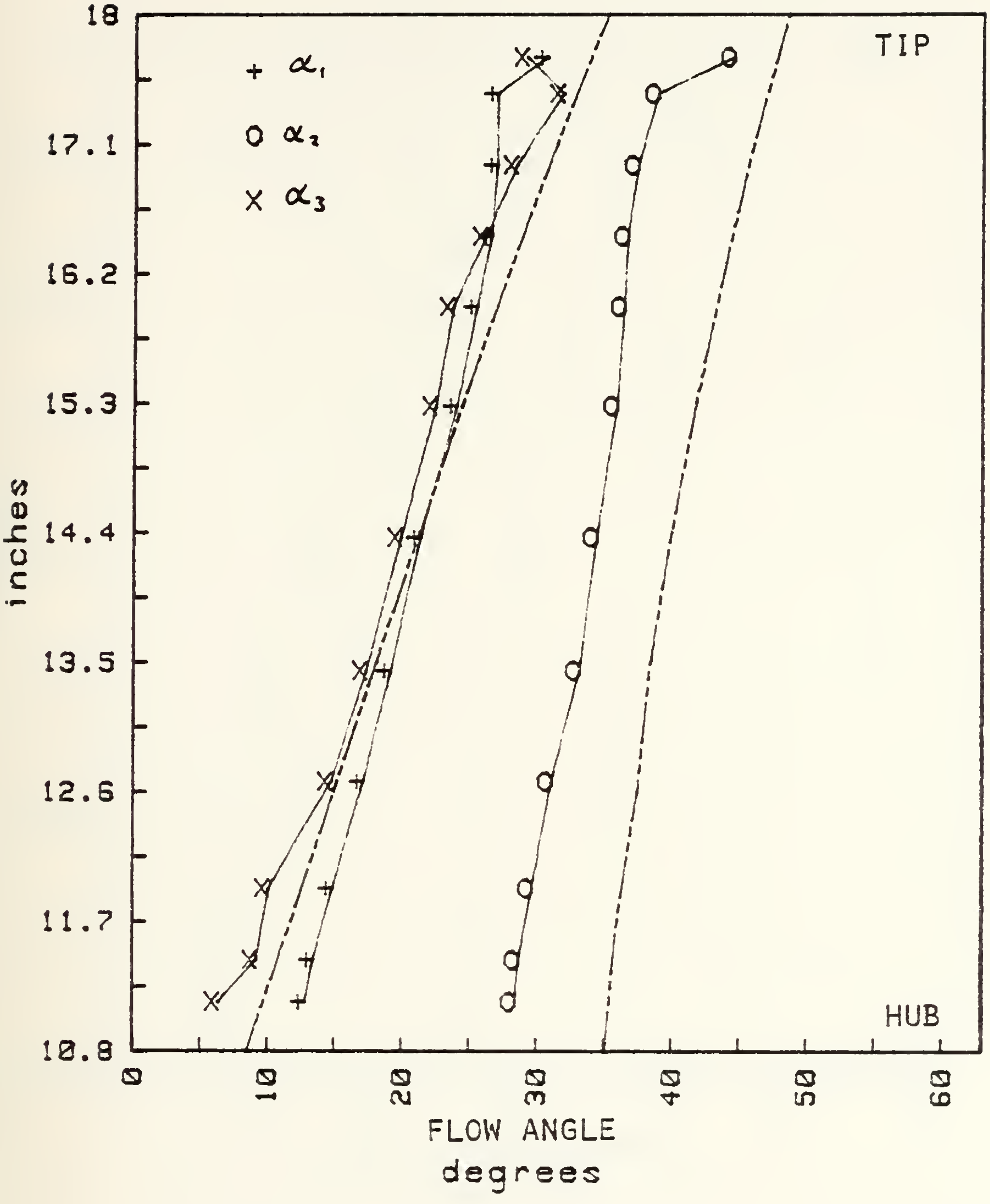

Figure 40. Off-design Measured Flow Angle Radial Distribution (IGVs 0°, S1; — - - — Design)

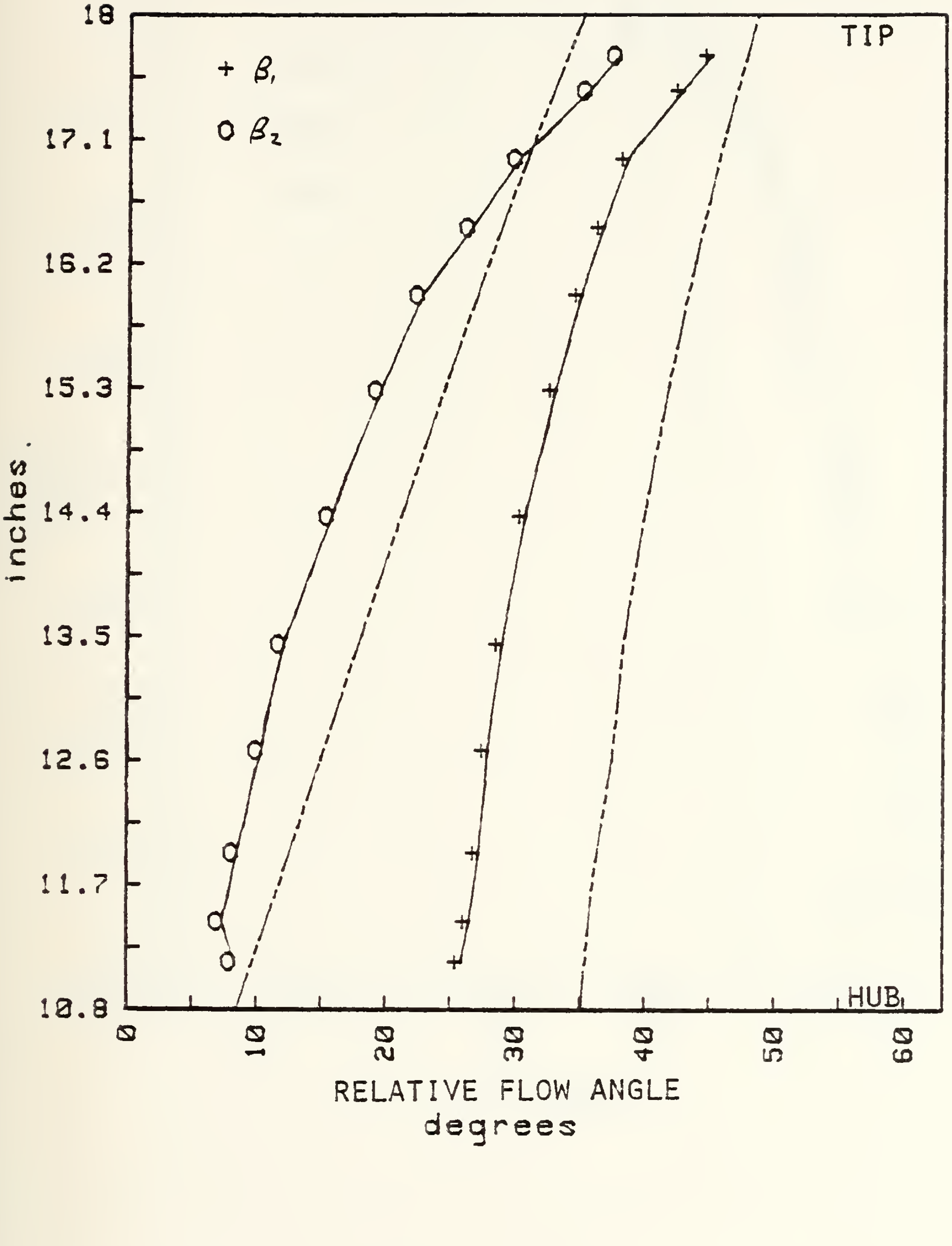

Figure 41. Off-design Relative Flow Angle Radial Distribution (IGVs 0°, S1; — - - — Design)

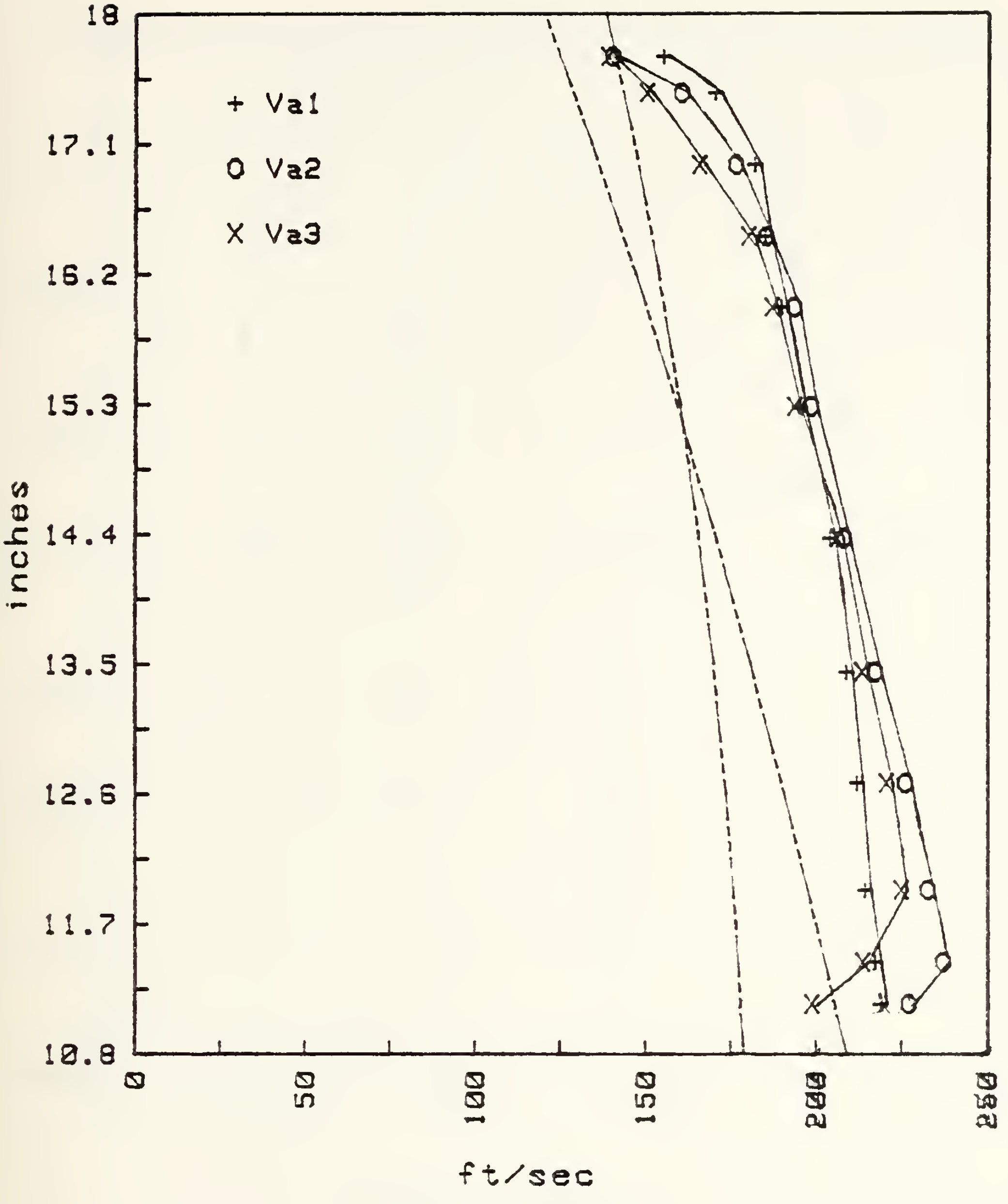

Figure 42. Off-design Axial Velocity Radial Distribution (IGVs 0°, S1; — - - - — Design)

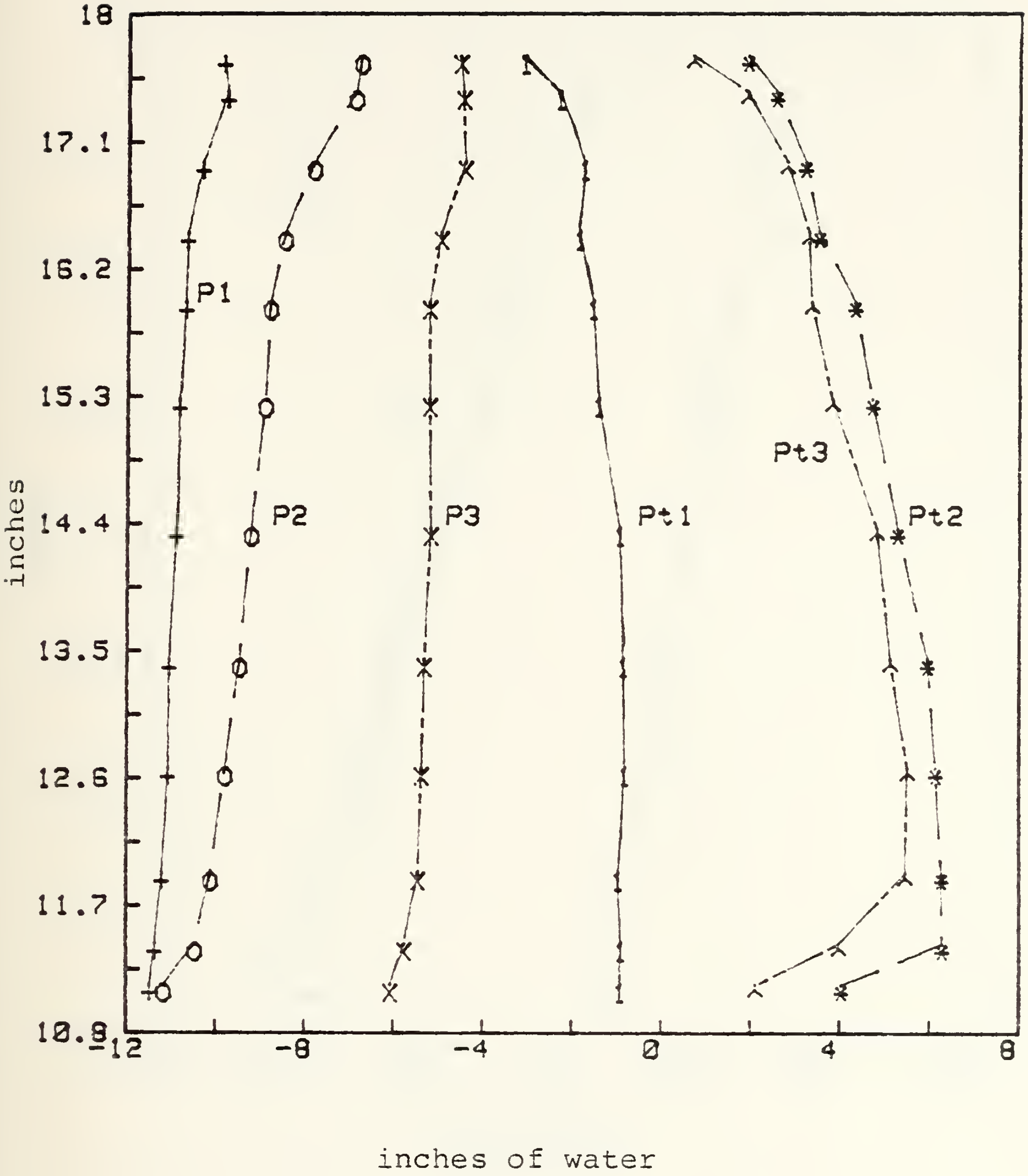

Figure 43. Off-design Intrastage Pressure Radial Distribution (IGVs 0°, S1)

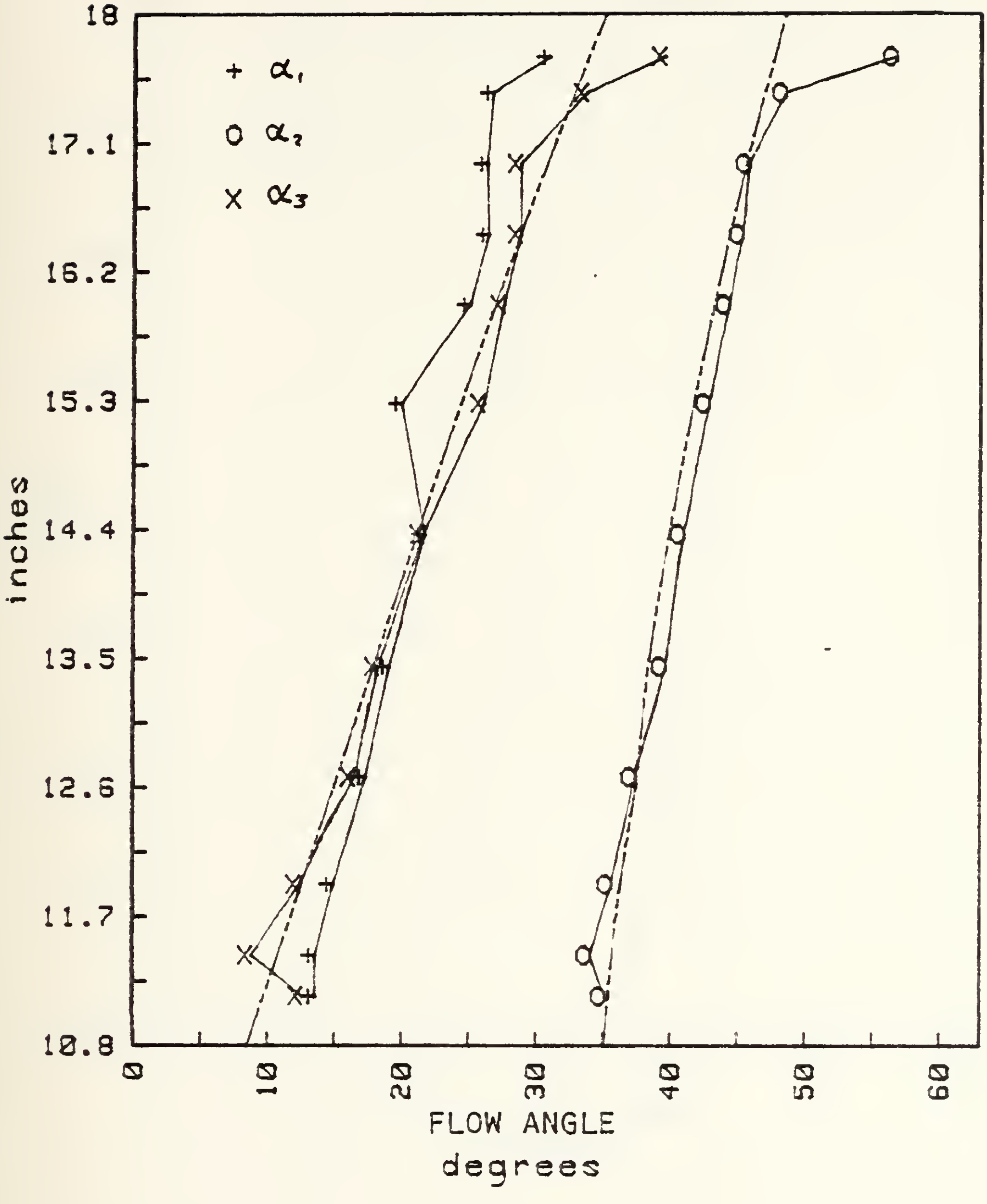

Figure 44. Off-design Measured Flow Angle Radial Distribution (IGVs 0°, S2+3+4; — - - — Design)

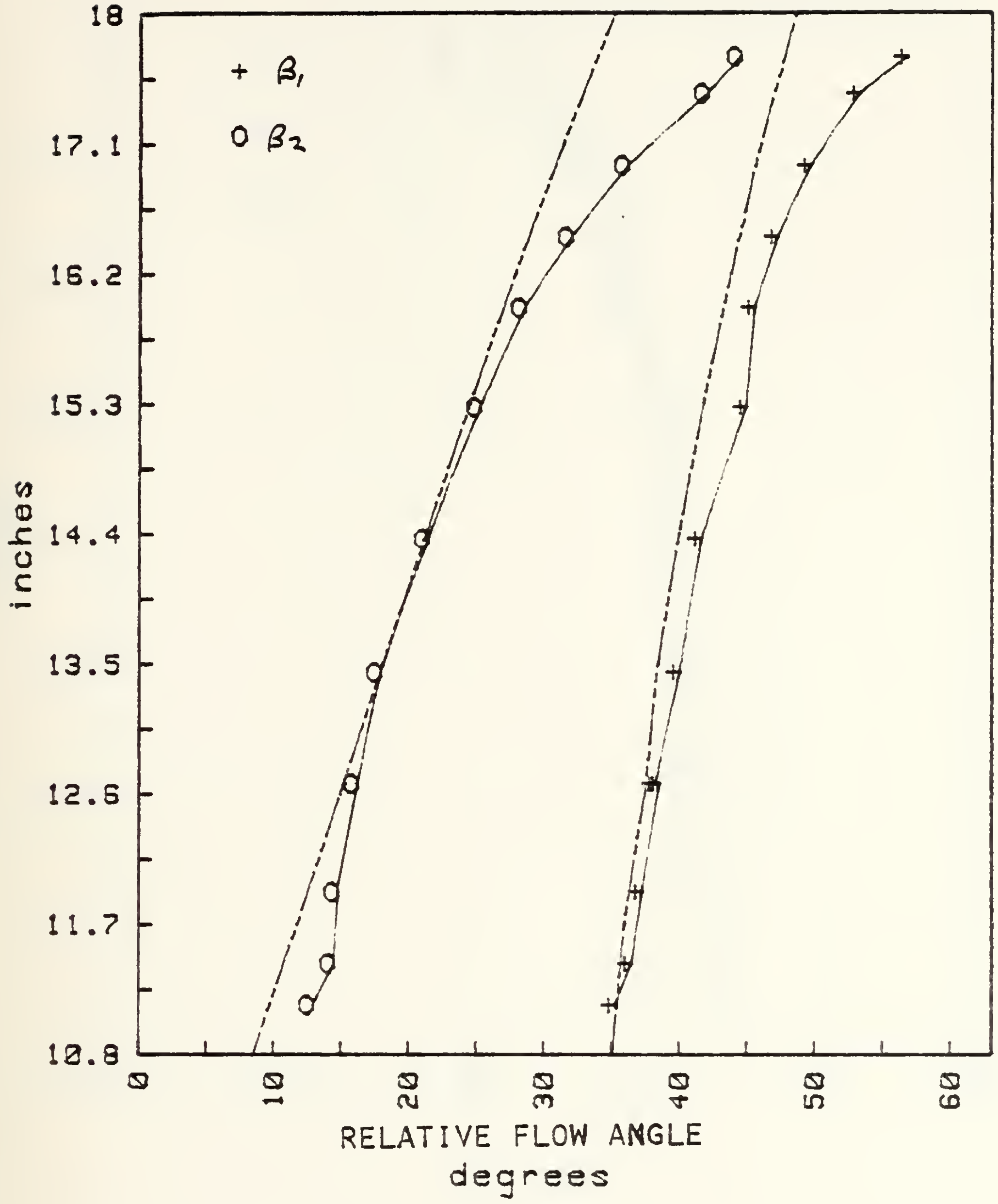

Figure 45. Off-design Relative Flow Angle Radial Distributions (IGV 0°, S2+3+4; — - - — Design)

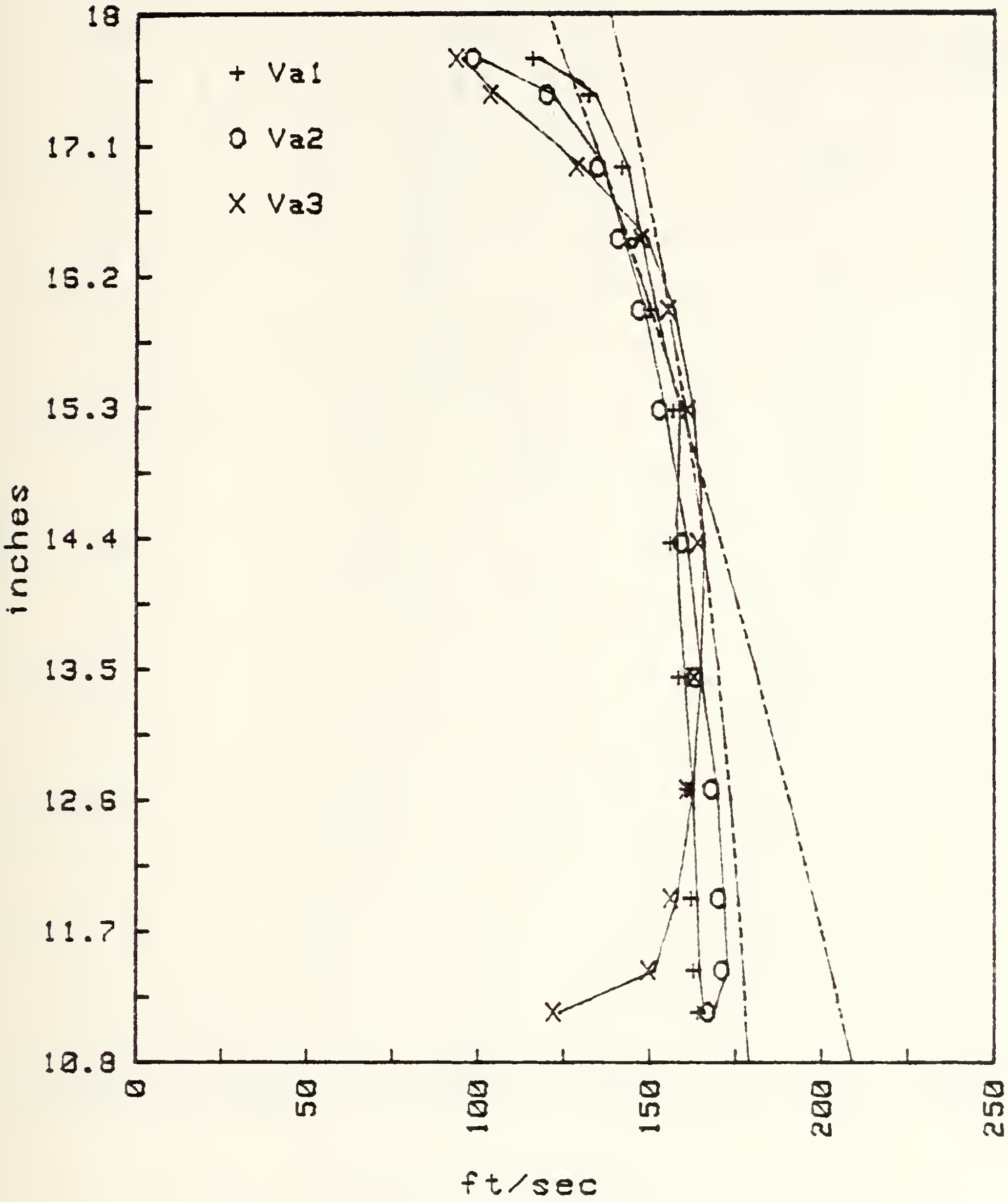

Figure 46. Off-design Axial Velocity Radial Distribution (IGVs 0°, S2+3+4; — - - — Design)

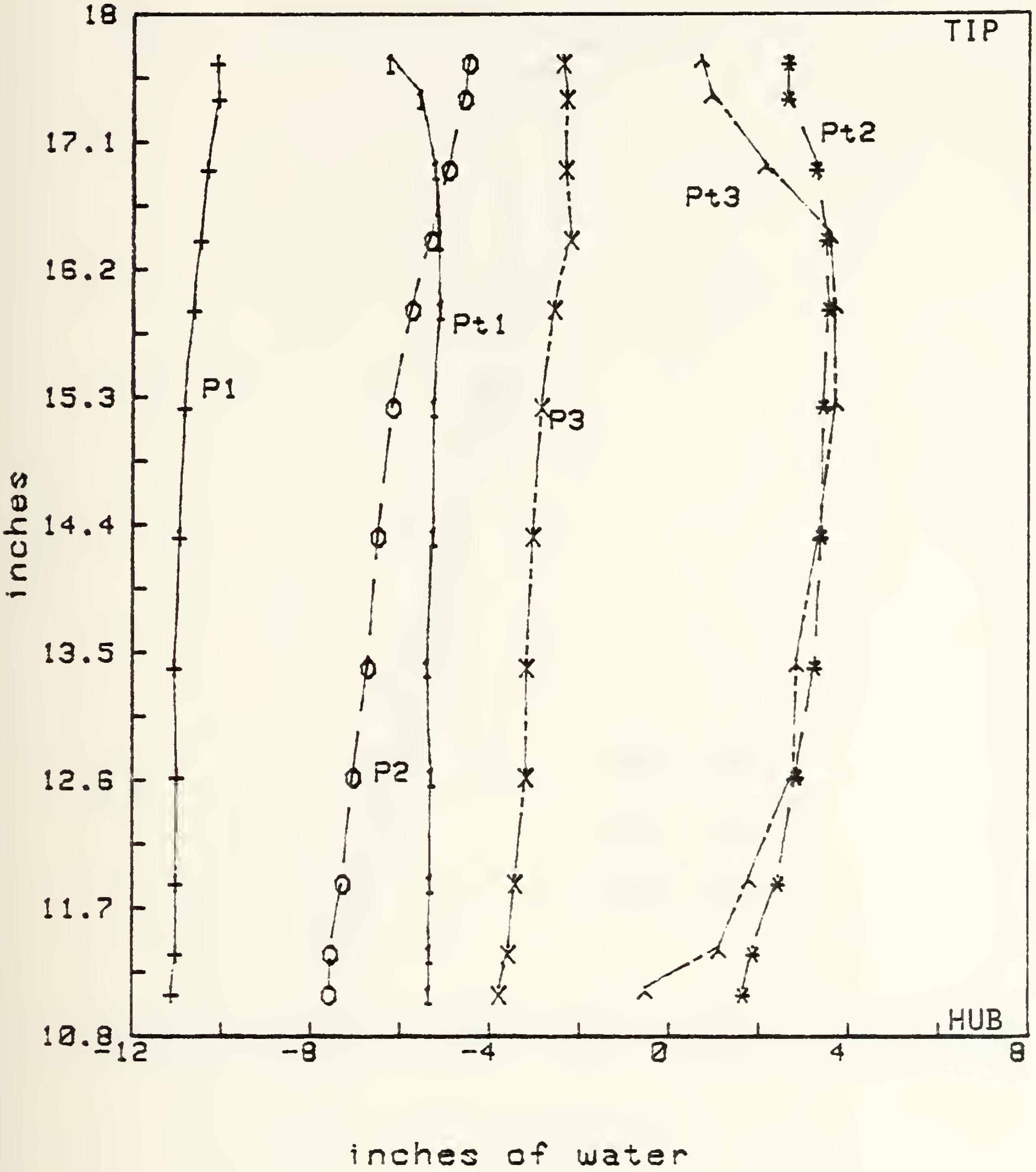

Figure 47. Off-design Intrastage Pressure Radial Distributions (IGV 0°, S2+3+4)

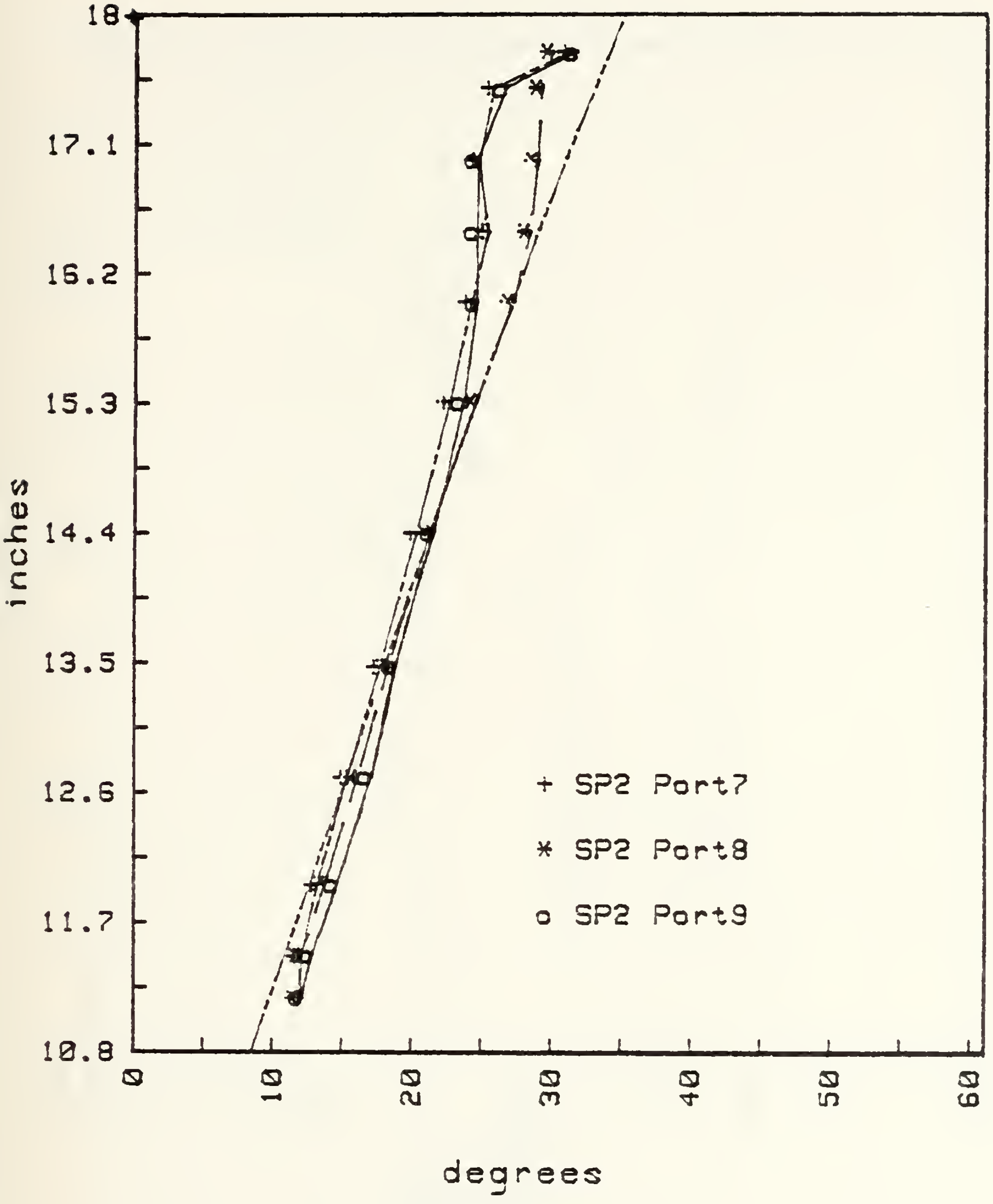

Figure 48. Comparison of Measured Flow Angle at Three Locations Relative to the Inlet Guide Vane Trailing Edge (IGVs 3°, S2+4; — - - — Design)

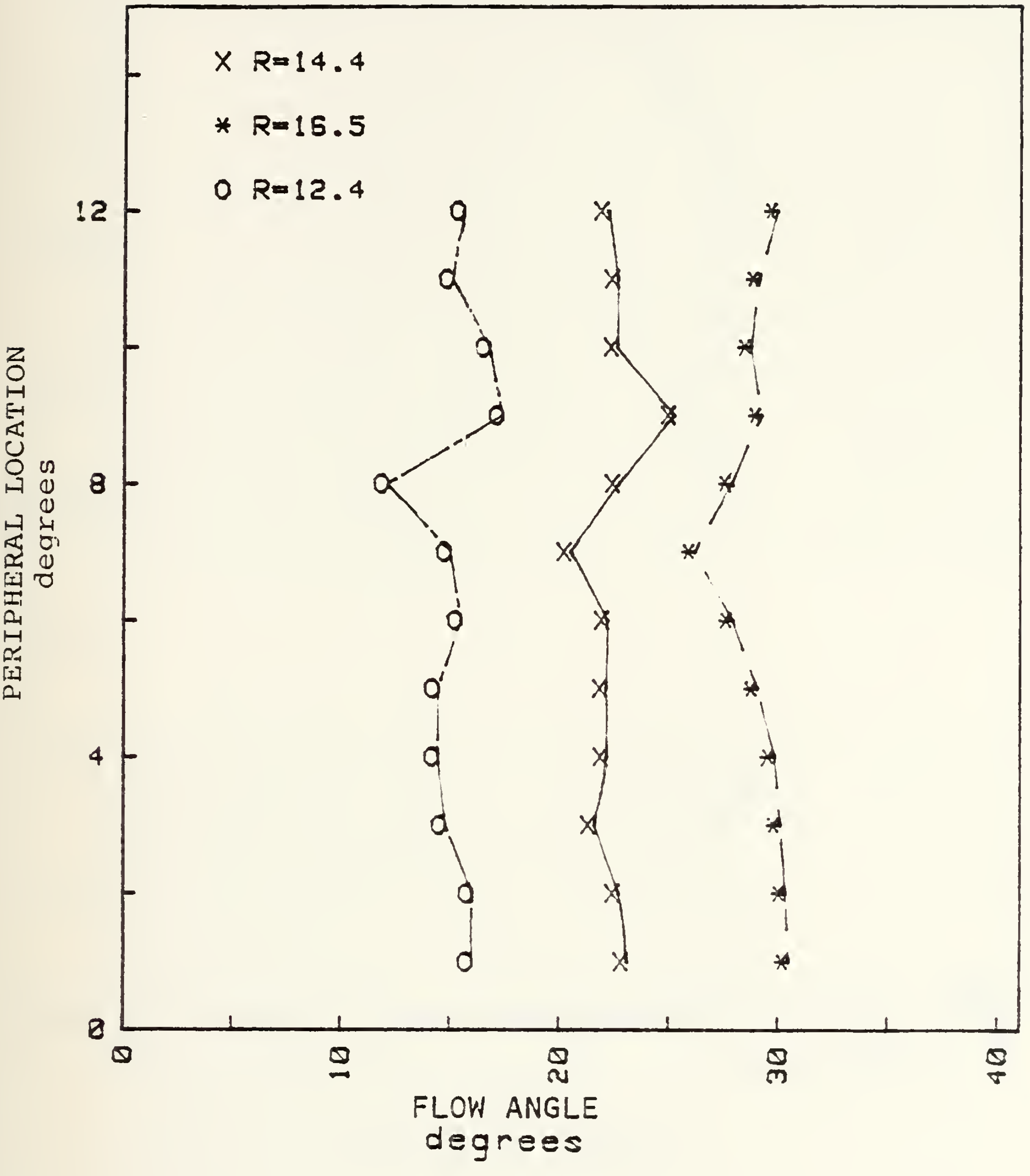

Figure 49. Stator Vane Exit Circumferential Survey at Three Radii

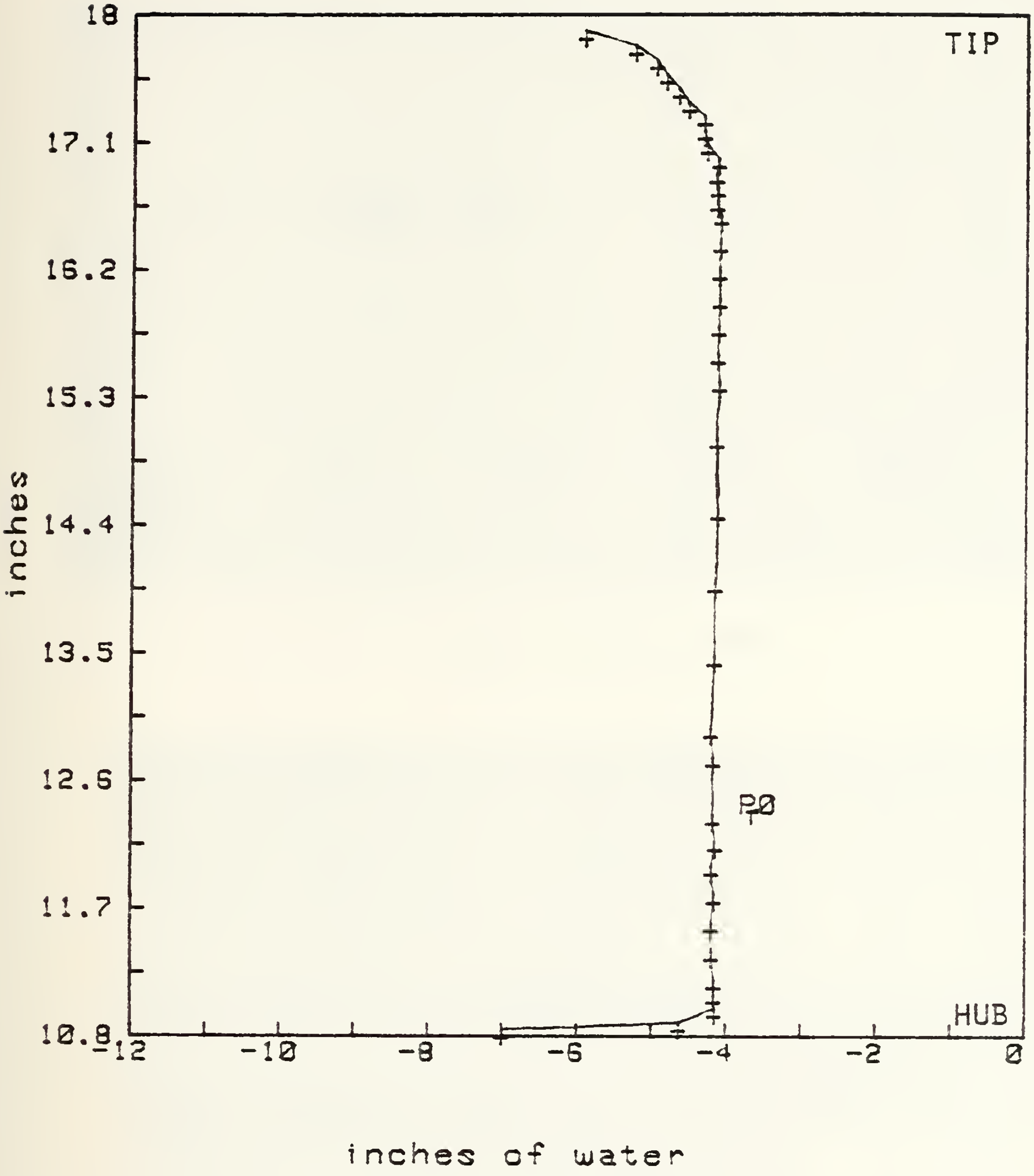

Figure 50. Inlet Total Pressure Radial Survey Results

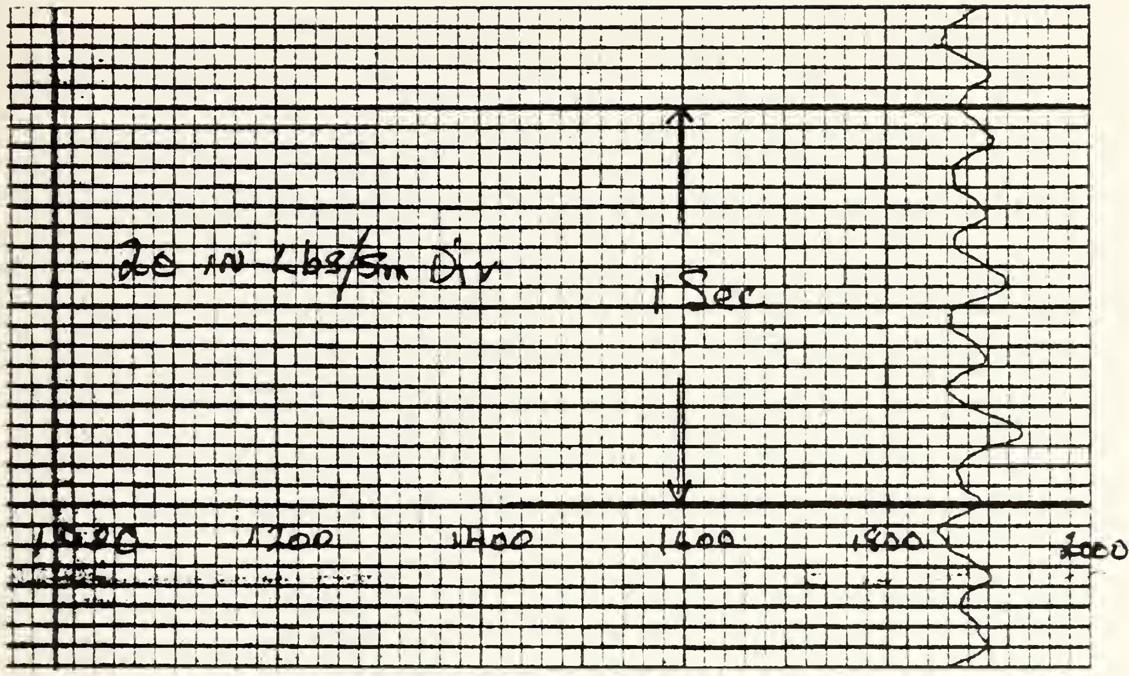

a. Torque Fluctuations

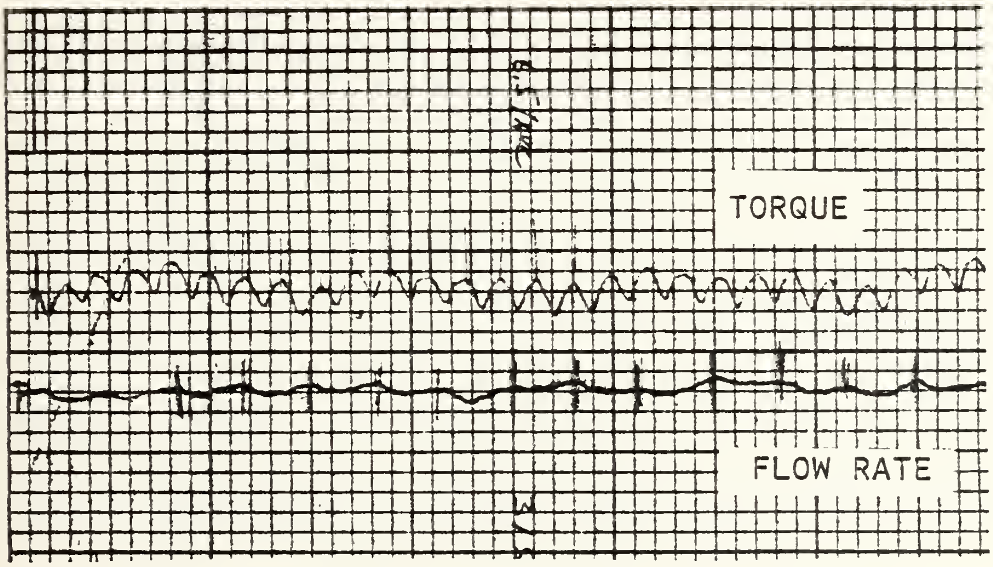

b. Torque and Flow Rate Fluctuations

Figure 51. Torque and Inlet Nozzle Pressure Fluctuations with Time

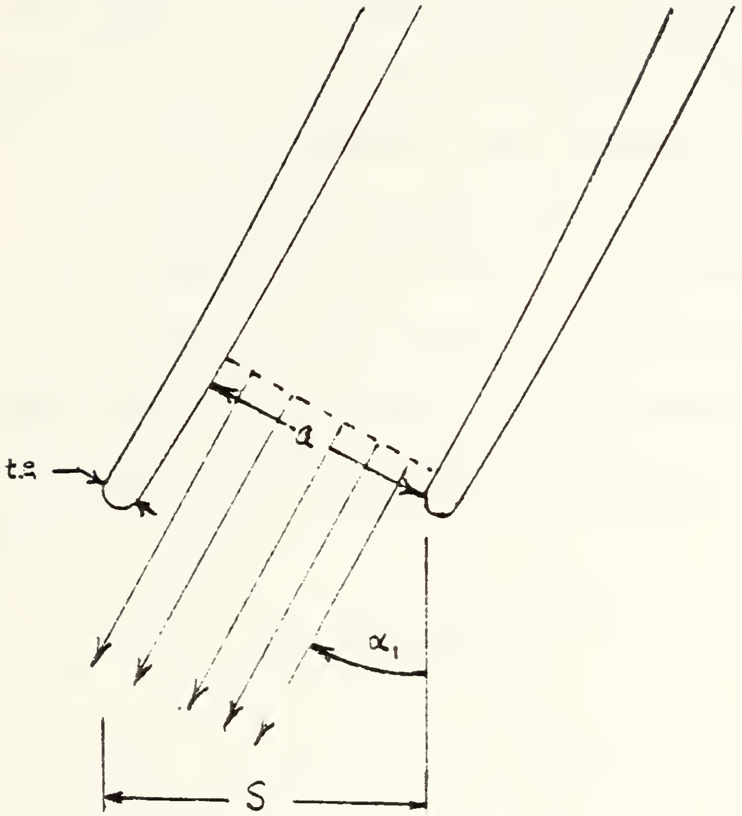

Figure 52. Schematic of Guide Vane Exit Geometry

APPENDIX A

SURVEY PROBE CALIBRATION

The United Sensor five hole probes can be used to measure three dimensional flow velocity vector, but first they must be calibrated. All probes used in the present study were calibrated in-house. The calibration process is described in Ref. 12. The probes were inserted in a known steady, free-jet flow and the pitch angle was varied at several fixed values of the velocity. Each probe was calibrated over a range from 90 to 350 feet per second and over a pitch angle range of at least -8 to 12 degrees. Probe pressure readings, p_1 to p_5, were used to evaluate the two coefficients

$$\beta = \frac{p_1 - p_{23}}{p_1} \qquad \text{A(1)}$$

and

$$\Gamma = \frac{p_4 - p_5}{p_1 - p_{23}} \qquad \text{A(2)}$$

These coefficients are related uniquely to the pitch angle and the dimensionless velocity, X, defined as

$$X \equiv \frac{V}{\sqrt{2\, c_p\, T_t}} \equiv \sqrt{\frac{\frac{\gamma-1}{2} M^2}{1 + \frac{\gamma-1}{2} M^2}} \qquad \text{A(3)}$$

The calibration involves a determination by least squares of the polynomial coefficients in the expressions for the surfaces which relate X and ϕ to β and Γ. The probe calibration is represented totally by the expressions

$$X = \sum_{i=1}^{L} \left\{ \sum_{j=1}^{M} C_{ij} \beta^{(j-1)} \right\} \cdot \gamma^{(i-1)} \qquad A(4)$$

and

$$\phi = \sum_{i=1}^{L} \left\{ \sum_{j=1}^{M} D_{ij} \beta^{(j-1)} \right\} \cdot \gamma^{(i-1)} \qquad A(5)$$

The surface approximations are obtained from the data obtained in the calibration tests. This establishes the values of C_{ij} and D_{ij}. When using the probe in the compressor, the measured values of p_1 to p_5 are used to calculate β and Γ from Eq. A(1) and Eq. A(2), and X and ϕ are then calculated from Eq. A(4) and Eq. A(5).

The generalized method used to derive the polynomial surface fits permitted the selection of the degree of the polynomial required. The selection was changed until the errors in the approximation were minimized. This was judged to have occurred when the differences between the values of velocity and pitch angle set in the calibration tests, and those calculated from Eq. A(1), A(2), A(4) and A(5) using probe pressure data, were least in the range of interest.

The probe coefficients and errors are given in Tables A1-A3. The three probes are identified by Serial Number 538, Serial Number 539 or "SMITH" (Serial Number unknown).

Table Ala. "SMITH" Probe Coefficients

$X = X(\beta,\Gamma)$

.017721	4.914135	-129.64795	2160.5117	-13594.146
-.012998	1.051538	-17.72818	-171.37476	4080.9478
-.128845	15.423376	-566.573	8227.793	-41897.953
-.23318	24.982849	-822.625	9909.4101	-37524.703

$\phi = \phi(\beta,\Gamma)$

9.470694	20.380249	-425.7713
50.877502	1288.4583	-13388.74
54.471558	6410.3359	16413.375
340.94336	1367.3125	687561.87
957.92676	-33787.813	2368447.
836.98584	-44216.656	2376007.

Table Alb. "SMITH" Probe Calibration Errors

Velocity Errors (Percent) at Each Point

Mach #	-8°	-6°	-4°	-2°	0°	2°	4°	6°	8°	10°	12°
.08	-.991	.670	.260	-.552	-.488	-.671	-.624	-.761	.158	-.431	.625
.12	.396	.361	.241	.239	.857	.976	.731	.078	.135	.611	-.194
.16	-.014	-.681	-.308	-.175	-.303	-.061	.003	.163	-.253	.175	-.303
.19	.233	-.123	-.448	-.157	-.086	-.204	-.292	-.447	.426	-.175	-.345
.23	-.213	.480	-.189	.678	.671	.106	.287	-.265	.013	.101	.339
.27	.079	.008	-.502	-.031	-.035	-.115	.057	-.166	-.518	-.024	.313
.30	-.072	.216	-.049	-.346	.372	.111	-.023	.120	-.172	.036	.006

Pitch Errors (Degrees) at Each Point

Mach #	-8°	-6°	-4°	-2°	0°	2°	4°	6°	8°	10°	12°
.08	-.384	-.284	.095	-.500	-.306	-.445	-.680	-.209	-.737	-.585	-.366
.12	.389	.407	.400	.505	.446	.556	.460	.808	.201	.856	.636
.16	-.180	-.035	-.220	-.083	-.183	-.109	-.055	.211	-.609	.230	.832
.19	-.270	-.003	-.144	.025	-.043	.158	.310	.395	.107	.166	.019
.23	-.016	.343	.124	-.368	.003	-.001	-.957	-.968	.084	.122	-.224
.27	.078	-.321	.117	-.351	-.043	.250	.373	-.288	-.166	.068	-.654
.30	-.011	-.063	.263	.021	-.090	-.005	.283	-.220	.169	.459	.204

Table A2a. 539 Probe Coefficients

$X = X(\beta,\Gamma)$

.017958	4.975449	-132.57974	2235.2759	-14266.232
.006145	-1.527235	84.993454	-1759.0627	12283.178
-.038944	10.301332	-706.33362	17228.191	-134440.53

$\phi = \phi(\beta,\Gamma)$

1.542056	-40.510986	442.36768	58.820313
39.597824	1622.3958	-60629.258	610474.37
-28.5937	4479.6377	-160191.12	1601539.2
490.11798	-71659.375	2483281.5	-24252884.

Table A2b. 539 Probe Calibration Errors

Velocity Errors (Percent) at Each Point

Mach #	-6°	-4°	-2°	0°	2°	4°	6°	8°	10°	12°
.09	.222	-.404	-1.306	-.975	-.969	-.030	-.336	-.394	-.797	-.042
.13	1.062	.430	.205	.414	.926	1.224	.721	.802	.421	.398
.16	.020	-.362	-.509	-.013	.169	.305	-.029	-.393	-.369	-.102
.20	-.103	-.353	-.546	-.408	-.173	-.094	-.308	-.495	-.293	-.002
.23	.684	-.007	-.040	.081	.291	.579	.142	-.036	.167	.397
.27	.252	-.527	-.648	-.029	.375	.267	.050	-.136	-.297	-.126
.30	.387	-.075	-.334	-.158	-.047	.297	.127	.100	.013	-.130

Pitch Errors (Degrees) at Each Point

Mach #	-6°	-4°	-2°	0°	2°	4°	6°	8°	10°	12°
.09	-.179	-.192	.578	.132	-.306	-.478	-.414	-.262	.061	-.453
.13	-.038	.105	-.342	.263	-.271	-.146	.604	.886	.521	.714
.16	-.071	.290	.287	.006	-.301	-.136	-.276	1.384	-.486	-.087
.20	-.271	.088	.166	.034	-.268	-.415	-.477	-.392	-.418	.063
.23	-.028	.094	-.211	.017	-.157	-.092	-.145	-.028	-.010	.211
.27	.110	-.008	-.098	.009	.197	.497	.260	.296	.167	-.134
.30	-.057	.010	.085	-.008	-.179	-.009	-.214	-.056	-.026	.004

Table A3a. 538 Probe Coefficients

$X = X(\beta,\Gamma)$

.017888	4.689008	-119.61237	1928.4517	-11789.381
.005678	-1.440922	46.716278	-413.83691	89.957031
-.089539	25.484783	-1580.9973	36027.414	-271594.37
.117867	-83.217896	6007.5342	-155905.84	1285755.7

$\phi = \phi(\beta,\Gamma)$

.646026	-120.9731	4189.3428	-45219.305
51.788132	2087.8091	-68312.375	639249.62
3.873146	4252.9238	-143912.28	1640178.5
247.91125	-48277.367	1752481.	-18214304.

Table A3b. 538 Probe Calibration Errors

Velocity Errors (Percent) at Each Point

Mach #	-8°	-6°	-4°	-2°	0°	2°	4°	6°	8°	10°	12°
.09	-.210	.047	-.612	-1.119	-.341	-.291	-.149	-.321	-.543	-.303	-.072
.12	.320	.663	.491	.420	.609	.630	.693	.359	.453	.035	.686
.16	-.162	-.086	-.167	.022	.132	.038	.121	-.194	-.236	-.454	-.187
.19	-.002	-.661	-.515	-.204	.053	-.110	-.258	-.138	-.173	-.243	.037
.23	.507	.142	.014	.122	.388	.190	-.014	.093	-.111	.260	.342
.26	-.065	-.192	-.194	-.122	.234	.103	.066	-.164	-.196	-.075	-.084
.29	.021	.131	-.162	.052	-.045	.050	.137	-.108	-.018	.000	.059

Pitch Errors (Degrees) at Each Point

Mach #	-8°	-6°	-4°	-2°	0°	2°	4°	6°	8°	10°	12°
.09	-.018	.061	-.064	-.120	.360	-.229	-.328	-.016	.231	-.206	.150
.12	.094	-.175	-.137	.060	-.077	.175	-.043	.113	.120	-.111	-.157
.16	-.138	.097	.165	.116	.118	.029	-.095	-.058	.258	.162	.060
.19	.048	.204	.018	.045	-.032	-.009	.040	.119	-.043	-.018	-.057
.23	-.204	.008	-.174	-.237	-.249	-.305	-.415	-.009	-.030	-.095	.009
.26	.060	.056	.154	.114	.199	.310	.204	.122	.195	.011	-.030
.29	-.056	.030	.004	-.090	-.057	-.147	-.092	-.057	.130	-.044	-.020

APPENDIX B

COMPRESSOR DESIGN DATA

The design data for the compressor with symmetrical blading are given in Table B1 and B2 and the calculated off-design behavior is shown in Fig. 4. Both Table B1 and B2 and Fig. 4 are from Ref. 1.

Table B1. Summary of Mid-span Design Flow Values

	Data at Mean Radius, R_m	Vavra Data
ROTOR INLET	$V_{a1}^* = V_{a1}/\omega R_m$	0.8138
	V_{u1}^*	0.3171
	W_{u1}^*	0.6829
	V_1^*	0.8734
	W_1^*	1.0624
	α_1	21.288
	β_1	40.0
	$\Delta V_u^* = V_{a2}/\omega W_u^*$	0.38323
ROTOR EXIT	$V_{a2}^* = V_{a2}/\omega R_m$	0.8380
	V_{u2}^*	0.7003
	W_{u2}^*	0.2997
	V_2^*	1.0921
	W_2^*	0.8900
	α_2	39.886
	β_2	19.68

Table B2. Summary of Off Design Calculations

β_1'	30.0	32.0	36.0	40.0	45.0	50.0
δ	9.79	9.89	11.11	10.39	10.83	11.36
β_2'	19.51	19.68	20.06	20.496	21.133	21.85
$V_{a1}^{*'} = V_{a2}^{*'} = \phi$	1.0520	1.0020	0.9094	0.8250	0.7284	0.6392
ΔV_u^*	0.2339	0.2670	0.3280	0.3832	0.4462	0.5048
Y'	0.0625	0.049	0.032	0.028	0.033	0.064
$\bar{\eta}_t'$	0.6025	0.7421	0.8753	0.9144	0.9221	0.8798
$\bar{\pi}_{t3}$	0.1345	0.1891	0.2740	0.3345	0.3927	0.3927
L'/L	0.778	0.846	0.943	1.00	1.028	0.946

APPENDIX C

EXPERIMENTAL DATA FROM BUILD 1

Performance data from build one is shown in Fig. 5 and mid-span velocities are listed in Table C1.

Table C1. Build 1 Velocities at Mid-Span

Screen	Alpha 1	Phi 1	V1
0	18.38	-3.22	159.9
1	18.00	-3.79	169.5
2	19.05	-2.92	174.3
3	19.06	-3.24	177.9
2+3	19.05	-.238	176.6
4	19.05	-3.27	174.5
5	19.08	-3.06	172.9
A	19.08	-3.46	155.5
1+A	19.06	-3.39	151.2
1+5	19.07	-3.12	169.1

Screen	Alpha 2	Phi 2	V2
0	31.67	1.34	250.3
1	32.67	.70	244.5
2	33.42	.97	239.9
3	34.78	.79	232.0
2+3	36.18	.58	222.6
4	36.67	.58	218.5
5	37.69	.58	216.0
A	41.18	.44	199.5
1+A	41.68	.84	198.5
1+5	37.93	.41	212.2

Table C1 (Continued)

Screen	Alpha 3	Phi 3	V3
0	20.30	-.01	201.3
1	20.30	-.00	196.9
2	20.30	-.00	193.0
3	19.60	.00	188.9
2+3	19.60	-.00	185.7
4	19.60	.01	182.3
5	19.60	.01	179.6
A	22.20	.01	131.7
1+A	22.20	.01	124.6
1+5	19.40	.01	173.9

APPENDIX D

INTEGRATION OF EXIT RAKES

The two total pressure rakes each consisted of twelve simple pneumatic tubes mounted radially along a common shaft as shown in Fig. D1. The distribution of sensors reflects the relatively even distribution of total pressure expected over most of the flow channel and the more rapidly changing conditions expected to occur near the hub and tip. The uneven radial distribution of sensors made averaging the pressure readings less convenient. Twenty equal flow areas were defined as shown in Fig. D2 and the value of the pressure for each of these areas was assigned based on the relevant probe pressure (Table D1). From the total pressure, assuming a uniform static pressure gradient from hub to tip, the relative mass flows for each area were determined. The mass flow weighted average total pressure was then calculated using the relationship

$$\overline{P}_t = \frac{\sum_{i=1}^{20} \dot{m}_i \, P_{t_i}}{\sum_{i=1}^{20} \dot{m}_i} \qquad D(1)$$

where

$$\dot{m}_i = A_i \sqrt{2\rho (P_{t_i} - P)} \qquad D(2)$$

Table D1. Sub-Area Pressure Determination from Probe Pressures

$P_t(1) = (\frac{1}{2}(P_t(1) + P_{hub}) + (P_t(1) + P_t(2)))/3$

$P_t(2) = P_t(2)$

$P_t(3) = P_t(3)$

$P_t(4) = (P_t(3) + P_t(4))/2$

$P_t(5) = P_t(4)$

$P_t(6) = (P_t(4) + P_t(5))/2$

$P_t(7) = (P_t(5) + P_t(6))/2$

$P_t(9) = P_t(6)$

$P_t(10) = (P_t(7) + P_t(6))/2$

$P_t(11) = P_t(10)$

$P_t(12) = P_t(7)$

$P_t(13) = (P_t(7) + P_t(8))/2$

$P_t(14) = P_t(8)$

$P_t(15) = (P_t(8) + P_t(9))/2$

$P_t(16) = (P_t(9) + P_t(10))/2$

$P_t(17) = P_t(10)$

$P_t(18) = (P_t(10) + P_t(11))/2$

$P_t(19) = P_t(11)$

$P_t(20) = (P_t(12) + P_{tip})/2$

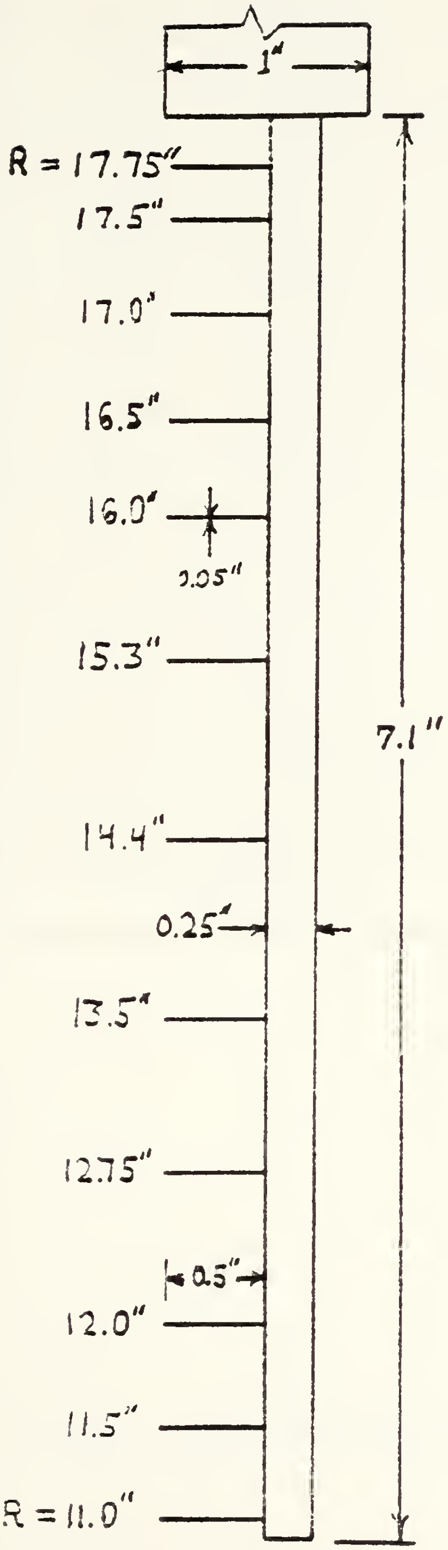

Figure D1. Total Pressure Rake Geometry

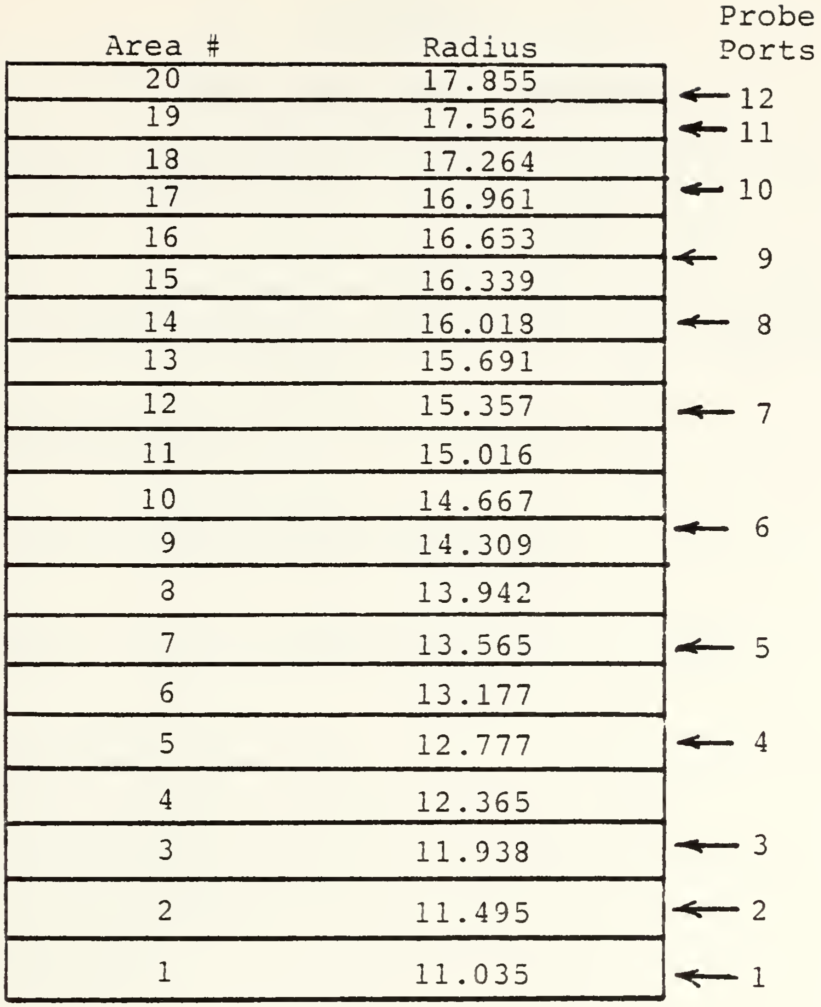

Figure D2. Pressure Mass Averaging Area Divisions

APPENDIX E

DATA REDUCTION EQUATIONS

$$\rho_0 = P_{amb} \cdot 5.1967/\left((T + 459.67) \cdot R\right)$$

$$\dot{m} = C_D \beta_N A_I \sqrt{2\rho_0\left(P_{t_I} - P_I\right) \cdot 5.1967} \left[1 - \frac{3}{4\gamma} \frac{P_{t_I} - P_I}{P_I}\right]$$

$$\bar{\phi} = \dot{m}/\left(\rho_0 \cdot A_C \cdot U_m\right)$$

$$\bar{\pi}_{t3} = \left(\bar{P}_{t8} - \bar{P}_{t1}\right) \cdot 5.1967/\left(\rho_0 U_m^{\ 2}\right)$$

$$\pi_i = \left(P_i - P_{t1}\right) \cdot 5.1967/\left(\rho_0 U_m^{\ 2}\right)$$

$$HP = \frac{2\pi}{60} RPM \cdot Tq/550/12$$

$$\overline{\underline{X}} = 2HP \cdot 550/\dot{m}\, U_m^{\ 2}$$

$$\bar{\eta}_t = \pi_{t3}/\overline{\underline{X}}$$

$$V_a = V \cos \alpha \cos \phi$$

$$V_u = V \sin \alpha$$

$$\beta = \tan^{-1}\left[\left(U - V_u\right)/V_a\right]$$

$$W = V_a/(\cos \beta \cos \phi)$$

$$U = \frac{2\pi}{60} RPM \cdot R/12$$

Note: Units are ρ (slugs/ft^3), P (ins water), T (°F), $\dot{m}$ (slugs/sec), Tq (in lb), R (in), velocities (ft/sec).

APPENDIX F

DATA REDUCTION SOFTWARE

```
10   !            ***** REDPLT ****
20   ! REDUCES DATA TAKEN BY GENUSE MOD1/MOD2
30   OPTION BASE 1
40   SHORT Phi1(64),V1(64),V2(64),Alfa1(64),Alfa2(64),Alfa3(64),Va1(64),Va2(64),
Va3(64),U(64),W1(64),W2(64),Beta1(64),Beta2(64),Betdel(64),Vudel(64),Mflw
50   SHORT Allsv(64,96),Allch(64,40),Phi3(64),Radius(64),V3(64),T(64),T3(64),Phi
2(64),Rho0(64),Pit3(64),Eta(64),X
60   SHORT Pt1(12),Pt8(12),Pt1av,Pt8av,Powr(64),Etaav(64),Cpt3(64),Cflwav(64),Cw
ork
70   DIM Nrdf$(10),Cx(4,5),Dx(6,3),Cy(4,5),Dy(4,4),Cz(3,5),Dz(4,4),Title$(13),Ti
tlx$(10),Titly$(10),Sym$(1)
80   !  READ THE DATA FILE
90   INPUT "DATA FILE NAME?",Nrdf$
100  INPUT "# of DATA POINTS?",Points
110  INPUT "TOTAL S/V PORTS?",Ports
120  INPUT "TOTAL NON-S/V CHANNELS?",Chans
130  REDIM Allsv(Points,Ports),Allch(Points,Chans)
140  ASSIGN #1 TO Nrdf$
150  MAT READ #1;Allsv,Allch
151  !  READ THE PROBE COEFFICIENTS
160  ASSIGN #2 TO "CALPRB:T14"
170  MAT READ #2;Cx,Dx,Cy,Dy,Cz,Dz
180  DEG
190  PRINTER IS 16
200    PRINT "       I  Cflow  POWER   Cwork  Cpt3   Etaav  Etats    T    T3-T  P
rise"
210  ! ************* ASSIGN VARIABLES TO DATA CHANNELS*************
220  FOR I=1 TO Points
230  Pamb=29.30*70.5190/5.1967         ! in H20
240  Ptare1=Allsv(I,1)
250  Ptare2=Allsv(I,45)
260  Px1=(Allsv(I,47)-Ptare2)*10000+Pamb  ! First Probe
270  Px23=(Allsv(I,48)-Ptare2)*10000+Pamb
280  Px4=(Allsv(I,49)-Ptare2)*10000+Pamb
290  Px5=(Allsv(I,50)-Ptare2)*10000+Pamb
300  Py1=(Allsv(I,51)-Ptare2)*10000+Pamb  ! Second Probe
310  Py23=(Allsv(I,52)-Ptare2)*10000+Pamb
320  Py4=(Allsv(I,53)-Ptare2)*10000+Pamb
330  Py5=(Allsv(I,54)-Ptare2)*10000+Pamb
340  Pz1=(Allsv(I,55)-Ptare2)*10000+Pamb  ! Third Probe
350  Pz23=(Allsv(I,56)-Ptare2)*10000+Pamb
360  Pz4=(Allsv(I,57)-Ptare2)*10000+Pamb
370  Pz5=(Allsv(I,58)-Ptare2)*10000+Pamb
380  Rpm=1616                              ! RPM
390  Ptnoz=(Allsv(I,3)-Ptare1)*10000+Pamb
400  Pnoz=(Allsv(I,4)-Ptare1)*10000+Pamb
410  Pos=Allch(I,10)*1000                  ! Radial Insertion
420  Alfa1(I)=Allch(I,11)*10000
430  Alfa2(I)=-Allch(I,13)*10000
440  Alfa3(I)=Allch(I,15)*10000
450  Te=Allch(I,1)
460  Te3=(Allch(I,2)+Allch(I,3))/2
471  Torq=Allch(I,9)*1000000*1.029
480  FOR K=1 TO 12                         ! Rake Pressures
490  Pt1(K)=(Allsv(I,K+6)-Ptare1)*10000
500  Pt8(K)=(Allsv(I,K+32)-Ptare1)*10000
510  NEXT K
511  Ps1=(Allsv(I,20)-Ptare1)*10000
512  Ps8=(Allsv(I,27)-Ptare1)*10000
520  ! ********REDUCTION   VELOCITY DIAGRAMS*************
530  T(I)=FNTemp(Te,32)
540  T3(I)=FNTemp(Te3,T(I))          ! REF TO T
550  Radius(I)=18-Pos
560  Um=.10472*Rpm*14.4/12
570  U(I)=Radius(I)*Um/14.4
580  Betax=(Px1-Px23)/Px1
```

```
590  Deltax=(Px4-Px5)/Px1
600  CALL Probe(Betax,Deltax,4,5,6,3,Cx(*),Dx(*),X,Phi1(I))
610  V1(I)=X*SQR(12018*(T(I)+459.67))
620  Va1(I)=V1(I)*COS(Alfa1(I))*COS(Phi1(I))
630  Vu1=V1(I)*SIN(Alfa1(I))
640  Beta1(I)=ATN((U(I)-Vu1)/Va1(I))
650  W1(I)=Va1(I)/COS(Beta1(I))/COS(Phi1(I))
660  Betay=(Py1-Py23)/Py1
670  Deltay=(Py4-Py5)/Py1
680  CALL Probe(Betay,Deltay,4,5,4,4,Cy(*),Dy(*),X,Phi2(I))
690  V2(I)=X*SQR(12018*(T3(I)+459.67))
700  Va2(I)=V2(I)*COS(Alfa2(I))*COS(Phi2(I))
710  Vu2=V2(I)*SIN(Alfa2(I))
720  Beta2(I)=ATN((U(I)-Vu2)/Va2(I))
730  W2(I)=Va2(I)/COS(Beta2(I))/COS(Phi2(I))
740  Betaz=(Pz1-Pz23)/Pz1
750  Deltaz=(Pz4-Pz5)/Pz1
760  CALL Probe(Betaz,Deltaz,3,5,4,4,Cz(*),Dz(*),X,Phi3(I))
770  V3(I)=X*SQR(12018*(T3(I)+459.67))
780  Va3(I)=V3(I)*COS(Alfa3(I))*COS(Phi3(I))
790  Vudel(I)=Vu1-Vu2                !CHANGE IN CIRCUMFERENTIAL COMPONENT
800  Betdel(I)=Beta1(I)-Beta2(I)    ! TURNING IN ROTOR
810  ! *************  PERFORMANCE ******************
820  Rho0(I)=Pamb*5.1967/((T(I)+459.67)*1716.56)
830  Mflw=1.026*7.0685*SQR(2*Rho0(I)*(Ptnoz-Pnoz)*5.1967)*(1-.535714*(Ptnoz-Pnoz
)/Ptnoz)
840  Cflwav(I)=Mflw/(Rho0(I)*4.53389*Um)
850  CALL Ptavg(Pamb,Ps1,Rho0(I),Pt1(*),Pt1av)
860  CALL Ptavg(Pamb,Ps8,Rho0(I),Pt8(*),Pt8av)
861  Rst=(Py23-Px23)/(Pz23-Px23)
862  Prise=(Pt8av+Pamb)/(Pt1av+Pamb)
870  Cpt3(I)=2*(Pt8av-Pt1av)*5.1967/(Rho0(I)*Um^2)
872  Cp=2*-Pt1av*5.1967/(Rho0(I)*Um^2)
880  Powr(I)=.10472*Rpm*Torq/550/12/55
890  Cwork=2*Powr(I)*550/(Mflw*Um^2)*55
900  Etaav(I)=Cpt3(I)/Cwork
910    PRINT USING "5X,2D,2D.4D,4D.3D,4(2D.4D),4D.2D,3D.2D,3D.3D";I,Cflwav(I),Po
wr(I)*55,Cwork,Cpt3(I),Etaav(I),Eta(I),T(I),T3(I)-T(I),Prise
930  NEXT I
940   PRINTER IS 0
960  ! *********** TABULAR VELOCITY DATA ***************
970  PRINT "Sta.1 Velocities"
980  PRINT "Radial Pos";"  V1 ft/sec";"  Alfa1 deg";"   Phi1 deg";"          Va1";
"        W1 ";"    Beta1"
990  FOR I=1 TO Points
1000 PRINT USING "7(7D.3D)";Radius(I),V1(I),Alfa1(I),Phi1(I),Va1(I),W1(I),Beta1(
I)
1010 NEXT I
1020 PRINT "  "
1030 PRINT "  "
1031 PAUSE
1040 PRINT "Sta.2 Velocities"
1050 PRINT "Radial Pos";"  V2 ft/sec";"      Alfa2";"   Phi2 deg";"        Va2";"
      W2 ";"    Beta2 "
1060 FOR I=1 TO Points
1070 PRINT USING "7(7D.3D)";Radius(I),V2(I),Alfa2(I),Phi2(I),Va2(I),W2(I),Beta2(
I)
1080 NEXT I
1090 PRINT "  "
1100 PRINT "  "
1110 PRINT "Sta.3 Velocities"
1120 PRINT "Radial Pos";"          V3";"       Alfa3";"        Phi3";"          Va3"
1130 FOR I=1 TO Points
1140 PRINT USING "5(7D.3D)";Radius(I),V3(I),Alfa3(I),Phi3(I),Va3(I),Vudel(I)
1150 NEXT I
1210 PRINTER IS 16
```

```
1211 ! ******  PLOTS OF DATA ******
1220 RAD
1230 DISP "FOR PLOTS OF DATA PRESS CONT "
1240 PAUSE
1250 ! ************** PLOT PERFORMANCE PARAMETERS **************
1260 PLOTTER IS "GRAPHICS"
1270 ! PLOTS AXIAL VELOCITY DISTRIBUTION
1280 Titles$="PERFORMANCE "
1290 Titlx$="Phi "
1300 Titly$=" "
1310 DATA .5,.4  ,1.2,1.0,.1,.1
1320 READ Xmin,Ymin,Xmax,Ymax,Xtic,Ytic
1330 GRAPHICS
1340 CALL Setup(Titles$,Titlx$,Titly$,Xmin,Ymin,Xmax,Ymax,Xtic,Ytic)
1350 Sym$="+"
1360 CALL Pltr(Sym$,1,Points,Cflwav(*),Cpt3(*))
1370 Sym$="O"
1380 CALL Pltr(Sym$,1,Points,Cflwav(*),Powr(*))
1390 Sym$="X"
1400 CALL Pltr(Sym$,1,Points,Cflwav(*),Etaav(*))
1410 LETTER
1420 EXIT GRAPHICS
1430 DUMP GRAPHICS
1431 PAUSE
1440 PLOTTER IS "GRAPHICS"
1450 PRINT PAGE
1460 ! ************* PLOT ANGLES ********************
1470 Titles$="FLOW ANGLES"
1480 Titlx$="Phi "
1490 Titly$="degrees"
1500 DATA .5, 0,1.2,60,.1,5
1510 READ Xmin,Ymin,Xmax,Ymax,Xtic,Ytic
1520 CALL Setup(Titles$,Titlx$,Titly$,Xmin,Ymin,Xmax,Ymax,Xtic,Ytic)
1530 Sym$="+"
1540 GRAPHICS
1550 CALL Pltr(Sym$,1,Points,Cflwav(*),Alfa1(*))
1560 Sym$="O"
1561 CALL Pltr(Sym$,1,Points,Cflwav(*),Alfa2(*))
1562 Sym$="X"
1565 CALL Pltr(Sym$,1,Points,Cflwav(*),Alfa3(*))
1570 LETTER
1580 EXIT GRAPHICS
1600 DUMP GRAPHICS
1610 !
1620 END
1630 !
1640 ! PROBE DATA REDUCTION SUBROUTINE
1650 SUB Probe(Beta,Delta,Ci,Cj,Di,Dj,C(*),D(*),SHORT X,Phi)
1660 OPTION BASE 1
1670 Gama=Delta/Beta
1680 X=FNVel(Gama,Beta,Ci,Cj,C(*))
1690 Phi=FNPhi(Gama,Beta,Di,Dj,D(*))
1700 SUBEND
1710 ! FUNCTION Vel
1720 DEF FNVel(Gam,Del,Ci,Cj,C(*))
1730 OPTION BASE 1
1740 X=0
1750 FOR I=1 TO Ci
1760 Tem=0
1770 FOR J=1 TO Cj
1780 Tem=Tem+C(I,J)*Del^(J-1)
1790 NEXT J
1800 X=X+Tem*Gam^(I-1)
1810 NEXT I
1820 RETURN X
1830 FNEND
```

```
1840 ! FUNCTION Phi
1850 DEF FNPhi(Gam,Del,Di,Dj,D(*))
1860 OPTION BASE 1
1870 P=0
1880 FOR I=1 TO Di
1890 Tem=0
1900 FOR J=1 TO Dj
1910 Tem=Tem+D(I,J)*Del^(J-1)
1920 NEXT J
1930 P=P+Tem*Gam^(I-1)
1940 NEXT I
1950 RETURN P
1960 FNEND
1970 ! FUNCTION Temp  CONVERTS VOLTAGE TO TEMP FOR `J` TYPE THERMOCOUPLES
1980 DEF FNTemp(Volt,SHORT Junc)
1981 Junct=(Junc-32)/1.8
1990 J1=5.0373743E1
2000 J2=3.0167011E-2
2010 J3=-7.4293513E-5
2020 Val=Volt+1E-6*((J3*Junct+J2)*Junct+J1)*Junct
2030 C0=-.48868252
2040 C1=19873.14503
2050 C2=-218614.5353
2060 C3=11569199.78
2070 C4=-264917531.4
2080 C5=2018441314
2090 Tc=((((C5*Val+C4)*Val+C3)*Val+C2)*Val+C1)*Val+C0
2100 Tf=Tc*1.8+32                  ! TEMP IN DEG F
2110 RETURN Tf
2120 FNEND
2130 ! SUBROUTINE Ptavg MASS FLOW WEIGHTED AVERAGE
2150 SUB Ptavg(Pamb,Ps,SHORT Rho,Pt(*),Pbar)
2160 OPTION BASE 1
2170 SHORT P(20)
2181 P(1)=Pt(1)
2182 P(2)=Pt(2)
2183 P(3)=Pt(3)
2184 P(4)=(Pt(4)+Pt(3))/2
2185 P(5)=Pt(4)
2186 P(6)=(Pt(4)+Pt(5))/2
2187 P(7)=Pt(5)
2188 P(8)=(Pt(6)+Pt(5))/2
2189 P(9)=Pt(6)
2190 P(10)=.667*Pt(6)+.333*Pt(7)
2191 P(11)=.667*Pt(7)+.333*Pt(6)
2192 P(12)=Pt(7)
2193 P(13)=(Pt(8)+Pt(7))/2
2194 P(14)=Pt(8)
2195 P(15)=(Pt(8)+Pt(9))/2
2196 P(16)=(Pt(10)+Pt(9))/2
2197 P(17)=Pt(10)
2198 P(18)=(Pt(10)+Pt(11))/2
2199 P(19)=Pt(11)
2200 P(20)=Pt(12)
2202 Mdot=0
2203 Psum=0
2210 FOR I=1 TO 20
2211  M=.22619*SQR(2*Rho*(P(I)-Ps)*5.1967)*1-.535714*(P(I)-Ps)/(P(I)+Pamb)
2212  Mdot=Mdot+M
2213  Psum=Psum+P(I)*M
2214 NEXT I
2220  Pbar=Psum/Mdot
2240 SUBEND
2250 !
2260 ! DRAW AXES AND LABEL TITLES
2270 SUB Setup(Title$,Titlx$,Titly$,Xmin,Ymin,Xmax,Ymax,Xtic,Ytic)
```

```
2280 DIM Title$(13),Titlx$(10),Titly$(10)
2290 CSIZE 3.3
2300 LIMIT 10,170,0,149
2310 MOVE 50,98
2320 LORG 6
2330 LABEL USING "K";Title$
2340 CSIZE 3.0
2350 MOVE 50,0
2360 LORG 4
2370 LABEL USING "K";Titlx$
2380 MOVE 10,50
2390 LDIR PI/2
2400 LORG 6
2410 LABEL USING "K,X";Titly$
2420 LOCATE 20,100*RATIO,10,90
2430 SCALE Xmin,Xmax,Ymin,Ymax
2440 FRAME
2450 AXES Xtic,Ytic,Xmin,Ymin
2460 LDIR 0
2470 LORG 8
2480 CSIZE 2.5
2490 FOR I=Ymin TO Ymax STEP 2*Ytic
2500 MOVE Xmin,I
2510 LABEL USING "K,X";I
2520 NEXT I
2530 LORG 8
2540 LDIR PI/2
2550 FOR I=Xmin TO Xmax STEP 2*Xtic
2560 MOVE I,Ymin
2570 LABEL USING "K,X";I
2580 NEXT I
2590 LDIR 0
2600 SUBEND
2610 ! PLOT DATA POINTS WITH (1) OR WITHOUT (2) LINES
2620 SUB Pltr(Sym$,Lintyp,Point,SHORT X(*),Y(*))
2630 OPTION BASE 1
2640 LINE TYPE Lintyp
2650 FOR I=1 TO Point
2660 PLOT X(I),Y(I),1
2670 LABEL USING "A";Sym$
2680 PENUP
2690 NEXT I
2700 PENUP
2710 SUBEND
```

APPENDIX G

SUMMARY OF TEST PROGRAMS

Date	Purpose
11 June 82	Comparisons of probes
16 June 82	Performance map. 0° IGV
13 July 82	(1) Examination of flow angles at 17" radius
	(2) Comparison of rakes and axisymmetry of flow
19 July 82	(1) Performance map @ 4° IGV
	(2) Radial survey S2+4 4° IGV
23 July 82	(1) Performance map @ 3° IGV
	(2) Radial survey S2+4
6 August 82	(1) Radial survey S1+4
	(2) Radial survey S2+4
	(3) Radial survey S1+2+4
12 August 82	(1) Radial survey Sta 1 probe hole #9 Circumferential Survey @ Sta 3 R = 14.4"
	(2) Radial survey Sta 1 probe hole #8 Circumferential survey @ Sta 3 R = 16.5"
	(3) Radial survey Sta 1 probe hole #7 Circumferential survey @ Sta 3 R = 12.4"
16 August 82	(1) Performance map @ 2° IGV
17 August 82	(1) Radial survey S2+4 2° IGV
	(2) Radial survey S1+4 2° IGV
19 August 82	(1) Check out of rake interference
	(2) Radial survey S2+4 2° IGV
	(3) Radial survey S1+4 2° IGV
23 August	(1) Detailed survey S1+4 @ 2° IGV

24 August 82	(1)	Detailed survey S1+4 @ 2° IGV with cobra probe Sta 0; with yaw probe Sta 1
26 August 82	(1)	Performance map @ 0° IGV
30 August 82	(1)	Survey S4
	(2)	Survey S1+4
	(3)	Survey S2+3
2 September 82	(1)	Off design survey S1
	(2)	Off design survey S2+3+4

Table G1. Performance Map, Throttle Configurations

Screen Combination	June 16 (IGV 0°)	July 13 (IGV 0°)	July 19 (IGV 4°)	July 23 (IGV 3°)	August 16 (IGV 2°)	August 26 (IGV 0°)
Zero Point	1, 2, 3	1, 2	1, 2, 3	1, 2	1, 2, 3	1, 2, 3
S1	4, 5, 6	3, 4	4, 5, 6	3, 4	---	---
S2	7, 8, 9	5, 6	7, 8, 9	5, 6	4, 5	4, 5, 6
S1+2	10,11,12	---	---	---	---	---
S3	19,20,21	7, 8	10,11,12	7, 8	6, 7	7, 8, 9
S1+3	13,14,15	---	---	---	---	---
S2+3	16,17,18	9,10	---	---	---	10,11,12
S1+2+3	25,26,27	---	---	---	---	---
S4	22,23,24	11,12	13,14,15	9,10	8, 9	13,14,15
S5	28,29,30	13,14	---	---	---	---
S1+4	31,32,33	---	16,17,18	11,12	10,11	16,17,18
S1+5	34,35,36	---	---	---	---	---
S2+4	37,38,39	15,16	19,20,21	13,14	12,13	19,20,21
S2+5	40,41,42	---	---	---	---	---
S1+2+4	43,44,45	17,18	---	17,18	14,15	22,23,34
S3+4	46,47,48	---	22,23,24	15,16	16,17,18	---
S1+2+5	49,50,51	---	---	---	---	---
S3+5	52,53,54	---	---	---	---	---
S1+3+4	55,56,57	---	25,26,27	19,20	19,20	25,26,27
S2+3+4	58,59,60	19,20	28,29,30	21,22	21,22	28,29,30
S2+3+5	61,62	---	---	---	---	---
S4+5	63,64	---	---	---	---	---
S5[1]		---	---	---	---	31,32,33

---

[1] Modified solidity

LIST OF REFERENCES

1. Naval Postgraduate School Report 57Va73121A, Redesign of the Low Speed Three Stage Axial Flow Compressor Test Facility, by W. Schlachter, P. F. Pucci and M. H. Vavra, 1973.

2. Welch, J. K., Experimental Investigation of the Effects of Tip Clearance and End Losses on Axial Compressor Performance, M.S. Thesis, Naval Postgraduate School, Monterey, California, 1973.

3. Naval Postgraduate School Report NPS-57Va70091A, Aerodynamic Design of Symmetrical Blading for Three-Stage Axial Flow Compressor Rig, by M. H. Vavra, 1970.

4. Turbopropulsion Laboratory, Naval Postgraduate School, Technical Note 80-09, Multistage Compressor--Initial Measurement with One Stage of Symmetric Blading, by I. N. Moyle, 1980.

5. Turbopropulsion Laboratory, Naval Postgraduate School, Technical Note 80-06, Multistage Compressor--Installation of Cast-Epoxy Blades, by I. N. Moyle and H. Zebner, 1980.

6. Turbopropulsion Laboratory, Naval Postgraduate School, Technical Note 82-01, Multistage Compressor--Flow Losses in Screens and Plates, by J. L. Waddell, 1982.

7. Turbopropulsion Laboratory, Naval Postgraduate School, Technical Note 82-04, GENUSE--General Purpose Data Acquisition Program for the HP 3052/9845A Acquisition System, by W. A. Proses and J. L. Waddell, 1982.

8. Vavra, M. H., Aero-Thermodynamics and Flow in Turbomachines, Wiley, 1960.

9. Horlock, J. H., Axial Flow Compressors, Butterworths Scientific Publications, 1958.

10. Naval Postgraduate School Report 1174VA1, Axial Turbine Design Data, by M. H. Vavra, 1974.

11. Turbopropulsion Laboratory, Naval Postgraduate School, Technical Note 81-03, Multistage Compressor--Fabrication of Cast Epoxy Blades, by I. N. Moyle, 1981.

12. Turbopropulsion Laboratory, Naval Postgraduate School, Technical Note 82-03, *Computer Software for the Calibration of Pneumatic and Temperature Probes*, by F. Neuhoff, 1982.

INITIAL DISTRIBUTION LIST

		No. Copies
1.	Defense Technical Information Center Cameron Station Alexandria, Virginia 22314	2
2.	Library, Code 0142 Naval Postgraduate School Monterey, California 93940	2
3.	Department Chairman, Code 67 Department of Aeronautics Naval Postgraduate School Monterey, California 93940	1
4.	Director, Turbopropulsion Laboratory, Code 67Sf Naval Postgraduate School Monterey, California 93940	20
5.	LT J. L. Waddell VC-5 Box 34 FPO San Francisco, California 96654	2

Thesis
W13
c.1

199638

Waddell

Evaluation of the
performance and flow
in an axial compressor.

199638

Thesis
W13
c.1

Waddell

Evaluation of the
performance and flow
in an axial compressor.

thesW13
Evaluation of the performance and flow i
3 2768 001 92831 0
DUDLEY KNOX LIBRARY